Åbo Akademi University

FACULTY OF TECHNOLOGY

Structural and Operational Optimisation – Applications in Energy Systems

Jarmo Söderman

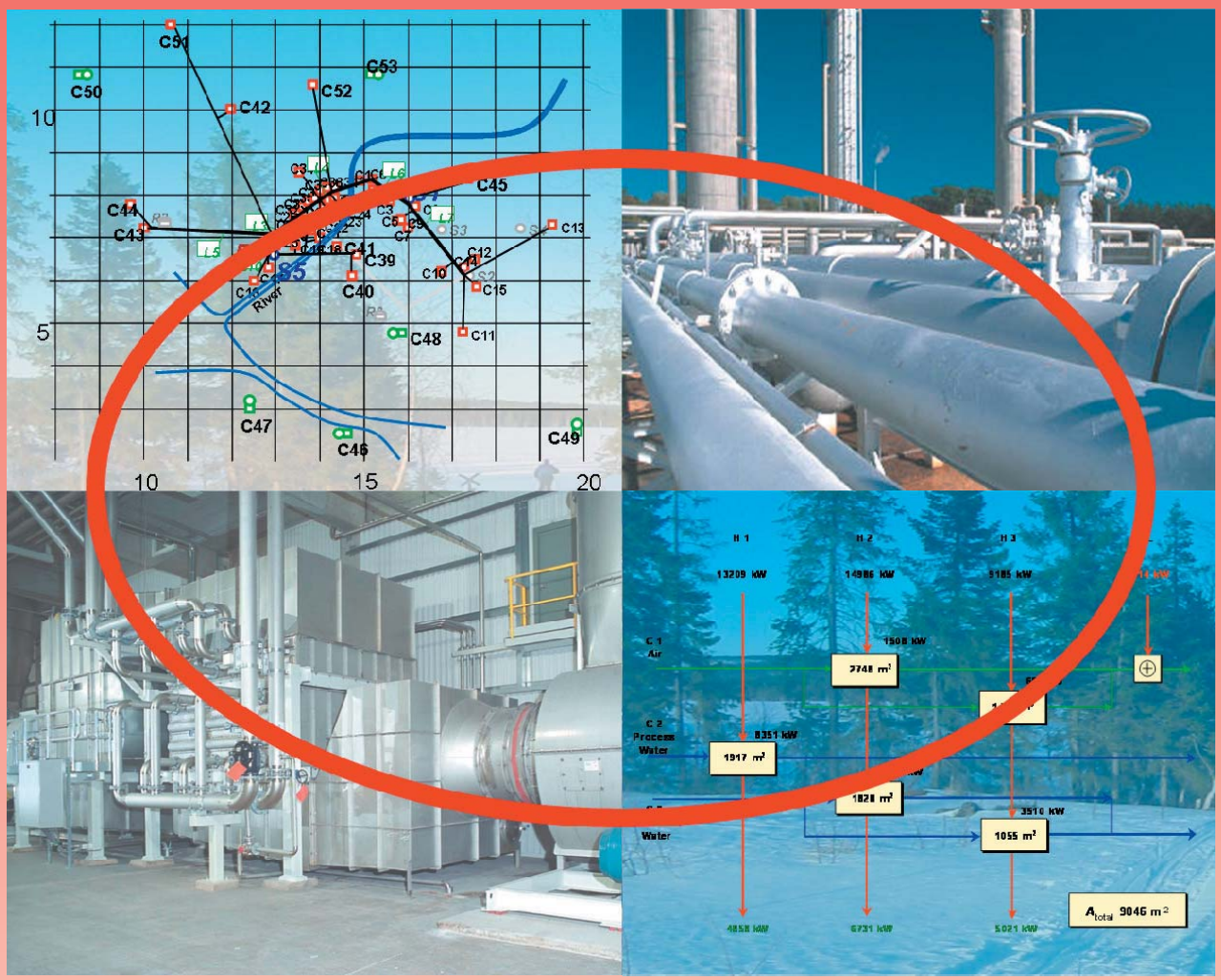

Heat Engineering Laboratory

ÅBO 2007

Structural and Operational Optimisation – Applications in Energy Systems

Jarmo Söderman

Heat Engineering Laboratory
Faculty of Technology
Åbo Akademi University

ÅBO 2007

Preface

The work in this thesis has been carried out at the Heat Engineering Laboratory, Faculty of Technology at Åbo Akademi University, under the supervision of Prof. Henrik Saxén. His support, encouragement and guidance have had an immense impact on the study. I want to thank him deeply for the impatient effort he has put forward during the work.

The applications that are presented in the thesis are based on regional and industrial cases. Part of the work is based on measurements in the paper industry. They were carried out in collaboration with Metso Paper Air Systems in Turku. I wish to thank the personnel of the unit for the information, discussions and support during the study. I wish to thank also the personnel of Turku Energia for the information, discussions and support in the regional energy systems part of the work.

I wish to thank especially docent Frank Pettersson. Collaboration with him has been highly fruitful throughout the study and discussions with him, comprised with continuous inspiration and encouragement, have been of utmost value for carrying out this work. I want to thank the colleagues at the Heat Engineering laboratory that have supported me in the study with help, ideas and valuable comments. My thanks are also due to Prof. Tapio Westerlund and the colleagues at the Process Design laboratory for their help and collaboration. I want to thank also the researcher colleagues at Helsinki University of Technology, Tampere University of Technology and VTT for the effective collaboration in our joint projects.

Finally, I want to express my deepest gratitude to my wife Marjaleena and my sons Henrik and Tuomas for their never ceasing encouragement during the work.

Åbo, December 2007

Jarmo Söderman

Abstrakt

Denna avhandling handlar om optimering av energisystem. Matematiska modeller har utvecklats för ett urval av energitekniska problem. De testfall som analyserats har tagits både från industriella processer och omfattande regionala energidistributionssystem. De utvecklade modellerna baserar sig på ett antal matematiska programmeringsmetoder: blandade heltals linjär programmering (Mixed Integer Linear Programming, MILP), blandade heltals icke-linjär programmering (Mixed Integer Nonlinear Programming, MINLP) samt i en hybrid modell icke-linjär programmering (Non-Linear Programming, NLP) och genetiska algoritmer (Genetic Algorithms, GA).

Modeller för optimering av energisystems struktur och drift i regioner har utvecklats i detta arbete. Modellerna inkluderar ett antal konsumenter som har varierande behov av elektricitet och värme under olika tidsperioder av året, samt ett antal platser i regionen där ett urval av energikonverteringsmetoder, som kombinerat värme och elproduktion (Combined Heat and Power, CHP), värmeproduktion med biobränsle och elproduktion med vindkraft kan installeras. Värmen kan distribueras till konsumenter via ett fjärrvärmenät eller ledas till varmvattenreservoarer som fungerar som värmeackumulatorer i systemet.

I avhandlingen behandlas också regionala fjärrkylenätverk där ett större antal konsumenter med varierande kylbehov har inkluderats. Systemets struktur och drift har analyserats med hänsyn till nuläget och långtidsprognoser för kylbehovet i regionen.

Avhandlingen omfattar också modeller för värmeåtervinningssystem vid torkpartiet av pappersmaskinen. Värmekällorna i detta sammanhang är fuktiga luftströmmar. Modellerna är uppbyggda så att man kan ta hänsyn till olika typer av prisfunktioner för de inkluderade värmeväxlarna. Modellerna baserar sig vidare på uppdelning av det totala temperaturområdet i temperaturintervall. Inom varje temperaturintervall kan man effektivt ta hand om kraftigt icke-linjära värmekapaciteter och värmeöverföringskoefficienter, förorsakade av kondenseringen av fukten i luftströmmarna i värmeväxlarna.

Inverkan av variationer i både kostnads- och processparametervärden på olika lösningar av värmeåtervinningssystem har också studerats. Punktoptimala lösningar med fixerade parametervärden har jämförts med robusta lösningar, som erhållits med givna variationsområden för processparametrarna.

Avhandlingen handlar även om användning av överskottsvärme, då torkpartiet delvis byggs med påblåsningstorkningsenheter, generering av elektricitet från värmeströmmar med låga temperaturer samt användningen av absorptionsvärmetransformator för att höja processströmmens temperatur över värmekällans temperatur.

Abstract

In this work mathematical programming models for structural and operational optimisation of energy systems are developed and applied to a selection of energy technology problems. The studied cases are taken from industrial processes and from large regional energy distribution systems. The models are based on Mixed Integer Linear Programming (MILP), Mixed Integer Non-Linear Programming (MINLP) and on a hybrid approach of a combination of Non-Linear Programming (NLP) and Genetic Algorithms (GA).

The optimisation of the structure and operation of energy systems in urban regions is treated in the work. Firstly, distributed energy systems (DES) with different energy conversion units and annual variations of consumer heating and electricity demands are considered. Secondly, district cooling systems (DCS) with cooling demands for a large number of consumers are studied, with respect to a long term planning perspective regarding to given predictions of the consumer cooling demand development in a region.

The work comprises also the development of applications for heat recovery systems (HRS), where paper machine dryer section HRS is taken as an illustrative example. The heat sources in these systems are moist air streams. Models are developed for different types of equipment price functions. The approach is based on partitioning of the overall temperature range of the system into a number of temperature intervals in order to take into account the strong nonlinearities due to condensation in the heat recovery exchangers.

The influence of parameter variations on the solutions of heat recovery systems is analysed firstly by varying cost factors and secondly by varying process parameters. Point-optimal solutions by a fixed parameter approach are compared to robust solutions with given parameter variation ranges.

In the work enhanced utilisation of excess heat in heat recovery systems with impingement drying, electricity generation with low grade excess heat and the use of absorption heat transformers to elevate a stream temperature above the excess heat temperature are also studied.

Structure of the thesis

The thesis comprises a general part concerning the type of processes that are addressed, the research on the addressed fields of technology and introductory notes for the included papers.

The following papers are included in the thesis:

Paper I

Söderman, J., Pettersson, F.,
Structural and operational optimisation of distributed energy systems,
Applied Thermal Engineering, 26, 2006, 1400–1408.

Paper II

Söderman, J.,
Optimisation of structure and operation of district cooling networks in urban regions,
Applied Thermal Engineering, 27, 2007, 2665–2676.

Paper III

Söderman, J., Westerlund, T., Pettersson, F.,
Economical optimisation of heat recovery systems for paper machine dryer sections, Proceedings of the 2nd conference on Process Integration, Modelling and Optimisation for Energy Saving and Pollution Reduction, 1999, 607–612.

Paper IV

Söderman, J., Pettersson, F.,
Influence of variations in cost factors in structural optimisation of heat recovery systems with moist air streams, Applied Thermal Engineering, 23, 2003, 1807–1818.

Paper V

Pettersson, F., Söderman, J.,
Design of robust heat recovery systems in paper machines,
Chemical Engineering and Processing, 46, 2007, 910-917.

Paper VI

Söderman, J., Pettersson, F.,
Searching for enhanced energy systems with process integration in pulp and paper industries,
Computer Aided Chemical Engineering, 14, 2003, 1055–1060.

Contents

1 Introduction

The use of energy is a precondition for the functioning of modern society. Electricity is used to run the production plants and the different equipment in offices and homes. Heat is needed for industrial processes and for hot water and space heating in buildings. Cooling is needed not only in the food industry processes and ware houses, but also in hospitals, offices, retail markets and houses for dwelling. The transportation of goods and people is growing quickly in all parts of the world. The benefits of this versatile energy utilisation are obvious but at the same time a world wide concern is growing to the negative environmental impact of energy use, especially of the greenhouse gas emissions and their impact on the climate change.

International Energy Agency (IEA) has predicted a continuous growth of the energy use in the world towards the year 2030 (IEA World Energy Outlook, 2004). The annual growth is assumed to be 1.6 % from 2002 to 2030. The transport sector is predicted to grow the fastest, 2.1 % per year, and to still rely in 2030 almost exclusively on oil. In other sectors, however, many different possibilities for primary energy sources are available. In recent years much focus in the debate has been directed to renewable energy forms, for instance biofuel, solar power and wind power. The share of the renewable energy sources in the world energy demand is predicted to be about 14 % in 2030. Hydro power, the main renewable energy form in the past, is predicted to maintain its present share of 2 % of the total world energy demand.

Due to the key role of the energy systems in society it is important that they are designed as optimally as possible with respect to both the investment costs of the equipment and the operational costs of the systems for their whole life cycle. Mathematical programming makes it possible to search for such optimal energy system solutions. For these solutions both effective models and solving methods are required.

The objective of the present work is defined from the basis of the importance of the energy in society to develop and apply mathematical programming models for structural and operational optimisation of energy systems. The structural aspect refers to the capital investment in the systems, i.e. the power, heating and cooling generation equipment, the distribution networks etc. The operational aspect refers to what the costs of running the energy systems are throughout their life time. Cases that are studied are taken from industrial processes and from large regional energy distribution systems. The transport sector is, however, excluded from the scope of this work.

The applications that are included are the distributed energy systems comprising a number of different energy conversation technologies, cooling plants and cold water storages for district cooling systems, heat recovery systems in connection with humid air streams and some technologies for enhanced utilisation of excess heat. The chosen applications are presented in sections 2, 3 and 4.

Distributed energy systems (DES) are studied as an alternative to conventional large central units generating electric power and heat. Generation plants that are smaller and

closer to the consumer sites can have a better overall economy and a reduced environmental impact. In this work distributed energy systems in a given region are studied and how they should be built optimally and with the most cost effective operation, with respect to the annual variations of the demands of district heating and electrical power. Many different technologies are available for heat and electricity generation, for instance hydro power, coal-, gas-, biomass- or oil-fired power plants, nuclear power plants, combined heat and power plants, wind turbines, photovoltaic cells, fuel cells etc.

Utilisation of district cooling (DC) for the supply of cooling to premises has increased in urban regions to replace the individual cooling machines in each room or building. Cold water at some degrees above freezing point is commonly used in DC systems. These systems are studied in this work with respect to optimal cold water supply networks in a region in different cooling demand situations. A cooling plant can be combined with cold water storages to add capacity at peak demand hours. The aim is to develop a model that can be used in the planning of DC system expansions based on predictions for the consumer cooling demand development.

The developed DES and DC system approaches are valuable tools for the stakeholders in the energy supply field: the energy plants, the equipment suppliers, the energy consumers and the authorities enabling them to take an active part in the decision and design process, before the regional energy systems are built.

Heat recovery in industrial processes reduces the operational costs of the industry by reducing the primary energy demand of the processes. Paper machine heat recovery systems (HRS) are taken in this work as examples of these systems. They are representative of any industrial heat recovery system, but have an additional feature to be taken into account in the modelling, namely the moisture content of the air streams, which are the heat sources in the systems. The condensation of water from the air streams inside the heat recovery exchangers means that both the specific heat transfer flow rates and the heat transfer coefficients become strongly nonlinear.

When industrial systems are designed they need to be considered against predictable variations of the operational parameters. In this work the influence of such variations is studied on solutions of heat recovery systems firstly by varying some cost factors and secondly by varying some process parameters. Point-optimal solutions, obtained by fixed parameters, are compared to robust solutions with given parameter variation ranges.

In energy utilisation systems low-grade heat is often abundantly available. Technologies that could enable the utilisation of such energy flows would decrease the primary energy demand and the environmental impact. As examples of such technologies enhanced heat use in paper machine heat recovery systems with impingement drying, electricity generation with low grade excess heat and the use of absorption heat transformers for elevation of process stream temperatures above the excess heat temperatures are studied.

The models that are developed rely on mathematical programming, using Mixed Integer Linear Programming (MILP), Mixed Integer Non-Linear Programming (MINLP) and a hybrid approach on combining Non-Linear Programming (NLP) and Genetic Algorithms (GA). A balance between the computation time and the inclusion of details in the models is sought in this work. The aim is also that in the optimisation problem the included

constraints and parameters can be taken into account simultaneously in one single optimisation run so that an economically optimal solution, based on these parameters, is obtained. The optimal solution will serve as a basis for the design process giving a suggestion of the system structure and operational parameters to be finally defined in the detailed engineering phase.

2 Distributed energy systems

A decentralised or distributed energy system (DES) comprises small scale generation plants of heat and electricity in a region and the needed distribution networks from the plants to the consumers, together with possible energy storages.

Conventionally both electric power and district heat have been generated in large central units. It has, however, been questioned, whether the generation plants should be smaller and closer to the consumer sites in order to achieve better overall economy and environmental benefits. Large power plants often have energy losses in the form of low-temperature waste heat. In the distributed generation the low-grade heat could often be better recovered. Other stated advantages of DES are shorter plant implementation times, capital need that is distributed both in time and by project, smaller transport pipelines for district heating and more flexible heat and power generation. It has been predicted that in the near future a considerable part of electricity and heat will be generated in distributed systems.

A DES is shown schematically in Fig. 2.1.

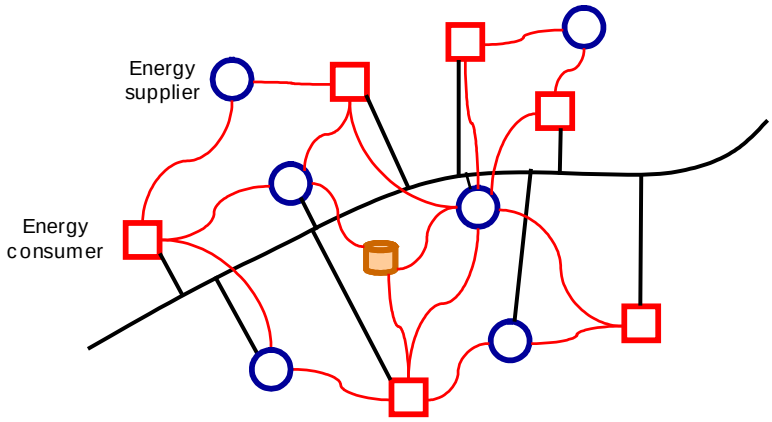

Figure 2.1. Schematic presentation of a distributed energy system in a region. Circles represent energy supplier units, squares energy consumers, tank a heat storage, fine curved lines district heating pipelines and bold lines electric power transmission lines.

2.1 Distributed energy system technologies

Energy conversion technologies

For a distributed energy system several energy conversion technologies are available. One important option is the combined heat and power (CHP), (e.g. Spets, 2002 and Savola, 2004). Additionally, many different types of boiler plants with a variety of fuels, for instance biofuels (e.g. Ranta, 2005 and Obernberger, 1998) are used. Other conversion technologies such as gasification technologies (e.g. Nieminen, 1998 and Marbe et al., 2004), geothermal plants (e.g. Bidini et al.), heat pumps (e.g, Aye, 2003), wind power (e.g. Fuglsang, 1999), solar power (e.g. Sen, 2004), water turbines (e.g. Paish, 2002), fuel cells (e.g. Khan et al., 2005), micro gas-turbines (e.g. Pilavachi, 2002), Stirling-engines (e.g. Kongtragool, 2003) etc. can be applied in a DES.

In a CHP plant both electrical power and heat are produced with high overall efficiency. Combined heat and power plants are used widely in countries where district heating is supplied. For example in Denmark and Finland 75 % of district heat is produced in CHP plants. An example of CHP plant flow sheet is shown in Fig. 2.2.

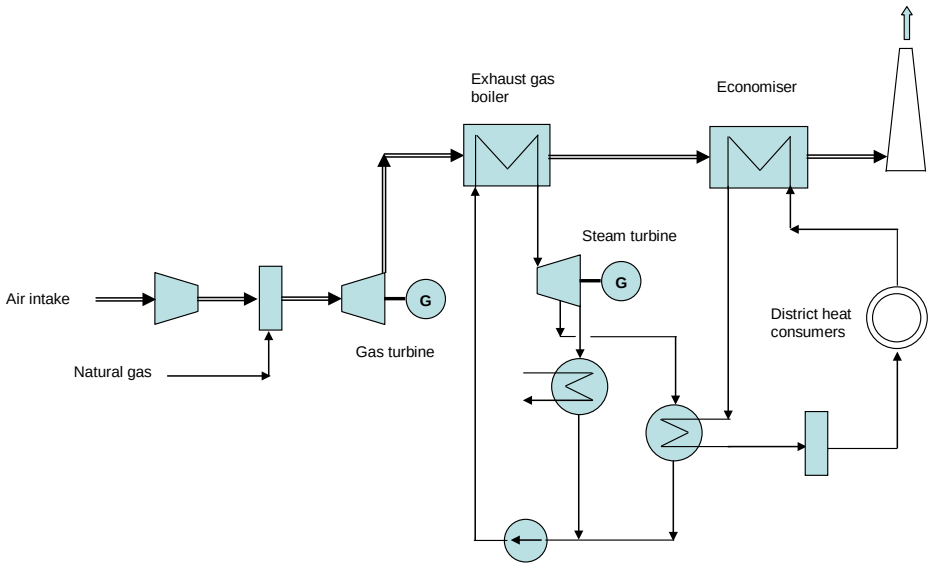

Figure 2.2. A CHP plant flow diagram with gas and steam turbine.

The main advantage of the CHP is its high total efficiency. Efficiencies up to 95 % are reported. The power to heat ratio depends on the type of the plant. For gas turbines the ratio is usually 0.4 – 0.5, while for gas engines and diesel engines it is 0.8 – 1.0. For solid fuel fired plants the ratio is 0.3 – 0.5.

Thermal boiler plants that produce only heat for the district heating are taken in this work as another studied option for DES. The plants use biomass as fuel. The boilers have high thermal efficiencies, typically up to 85 %.

For wind turbines the installed capacities have steadily increased and are today from 2 to 5 MW per unit. Large wind power parks have been built especially in Germany, Spain

and Denmark, comprising even hundreds of wind turbine units. The annual peak capacity hours are often relatively low, for instance in Finland 2000 to 3000 hours on the best coastal sites.

Compressor-driven heat pumps are considered as an option for the district heat consumers to produce their own heat. Evidently, there is a trade-off between the electricity price together with the heat pump price and the cost of the district heat.

District heating pipelines

District heating (DH) pipelines with two parallel steel pipes, with foam insulation and a plastic mantel, are considered in the study. The costs of all civil work, namely excavation, installation, filling of the excavation and surface works are considered in the analysis. The temperature level of the DH feed water to consumers is usually from 90 to 115 °C. The temperature drop at the consumer premises is usually approx. 50 °C, i.e. the DH return water temperature is 40 - 60 °C.

Design of heat storages

Heat storages in this work are modelled as insulated, cylindrical steel tanks, built above the ground as shown in the Fig. 2.3.

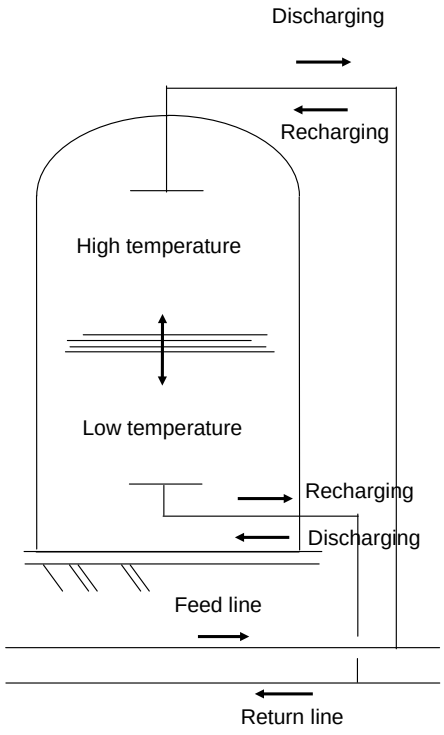

Figure 2.3. Working principle of a hot water storage.

The storage tank is kept nearly full all the time. The tank operates at a small over pressure, 10-15 mmH_2O over the normal air pressure. The free room at the top of the

tank is filled with steam to avoid air content increase in the tank water. During charging hot water from the DH feed line is pumped in at the top of the tank. At the same time cold water is taken out to the return line from the bottom of the tank. If the charging takes place at night-time then the discharging is done during the following period (day-time). The same lines are utilised but now in opposite directions, as shown in Fig 2.3. DH return water is pumped into the tank from the bottom and the hot water is taken out to the DH feed line from the top of the tank.

A transition zone is formed in the tank between the hot feed water at the top and cooled return water at the bottom. The zone moves up and down in the tank. When the tank is fully charged the zone is near the bottom. During discharge the zone moves up.

In Fig. 2.4 the heat capacity variation of the storage tank is shown during two consecutive periods.

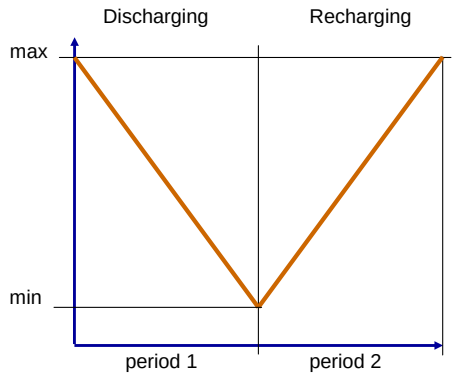

Figure 2.4. Variation of the heat capacity of a hot water storage in two consecutive periods.

2.2 Basic features of the optimisation model of DES

An MILP model is developed for structural and operational optimisation of DES in a region. The Branch and Bound method is applied in solving the optimisation problem. The approach guarantees a global optimal solution to the problem. Basic features of the model are presented below.

An energy supplier can be situated inside the region in a number of predetermined locations. There can be many types of heat and power generation units or combinations of these. Sites can have any number of the given types of production units or there can be restrictions. For example, a coastal site may have been reserved only for wind power. The solution will then show whether the wind power at that site is economically viable in respect to the optimality of the whole regional energy system.

The variations in the consumption of heat and power are taken into consideration by dividing a year into a number of periods. Consumers can produce their own heat in competition with the district heat. If a heat pump is installed at a consumer site, there will be additional electricity consumption at that site.

The region is considered as self-contained in respect of satisfying the total heating demand. For the electric power the demand can be satisfied with power produced within the region and/or from the grid. The power from the grid is considered to be abundant and purchased with given tariffs that can have differences between day and night and between seasons.

2.3 District heating and electricity generation

Some data concerning the development of district heating and electricity markets is presented here as a background to the distributed energy system development.

District heating is delivered to approx. 100 million people in Europe (Russia excluded), i.e. 23 % of the European population (CHP-info, 2005). The largest share of district heating used in the dwelling house heating in Europe has been reported from Latvia with a 70 % share, while for example in United Kingdom the share is only 1 %.

The world electricity consumption in 2002 was approx. 16070 TWh. A growth of 2.5 % per year from year 2002 to year 2030 has been predicted, which would mean a consumption of 31660 TWh by 2030. By this time the distributed energy systems are predicted to have grown by about 4 % per year. (IEA, World Energy Outlook, 2004).

Table 2.1. Electricity generation in the world 2002 and 2030

	generation 2002 TWh	generation 2030 TWh	share 2002 %	share 2030 %	change/a 2002-2030 %
World electricity generation	16070	31660	100	100	2,5
Coal	6240	12090	39	38	2.4
Natural gas	3070	9330	19	29	4.0
Hydro power	2610	4250	16	13	1.8
Nuclear	2650	2930	17	9	0.4
Oil	1180	1180	7	4	0.0
Renewables (excl. hydro power)	320	1890	2	6	6.1
Biomass and waste	210	630			3.8
Wind	50	930	0.3	3	10.1
Geothermal	60	170			3.7
Solar	1	120			17.2

The electricity generation capacity in the world is expected to grow from 3400 GW in 2002 to 7200 GW by 2030. Additionally, it is predicted that some 1000 GW of old capacity will be replaced with new plants. The largest part of electricity is expected to be generated by coal. Its share would decrease slightly, from 39 % in 2002 to 38 % by 2030. The share of natural gas would increase strongly, from 19 % in 2002 to 29 % by 2030.

In the group of renewable energy sources comprising biomass, wind, geothermal and solar power the electricity generation is expected to grow strongly. Electricity generation

by biomass is expected to grow by about 4 % a year to 630 TWh by 2030. Wind power is expected to grow by 10 % a year to 930 TWh and solar power by 17 % a year to 120 TWh by 2030.

2.4. Energy planning models

Regional energy planning models

During last three decades many linear programming optimisation models have been developed for regional energy planning scenarios. MARKAL Market allocation model (e.g. Fishbone and Abilock, 1981) and EFOM energy flow optimisation model (e.g. Van der Voort et al., 1984) are examples of the models developed. The models are general optimisation models for large scale energy planning and do not conventionally deal with the individual consumers and suppliers or the energy network routing.

An example of regional energy planning modelling is presented in the work of Cormio et al. (2003). A bottom-up energy system optimisation model was used to support the regional decision making on energy issues, applying the EFOM model. Several different energy options were included and a relatively large region was simulated. The model does not take into account the locations of power plants or consumers. Instead, it handles the whole region as a single supplier/consumer place. District heating is not discussed in the paper as the region is in the Mediterranean climate. In an attempt to include the environmental impacts the authors have included external costs to cover the emission costs. The external costs are based on questionnaires of how much people are willing to pay for a cleaner environment. The authors state that the inclusion of the external costs in the objective function made the conventional thermo electric power plants so expensive that they were excluded from the regional plan.

Decentralized energy planning models

A review of decentralized energy planning models is presented in Hiremath et al. (2007). An example is given in the paper of Chinese and Meneghetti (2005), presenting an MILP model for optimisation of district heating in an industrial district. The model is built from the heat supplier side with the objective to maximise the profit of the suppliers. The consumer side is modelled as the heat demand but, for example, the consumer's possibility of using a heat pump is not considered. The model does not take into account the locations of the individual consumers, pipelines or supplier plants. Neither are the heat storages considered, nor the electricity demands of the consumers. Thus different possibilities for producing electricity, e.g. wind power or CHP, are not discussed. The authors consider also the environmental aspects, using another model, where the objective is to minimise the CO_2 emissions.

Environomic energy system models

Recently, as the concern for the impact of energy systems on the global environment has increased, combined models of optimisation of energy systems and emission reduction

have been developed. For example, in two papers of Curti et al. (2000a and 2000b) space heating in an urban district was studied. The buildings in the district were classified in four different categories with respect to the needed temperature levels at the space heating radiators. The model includes a central heat pump as the main heat supplier and a number of satellite heat pumps that serve as local, decentralised upgrading units of the district heating water temperature. The system allows the use of the return line as heat source for those buildings that belong to the lowest category in the temperature level classification. The problem is an MINLP problem and is solved by a genetic algorithm. The environmental aspects are taken into the model as pollution costs. From conventional equipment and resource costs augmented equipment and resource costs are formed by adding to them specific pollution costs.

In the work of Weber et al. (2006) a two-step approach is presented for the optimisation of the structure of district energy systems. In the first stage, an evolutionary algorithm is used for the choice of structural parameters. In the second stage an MILP problem is solved with the chosen structural parameters fixed. A solution is obtained showing a Pareto front considering CO_2 emissions and the structural costs of the network.

3 District Cooling

In recent years utilisation of district cooling (DC) has increased in urban areas. Instead of each cooling consumer investing, maintaining and operating his own cooling machine central cooling generation plants and cold media distribution networks are built. In the evaluations one should also take into account the space for the cooling machine that becomes vacant for other purposes as the consumer is connected to the DC network. An additional advantage in the dwelling and office houses is that the noise of the cooling machine is avoided.

For the distribution of cooling, cold water at some degrees above the freezing point has been the common choice, but other media like ice slurry and CO_2 have also been suggested. Cold water is distributed in similar pipelines as hot water in district heating (DH) networks. However, the temperature difference between the feed water and the return water is only around 10 °C, while it in DH networks is normally 40 - 60 °C. Thus the pipeline dimensions have to be considerably larger in DC networks than in DH networks for the same energy transport capacity.

A cooling plant can be combined with cold media storages to add capacity at the peak demand situations. Alternatives for cold media in storages are e.g. cold water, snow, ice, ice slurry or different phase changing materials like paraffins.

With a compressor-driven cooling machine the evaporation temperature of the refrigerant is near 0 °C, while the condensation temperature can be chosen in some limits depending of the system, to which the condensation heat is transferred. Absorption cooling machines can be used in cases where excess heat is available at suitable temperature level from a process industry plant situated sufficiently close to the cooling consumers.

3.1 Heat pumps as refrigerators

Heat pumps have been used as refrigerators since the end of the 18th century. Earliest refrigerators were absorption engines for production of ice with sulphuric acid and water as absorbent and refrigerant media. The first ammonia and water absorption refrigerators were developed in the middle of the 19th century. From 1880 onwards vapour compression heat pumps started to replace the absorption machines.

Absorption heat pumps regained new interest in the 1920's, especially for upgrading waste energy. The interest in all types of heat pumps faded, however, in 1940's and 50's, as the primary energy resources were seen overwhelmingly abundant. The two oil crises in the 1970's changed the attitude back towards the energy saving and led to a renewed interest in the heat pump technologies.

Cooling technologies can be divided into technologies in the temperature range from the ambient temperature to 0 °C and technologies below 0 °C. In the present study only the temperature range above the freezing point was considered.

3.2 Compressor cooling machines

A compressor-driven cooling machine is a heat pump, shown schematically in Fig. 3.1. In the figure the heat pump is connected so that both district cooling and district heating networks are served. The cooling machine generates cooling effect to a district cooling network and delivers the condensation heat to a district heating network.

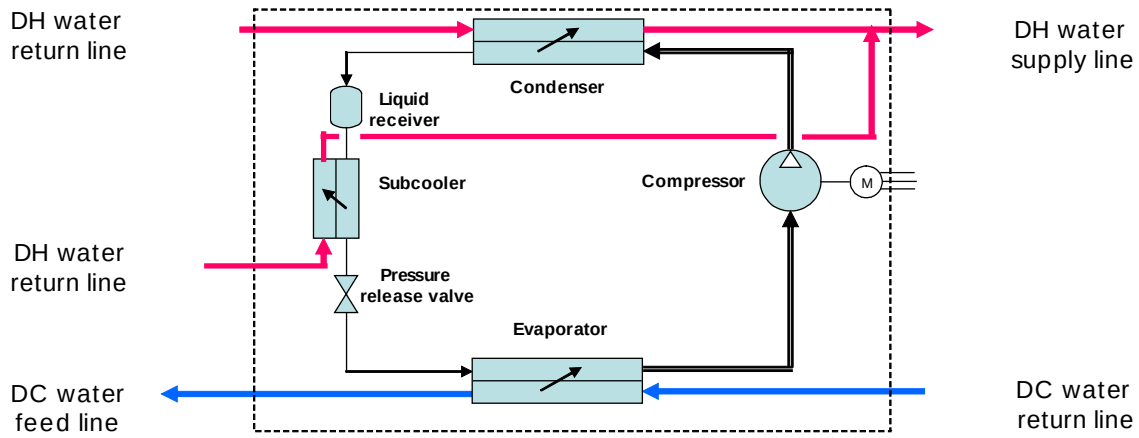

Figure 3.1. Compressor cooling machine.

A compressor cooling cycle is presented in a *p*,*h*-diagram in Fig. 3.2. The cycle comprises expansion of the refrigerant liquid from a higher pressure p_2 and temperature T_S to a lower pressure p_1 and temperature T_L (from point 1 to point 2) with partial evaporation, heat transfer $\dot{Q}_1$ into the refrigerant fluid (from 2 to 3) with complete evaporation at the temperature T_L and slight overheating to temperature T_O , compression from p_1 and T_O to p_2 and T_H , (from 3 to 4) and heat transfer $\dot{Q}_2$ from the system with cooling from T_H to T_C with condensation at the temperature T_C and following subcooling to the temperature T_S (from 4 to1).

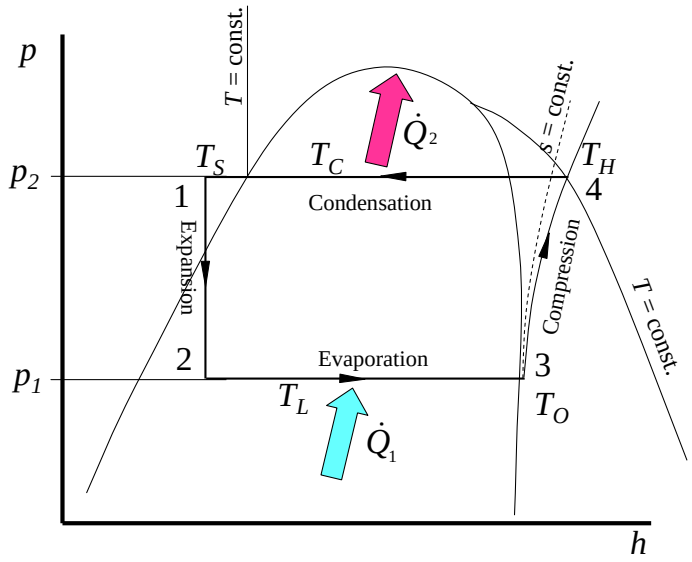

Figure 3.2. Compressor cooling machine cycle in *p,h*-diagram.

The effect balance for the cycle is

$$\dot{Q}_1 + P_{in} = \dot{Q}_2 \tag{3.1}$$

where P_{in} is the net effect of the compressor.

Coefficient of performance

The coefficient of performance, COP, for refrigerators and cooling machines is defined as the ratio between the heat flow from the heat source and the inserted effect

$$\mathrm{COP}_{\mathrm{Re}} = \frac{\dot{Q}_1}{P_{in}} = \frac{\dot{Q}_1}{\dot{Q}_2 - \dot{Q}_1} \tag{3.2}$$

For a heat pump COP is defined as the ratio between the heat flow delivered to the heat sink and the inserted effect

$$\mathrm{COP}_{\mathrm{HP}} = \frac{\dot{Q}_2}{P_{in}} = \frac{\dot{Q}_2}{\dot{Q}_2 - \dot{Q}_1} \tag{3.3}$$

The relation between COP for a heat pump and a refrigerator becomes, by combining Eq. (2) and Eq. (3)

$$\mathrm{COP}_{\mathrm{HP}} = \mathrm{COP}_{\mathrm{Re}} + 1 \tag{3.4}$$

A Carnot-COP, COP_C can be defined for an ideal cooling cycle with assuming constant temperatures for heat inlet, θ_1 and heat outlet, θ_2. COP_C is defined with the respective absolute temperatures, T_1 and T_2 as

$$COP_C = \frac{T_1}{T_2 - T_1} \tag{3.5}$$

This defines the maximum possible COP for the system. An efficiency factor for a cooling cycle can be defined as the ratio between the ideal cycle COP_C and the actual COP, as given in Eq. (3.6)

$$COP = \eta \cdot COP_C = \eta \cdot \frac{T_1}{T_2 - T_1} \tag{3.6}$$

In a district cooling network the supply water is for instance 6 °C and the return water about 10 °C higher. The evaporation temperature of the refrigerant is some degrees centigrade below the DC feed water temperature. Typical COP values for compressor cooling machines are from 2 to 4. The performance can be improved, for instance, by a two-stage cascade process or by using a number of one-stage cycles in series.

3.3 Absorption cooling machines

In an absorption cooling machine, Fig. 3.3, the compressor is replaced by an absorber/generator process step. A secondary working fluid, a solvent, is needed to be circulated between the absorber and the generator. In other aspects the system operates with same principle as the compressor cooling machine.

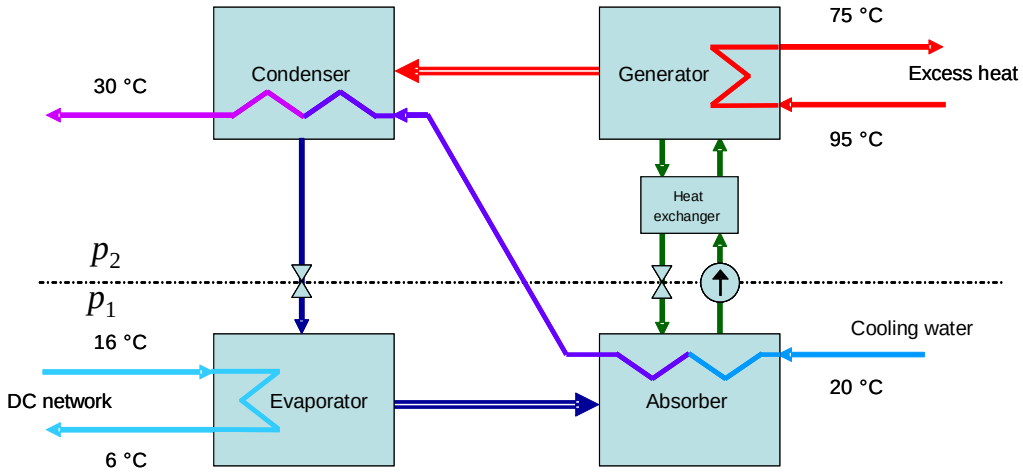

Figure 3.3. Absorption cooling machine.

The refrigerant vapour is generated at the evaporator at a low pressure p_1 and let to the absorber, where it is absorbed by the solvent. Thereby it releases its heat of condensation and absorption. As the boiling point of the solution is higher than that of a pure refrigerant, the temperature of the solution would increase in the absorber without cooling. The absorber is cooled by a suitable cooling medium. The solution, which now has a lower concentration because of the absorbed vapour, is pumped to a higher pressure by a liquid pump. The solution is heated in the generator by a hot process stream causing the solution to boil. The obtained refrigerant vapour is condensed in the condenser by the cooling medium, which is pumped from the absorber. The condensed refrigerant is let via the expansion valve to the evaporator to complete the cycle. The resulting cooling effect output is approximately the same as the heat input from the heat source. An intermediate heat exchanger between the absorber and the generator improves the machine performance.

The absorption cooling process is presented in a *p,T*-diagram, Fig. 3.4. The input of process heat in the generator is denoted by $\dot{Q}_D$ and the input of heat from the cooling network in the evaporator by $\dot{Q}_E$. The heat from the condenser and the absorber into the cooling water are denoted by $\dot{Q}_C$ and $\dot{Q}_A$ respectively.

The temperature levels are chosen so, that the condensation and absorption are run approximately at the same temperature level, so that the cooling water can be circulated through both units in series.

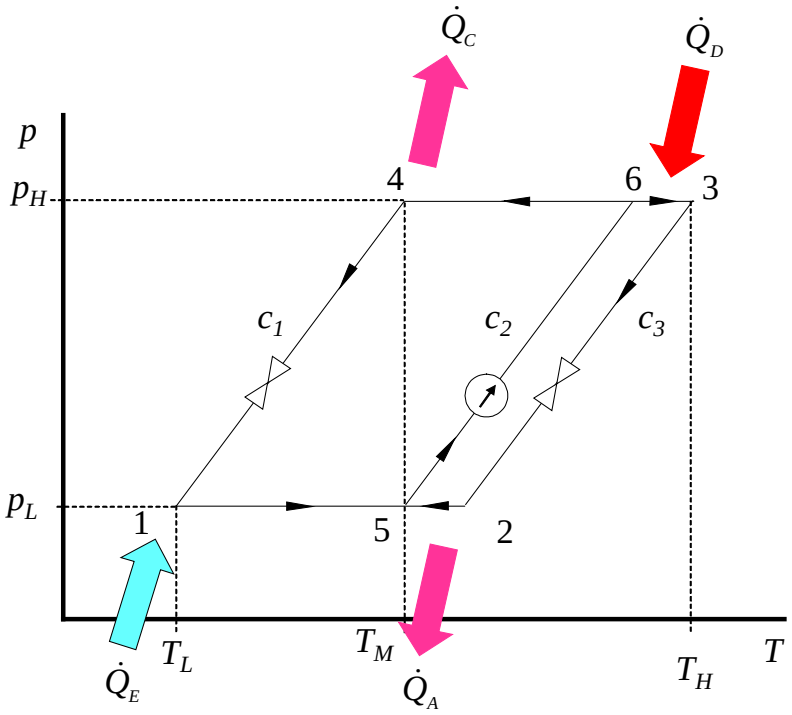

Figure 3.4. Absorption cooling process.

The COP for absorption cooling process is defined as

$$\mathrm{COP}_{\mathrm{ACM}} = \frac{\dot{Q}_E}{\dot{Q}_D} \tag{3.7}$$

In absorption cooling machine the input of mechanical work is small. The compressor work in a compressor-driven cooling machine is replaced by a liquid pump. The major advantage of the absorption cooling in comparison with the compressor cooling is the use of low exergy excess heat instead of high exergy source, electricity.

From a large variety of possible working fluid pairs for the absorption cooling process most common pairs today are water/ammonia, H_2O/NH_3 and lithium bromide/water, $LiBr/H_2O$. The H_2O/NH_3 pair is suitable for a wide temperature range but is usually used in processes with temperatures below 0 °C. $LiBr/H_2O$ is used only in the temperature range above 0 °C due to the risk of ice formation in the equipment.

4 Paper machine heat recovery systems

A paper machine comprises normally three sections, the wire section, the press section and the dryer section. Fiber stock enters the wire section from a head box, at a consistency of 0.2 to 1.0 % fibers in water. In the wire section a paper web is formed by draining water from the stock by gravitation and under-pressure. In the press section the dry solids content is increased to 33 - 55 %, depending on the paper grade and the press section design. In the dryer section water is evaporated from the web by direct or indirect heating. After the dryer section the moisture content of the paper is 5 - 9 % (Karlsson, 2000).

Paper machines are often integrated with a pulp mill. Pulp is produced mainly by chemical or mechanical pulping processes. Chemical pulping can today be self-sustained, converting around half of the wood raw material to energy. Mechanical pulping has in recent years been built more often than earlier, as it gives higher yields of the wood raw material than what is obtained by chemical pulping. Mechanical pulping is, however, an energy demanding process. For example, production of thermo-mechanical pulp (TMP) requires typically 2000 – 3000 kWh electric power per ton of pulp. Around 70 % of the power can be recovered in the form of low-pressure steam. The low-pressure steam can be used, for instance, at the dryer section of an integrated paper machine.

4.1 Paper drying

The most common drying technology in paper machines is cylinder drying. The paper web is brought into contact with hot outside surfaces of rotating steel cylinders. The cylinders are heated with low-pressure steam condensing inside the cylinders.

Cylinder drying requires a large space due to relatively low specific evaporation rates, usually around 30 kg H_2O/m^2h paper web contact area. The trend has been to increase the machine speeds and capacities, which mean longer drying sections than earlier. New drying methods such as impingement drying have been developed in order to improve the drying rates and decrease the dryer length. Impingement drying has a specific evaporation rate around 100 – 120 kg H_2O/m^2h.

Steam consumption in paper drying is typically about 1500 kWh/ton paper and electricity consumption about 630 kWh/ton paper (Kuhasalo, 2000). It is often difficult to utilise all the available secondary heat for conventional purposes at the mills. Therefore, additional heating applications, such as district heating, waste water evaporation, sludge dewatering etc. have been studied and implemented.

4.2 Heat recovery at dryer section

At a paper machine the secondary heat can be used for several purposes, for example for the heating of the incoming air into the dryer hood, various process waters and the machine hall ventilation air, as well as outside the mill for example for district heating.

A heat recovery system at a paper machine comprises heat exchangers and blowers for the supply air and the exhaust air together with a number of heat exchangers for other process streams. Usually several recovery towers are built along a paper machine dryer section. The exhaust air temperatures and moisture contents vary slightly in different towers.

The exhaust air moisture starts to condensate on the heat transfer surfaces when the temperature in the air fluid layer near the surface has sunk to the saturation temperature. The condensate runs down to the bottom of the tower. The condensate has a temperature of around 50 – 60 °C and contains fine cuts of fibers and other impurities from the paper web. The condensate can be purified and reused to minimise the overall water consumption of the mill.

The humidity of the air in the dryer section hood must be kept sufficiently low to prevent condensation on the inside surfaces of the hood. Condensation would mean a risk of water dropping down to the paper web and deteriorating the paper quality. In a conventional cylinder dryer the air humidity is kept below 160 – 180 g H_2O/kg d.a., at an air temperature of 80 – 85 °C. In an impingement dryer the humidity can be considerably higher, from 250 to 300 g H_2O/kg d.a., due to a much higher air temperature, 250 – 350 °C, and a closed circulation of the impingement air (Sundqvist, 2000).

Figure 4.1. Heat Recovery Tower.

A heat recovery tower is shown in Fig. 4.1. A schematic drawing of the tower is shown in Fig. 4.2. The tower is built with the under-pressure arrangement.

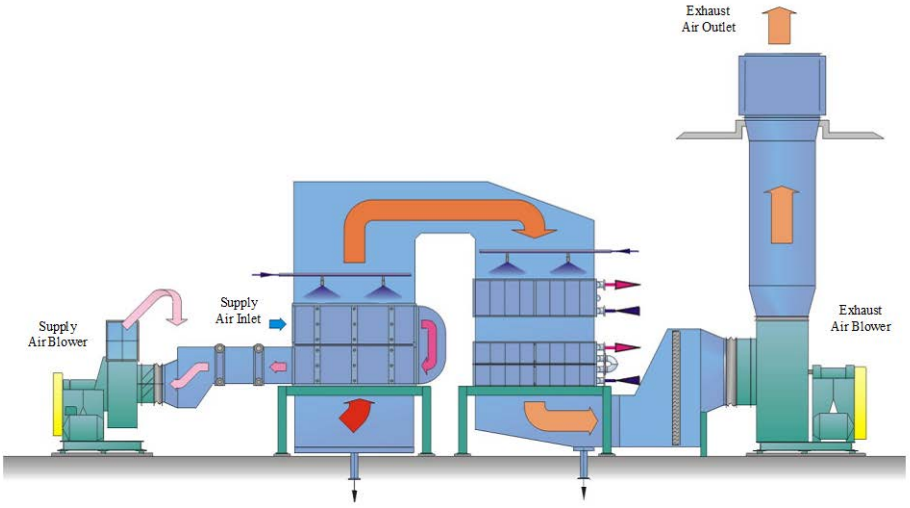

Figure 4.2 Heat recovery tower with under-pressure arrangement. (Metso Air Systems)

The supply air to the dryer section is drawn from the machine hall and heated first in an air-to-air heat exchanger. After that the air is heated further by steam to reach the target temperature, 90 - 95 °C, before it is blown into the dryer section.

The exhaust air from the dryer section is drawn through the tower with the exhaust air blower, placed after the heat exchangers. The first exchanger is the above mentioned air-to-air heat exchanger in the ascending part of the tower, and two air-to-water heat exchangers in the descending part. Above the exchanger units efficient spray nozzles are installed for washing of the exchanger surfaces. Sprays are used for a short moment at selected washing intervals. The wash water is mixed with the condensate at the tower bottom.

In a tower with the over-pressure arrangement the exhaust air blower is placed before the heat exchangers. Considerably smaller equipment for noise attenuation is needed than in an under-pressure tower, due to the attenuation effect of the exchanger units.

A schematic flow diagram of a heat recovery tower is shown in Fig. 4.3. Exhaust air is utilised first to heat the dryer hood supply air, then to heat the circulation water for the heaters of the machine hall ventilation air. In colder climates, the machine hall ventilation air must be warmed and a risk of freezing the circulation water exists, so the water contains usually around 10 % of glycol.

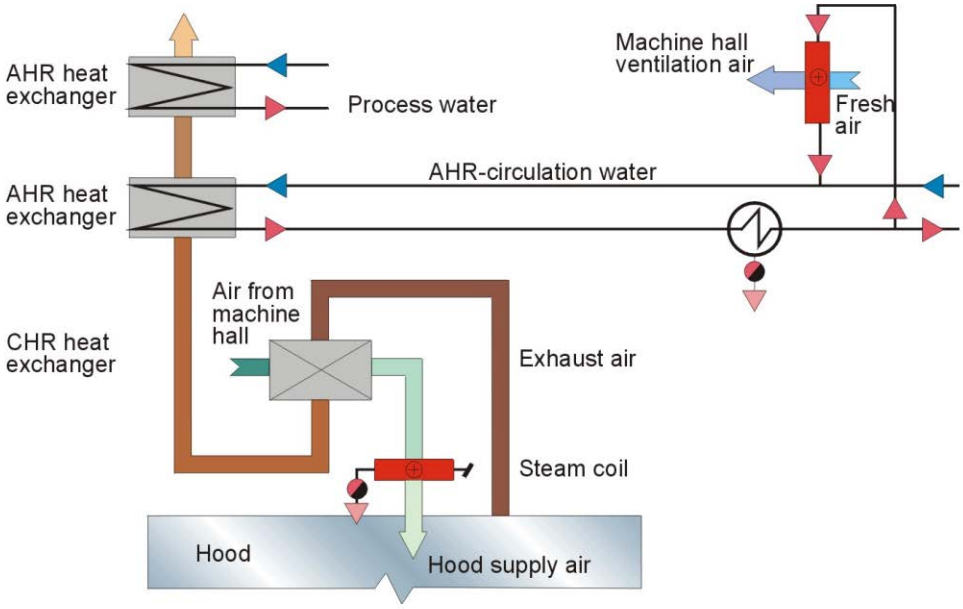

Figure 4.3. Flow diagram of a heat recovery tower. (Metso Air Systems)

An example of a heat flow Sankey-diagram of a paper machine dryer section is shown in Fig. 4.4. The paper machine has a production capacity of 300 000 ton/year paper. The heat flow with the exhaust air out from the dryer section is about 42 MW. Around 3 MW is recovered into the supply air and about 24 MW into different water streams. Finally, low temperature air with approximately 15 MW is discharged.

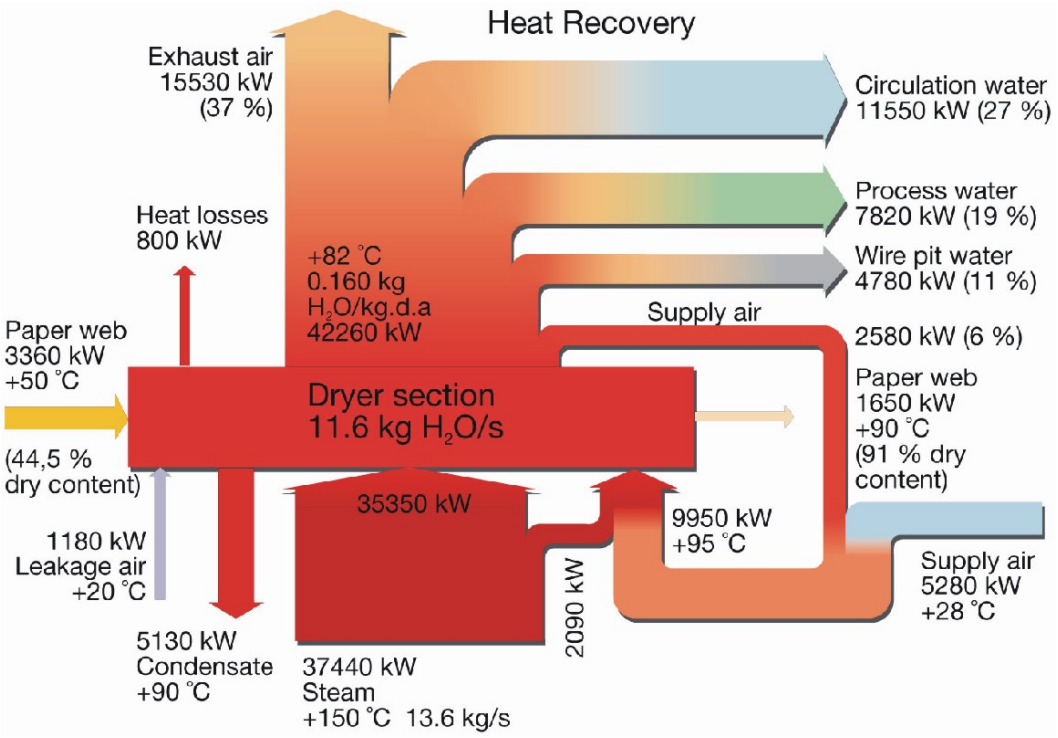

Figure 4.4. Example of a Sankey-diagram of heat flows at a paper machine dryer section. (Metso Air Systems)

The heat demand and recovery are strongly dependent on the outdoor air temperatures at the mill site and the incoming water temperatures. An example of the annual duration curves of the outdoor air temperature together with the heat loads for a heat recovery system and the steam consumption at a Nordic mill site are shown in Fig. 4.5.

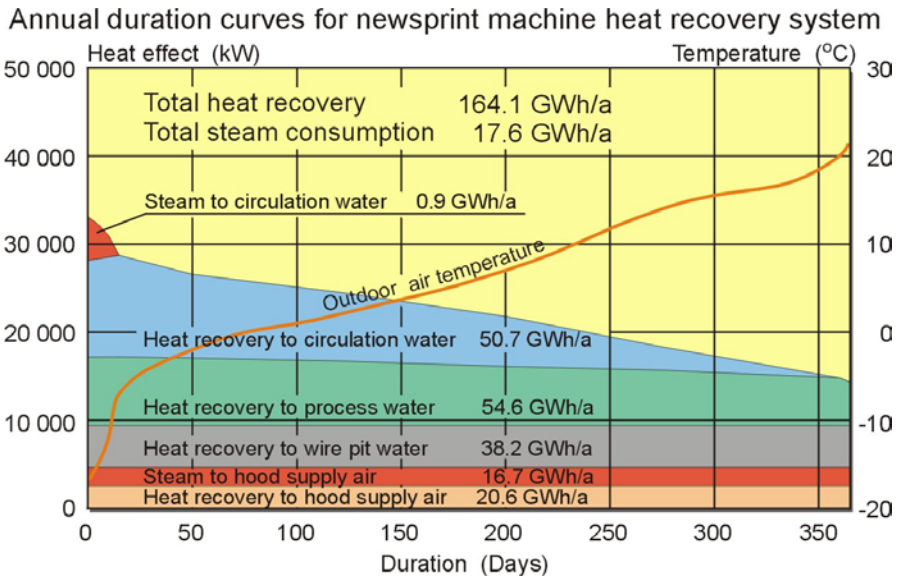

Figure 4.5. Example of annual duration curves for the outdoor air temperature and the heat loads for a heat recovery system at a paper mill site. (Metso Air Systems)

The heat recovery into the circulation water (for warming the mill's premises) varies strongly during a year, while heat recovery to other streams remains fairly constant. Steam is needed all the year for heating of the supply air and on the coldest days also for heating the circulation water. HRS is sufficient throughout the year for all other heating purposes that are included.

4.3 Heat exchanger networks synthesis

Heat exchanger network synthesis problems are often modelled with both discrete variables and non-linear objective function and constraints. This means that they must be solved with methods applicable for mixed-integer nonlinear programming (MINLP) problems. If, on the other hand, the objective function and the constraints can be expressed linearly the problem can be solved by methods for mixed integer linear programming (MILP) problems.

Heat Exchanger Network (HEN) synthesis has been discussed in a very large number of papers. Comprehensive reviews of the HEN synthesis are given by Gundersen and Naess (1988), Biegler et al. (1997) and Furman and Sahinidis (2001). Here, some papers are referred to that have their focus relevant to the present work.

An early approach to the HEN Synthesis is presented by Kesler and Parker (1969). In their model, heat of both hot and cold streams is partitioned into a number of equal sized heat units. The hot stream heat units are transferred either individually or in combination with adjacent units to the same number of cold stream heat units at lower temperatures. The problem is solved as an assignment problem. The model is illustrated in Fig. 4.6 with two hot and two cold streams. The heat flows, the heat units and the obtained solution are shown in the figure.

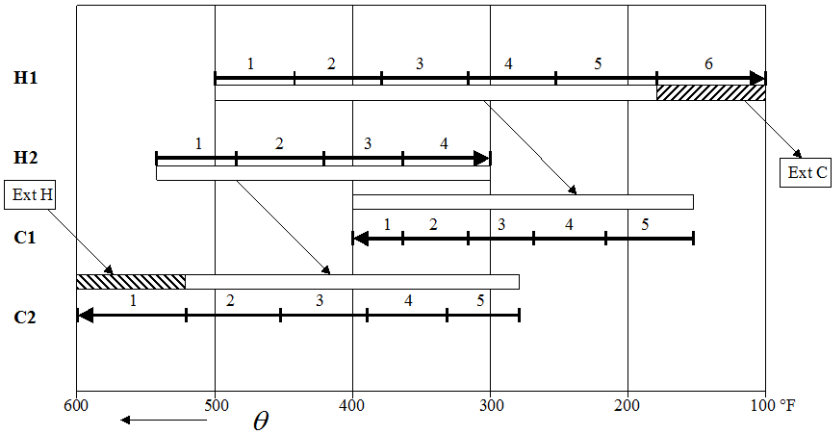

Figure 4.6. Solution of a HEN synthesis sample problem of Kesler and Parker (1969) with two hot and two cold streams. Heat flows are partitioned in equal size heat units.

Heat transfer matches in Fig. 4.6 are obtained between H1 and C1 and between H2 and C2. The last heat unit of H1 is cooled by a cold utility (Ext C) and the first unit of C2 is heated with a hot utility (Ext H).

Lee et al. (1970) introduced the branch and bound method to HEN synthesis. Later, Pho and Lapidus (1973a, 1973b) proposed a procedure with a decision tree, which becomes, however, very large in realistic problems. In the papers by Cerda and Westerberg (1979) and by Mason and Linnhoff (1979) a transportation model was applied for determining the minimum utility demand. In the paper by Cerda et al. (1983) the approaches from the two papers were merged and extended. The overall temperature range was partitioned into temperature intervals. No a priori defined heat transfer units were required. The model was further developed by Cerda and Westerberg (1983).

Papoulias and Grossmann (1983) proposed a transhipment model for targeting the utility costs and the number of heat exchanger units. Heat is shipped from hot streams (sources) to cold streams (destinations) through intermediate temperature intervals (warehouses). Heat flows from hot streams to a temperature interval and then to cold streams in the same interval or as a residual heat to the next lower interval. One temperature interval is shown in Fig. 4.7.

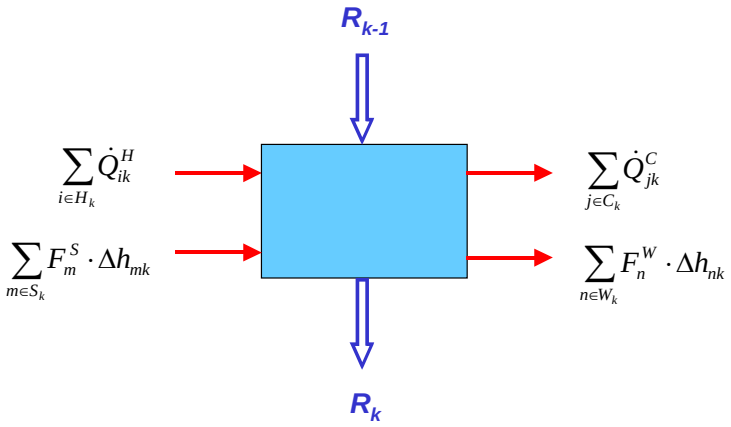

Figure 4.7. A temperature interval in the transhipment model of Papoulias and Grossmann, (1983).

The partitioning of the overall temperature range into temperature intervals is made with a chosen difference, the minimum heat recovery approach temperature (HRAT) for the heat exchange between the hot and cold side temperatures. HRAT determines the required heat transfer areas in the intervals.

The model comprises two sequential problems, the minimum utility cost problem and the minimum number of heat exchanger units problem. The minimum utility cost problem is formulated as a linear programming (LP) problem. No binary variables are used at this phase. The minimum number of heat exchanger units problem uses the solution from the minimum utility cost problem. The utility flow rates are then known. The problem is an MILP problem, partitioned in sub-networks at each pinch point. The temperature intervals are formed in each sub-network, applying binary variables to define the existence of heat transfer matches in the sub-networks between the hot and cold streams.

Floudas et al. (1986) extended the two step model of Papoulias and Grossmann (1983) with a third step, the minimum investment cost step. For this step a superstructure was built and a nonlinear programming problem (NLP) was formulated. For each stream in the problem a separate superstructure is defined. The stream superstructures are then combined into an overall system superstructure. A stream superstructure is shown in Fig. 4.8 for a cold stream that can be matched with three hot streams.

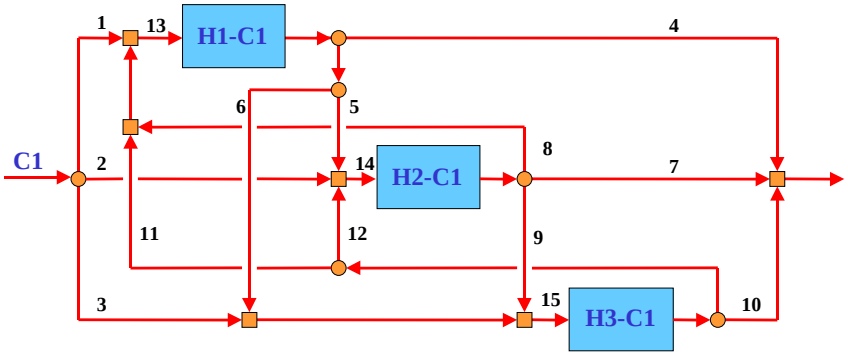

Figure 4.8. Superstructure of a cold stream with matches to three hot streams, Floudas et al. (1986).

An important feature of the applied model is that its superstructures will always include a solution of the minimum unit problem, obtained by the MILP-transhipment model. The problem will thus always have a feasible solution. The heat balances in the model contain bilinear terms, namely multiplications of heat capacity flows and temperatures. This makes the problem non-convex.

A sequential targeting and optimisation approach has the advantage of decomposing a synthesis problem into smaller sub-problems so that they are easier to solve. The disadvantage is that the trade-offs between heat loads, number of units and heat transfer areas are not taken into account rigorously.

A sequential problem can be defined as (Floudas, 1986)

$$\left\{ \begin{array}{l} \text{minimise area costs} \\ \quad \text{s.t.} \quad \text{minimise number of units} \\ \quad\quad \text{s.t.} \quad \text{minimum utility costs} \end{array} \right\} \qquad (4.1)$$

A simultaneous optimisation model can take into account all the costs in the same run. The respective simultaneous problem can be defined as

$$\min \text{Total costs} = \text{Area Costs} + \text{Fixed Cost of Units} + \text{Utility Costs} \qquad (4.2)$$

The sequential formulation is an approximation of the simultaneous formulation. Depending on the problem and the unit costs involved, the solution of a sequential problem can be the same as or very different from the solution of the respective simultaneous problem.

Floudas and Ciric (1989) developed an MINLP model to simultaneously optimise a set of process streams and a network topology for a fixed level of heat recovery. The formulation is based on the similar superstructures as in Floudas et al. (1986).

Yee and Grossmann (1990) presented a simultaneous HEN synthesis model, called SYNHEAT model. The proposed approach includes a superstructure of HEN containing a number of stages for the heat transfer between the hot and cold streams. Both parallel-coupled alternatives with stream splits and series-coupled alternatives are included in the superstructure. A superstructure comprising two hot streams, two cold streams and two stages is shown in Fig. 4.9.

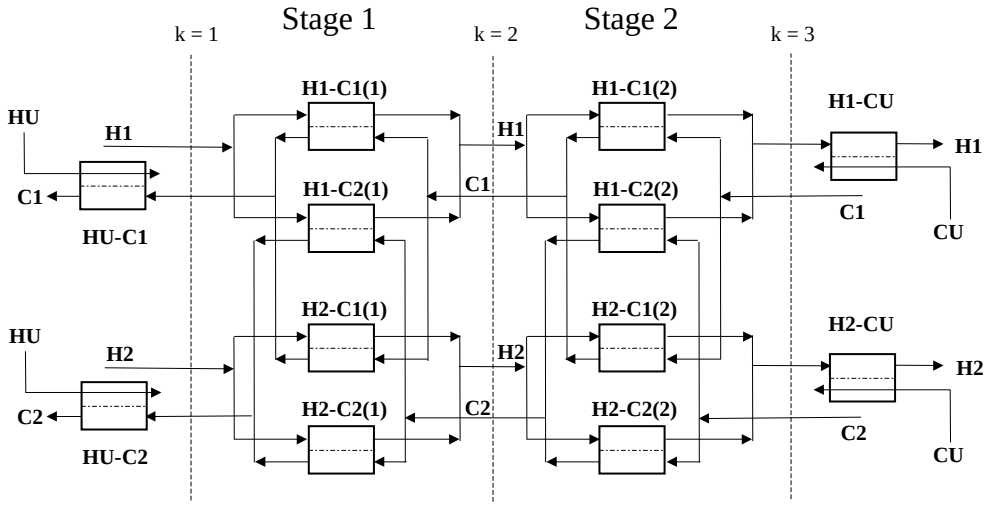

Figure 4.9. Superstructure for a HEN problem by Yee-Grossmann, (1990).

In Fig. 4.9 two stages with three boundaries, denoted by *k*, are defined. Cooling by a cold utility can only take place after the last stage and heating by a hot utility only before the first stage. The objective is to find the network that shows the lowest annual cost, i.e. the sum of the annual utility costs and annualised investment costs.

Overall heat balances for hot and cold streams are built with constant heat capacity flow rates. Heat balances for each stage are built in a similar manner, using stage-wise temperature differences. Binary variables are included in the existence constraints.

The concept of isothermal mixing is applied in the model in order to make the constraints linear. The isothermal mixing is, however, seldom realistic in practical design work.

Ciric and Floudas (1991) presented a four-step approach for simultaneous HEN synthesis problems. The first step is to choose either strict pinch synthesis or a pseudo-pinch synthesis. In the strict pinch synthesis, two independent sub networks are created with partitioning the system at the pinch point, whereas in the pseudo-pinch problem heat is allowed to cross the pinch point and only one network is created.

The second step is to define the utility consumption. For a pseudo-pinch problem, the hot and cold utility consumption can be treated as independent variables, whereas in a strict

pinch problem the utility levels must be determined as a function of the heat recovery approach temperature, HRAT.

In the third step an MINLP problem applying the hyperstructure of Floudas and Ciric (1989) and the transhipment model of Papoulias and Grossmann (1983) is solved. The final step is to solve the MINLP problem with Generalised Benders Decomposition. The authors pointed out that the model involves a nonlinear, non-convex objective function and contains nonlinear, non-convex constraints. A number of local optima may exist and the global optimum may not be found.

Daichendt and Grossmann (1994) proposed a preliminary screening procedure for the SYNHEAT model of Yee and Grossmann (1990). The transhipment model of Papoulias and Grossmann (1983) was utilised as a pre-screener. The number of alternative structures could be reduced by the pre-screening techniques and thus reduce the overall computation time. The pinch technology was used to create a superstructure as an upper bound on the number of units for the SYNHEAT model.

In the work of Galli and Cerdá (1998) the simultaneous algorithmic methods of Yee and Grossmann, 1990; Ciric and Floudas, 1991 and Daichendt and Grossmann, 1994 were criticised for all having a major disadvantage of the passive role of the design engineer. They proposed a designer-driven HEN synthesis approach, where the designer can give topology restrictions before solving the problem. In this way the number of binary variables can be reduced and the computational times be shortened. Heat transfer areas and the costs of equipment (exchangers, piping, splitters etc.) were not included in the model. The concept of pseudo-pinch of Trivedi et al. (1989) was utilised. By relaxing the pinch rule, so that heat can cross the pinch point, better networks were obtained. In a later paper, Galli and Cerdá (2000) presented a revised model where standard sizes of the heat exchangers were included.

In the paper of Shetna et al. (2000) an MILP approach with transportation formulation was presented for HEN synthesis with temperature intervals, instead of fixed $\Delta T_{\min}$. Two linear relations were applied, the specific heat capacity vs. temperature and the heat transfer coefficient vs. temperature. A large industrial heat exchanger network was treated as an example. Some of the streams had temperature-dependent specific heats, while the heat transfer coefficients were the same for all the streams.

Barbaro and Bagajewicz (2005, with Corrigendum 2006) proposed an approach for heat exchanger network synthesis based on temperature intervals. The model allows non-isothermal mixing and several exchangers for the same match. Linear costs are applied and constant values for heat transfer coefficients, the same on both sides of the heat exchangers are used. The specific heat capacity is taken as constant in all presented examples.

Pettersson (2005) formulated a general MILP transportation problem that is modified to reduce sequentially the number of possible matches until a chosen number of allowed matches are included in the problem. A further step, grouping, is applied to reduce the search space. The obtained subgroups are designed separately and combined for the final design.

4.4 HEN synthesis using thermodynamics and heuristic rules

Heuristic rules were introduced in HEN synthesis by Masso and Rudd (1969), one of the first reported attempts to systematically solve a HEN synthesis problem. Hohmann (1971) proposed a feasibility table as a rigorous way to establish the minimum utility target ahead of design. Hohmann also defined a feasible solution space in the area vs. energy diagram.

The idea of defining a bottleneck in the temperature vs. energy diagram of hot and cold composite curves was introduced by Huang and Elshout (1976). The authors placed hot and cold composite curves in the heat availability diagram so that the curves were touching each other at one point. The diagram then showed the limit of how much heat can be transferred between the hot and cold streams. Umeda et al. (1978) called the touching point of the two composite curves the *pinch point* and discussed the influence of the minimum approach temperature on the heat transfer areas. Linnhoff and Flower (1978) presented a systematic procedure for generation of energy optimal heat exchanger networks. The authors called the procedure the Problem Table Algorithm. Later, these ideas were developed into the pinch technology as presented, for example, in the paper by Linnhoff and Hindmarsh (1983) and in a state-of-the-art review by Linnhoff (1993).

One of the basic rules of the pinch technology is that heat must not cross the pinch-point. However, this rule has been shown by several authors not to lead to optimal solutions. Instead of the strict pinch rule, formation of a pseudo-pinch boundary was proposed by Trivedi et al. (1989). Two different approach temperatures were defined, the overall heat recovery approach temperature, HRAT, and the minimum exchanger approach temperature (EMAT). By letting EMAT have a smaller value than HRAT the strict pinch rule is relaxed and a pseudo-pinch boundary formed.

5. Introduction to the applied optimisation methods

Two classes of optimisation methods have been used in this work. Deterministic methods strive to solve the problem exactly, while the stochastic methods are searching for the best solution by combining the random choice of solution candidates and the selection of the best fitted candidates from the solution population.

5.1 Deterministic methods

A mathematical programming problem with constraints can be generally formulated as

$$\begin{aligned} &\min_{x} \ f(\mathbf{x}) \\ &\text{s.t.} \\ &\mathbf{h}(\mathbf{x}) = \mathbf{0} \\ &\mathbf{g}(\mathbf{x}) \le \mathbf{0} \\ &\mathbf{x} \ge \mathbf{0}, \ \ \mathbf{x} \in \mathbf{X} \subseteq R^n \end{aligned} \qquad (5.1)$$

The objective function, denoted by $f(\mathbf{x})$, is minimised or maximised, subject to a set of constraints. $\mathbf{x}$ is a vector of variables in the variable set $\mathbf{X}$. The set of equality constraints is denoted by $\mathbf{h}(\mathbf{x})$ and the set of inequality constraints by $\mathbf{g}(\mathbf{x})$. The variables $\mathbf{x}$ are the unknown conditions of the system. They can be either continuous or discrete. If variables from both categories are applied in a problem then the problem is a mixed integer problem. The problem can comprise different parameters that define the unit costs, etc.

LP problems

A linear programming (LP) problem is a problem that has a linear objective function, linear constraints and continuous variables. The Simplex method proposed by Dantzig (1963), and the interior point method by Karmarkar (1984) have, for example, been applied for solving LP problems.

An LP problem can be written in general form as

$$\begin{aligned} &\min_{x} \mathbf{c}_x^T \mathbf{x} \\ &\text{s.t.} \\ &\mathbf{Ax} = \mathbf{d} \\ &\mathbf{Ex} \le \mathbf{k} \\ &\mathbf{x} \ge \mathbf{0} \quad \mathbf{x} \in \mathbf{X} \subseteq R^n \end{aligned} \tag{5.2}$$

The vector **c** denotes the parameters of the vector **x** of the continuous variables. The parameters are for instance different unit costs, when the objective is to minimise the overall costs of the target system. **A** and **E** are the constraint matrices. A constraint matrix has the size $m \times n$, when the number of constraints is m and the number of variables n. The parameter vectors **d** and **k** denote the right-hand-side values of the constraints, i.e. the constant terms.

MILP problems

In mixed-integer linear programming (MILP) problems, only linear constraints and a linear objective function are included. Some of the variables are discrete in the problem formulation (5.3).

The problem can be formulated as

$$\begin{aligned} &\min_{x,y} \left\{ \mathrm{c}_x^T \mathrm{x} + \mathrm{c}_y^T \mathrm{y} \right\} \\ &\text{s.t.} \\ &\mathbf{Ex} + \mathbf{Fy} = \mathbf{k} \\ &\mathbf{Ax} + \mathbf{By} \le \mathbf{d} \\ &\mathbf{x} \ge \mathbf{0} \quad \mathbf{x} \in \mathbf{X} \subseteq R^n \\ &\mathbf{y} = \mathbf{0,1} \quad \mathbf{y} \in \mathbf{Y} \subseteq R^n \end{aligned} \tag{5.3}$$

x denotes a vector of continuous variables, corresponding to mass and heat flow rates, temperatures, heat transfer areas, etc., and **y** denotes a vector of integer variables, often binary variables, that correspond to the existence or non-existence of the different system parts. The discrete variables define the structure of the solution system. The linear objective function is a sum of linear terms, for example different costs. The linear process constraints are given by a set of inequalities and by a set of equations, where **A, B, E** and **F** denote the constraint matrices and $\mathbf{c}_x$, $\mathbf{c}_y$, **d** and **k** parameter vectors.

Land and Doig (1960) proposed a branch and bound method for solving MILP problems. The method is based on the search of continuous solutions where the values of discrete variables eventually are forced to take discrete values. The method is, however, slow and requires rather large computer memory capacity. Dakin (1965) proposed an improved algorithm based on the same search principle. Later, improvements have been proposed

by different authors (e.g. Pardalos and Rosen, 1987). The branch and bound method is today used in most of the commercial solvers for MILP problems.

Another approach, applying of cutting planes, for solving the MILP problems was initially proposed by Gomory (1960). Method improvements have been proposed, e.g., by Crowder et al. (1983).

In the branch and bound method with binary (0,1) variables the enumeration is performed in a systematic way in order to avoid the examination of every binary variable combination. A search tree with the branches on different binary variables is formed. The problem is solved first on the root node with an integer relaxation. Branching is made so that the two discrete values of the variable are taken from both sides of the continuous value of the variable at the root node solution. Two sub-problems are created and solved. With different fathoming criteria of the algorithm the branches that cannot have a better solution value than the incumbent solution are pruned. The global optimal solution is found if there is a feasible solution to the problem. The computation time can be influenced with different search strategies to move in the search tree, like depth-first and breadth-first.

MINLP problems

Process synthesis problems can involve both continuous and discrete variables together with nonlinear constraints and a nonlinear objective function. These problems are solved with methods applicable for mixed-integer nonlinear programming (MINLP) problems.

An MINLP problem is defined by adding the sets of nonlinear equality and inequality constraints, denoted by **h**(**x**,**y**) and **g**(**x**,**y**), into formulation (5.3).

$$
\begin{aligned}
&\min_{x,y} \; f(\mathbf{x},\mathbf{y}) \\
&\text{s.t.} \\
&\mathbf{Ax} + \mathbf{By} \le \mathbf{d} \\
&\mathbf{Ex} + \mathbf{Fy} = \mathbf{k} \\
&\mathbf{h(x,y)} = \mathbf{0} \\
&\mathbf{g(x,y)} \le \mathbf{0} \\
&\mathbf{x} \ge \mathbf{0} \qquad \mathbf{x} \in \mathbf{X} \subseteq R^n \\
&\mathbf{y} = \mathbf{0,1} \quad \mathbf{y} \in \mathbf{Y} \subseteq R^n
\end{aligned}
\tag{5.4}
$$

Different MINLP-methods are reviewed for example in Grossmann (1996). The Outer Approximation (OA) method was introduced by Duran and Grossmann (1986) for the solution of MINLP problems, where the non-linear functions are convex.

Methods to handle the non-convexities were presented by Kocis and Grossmann (1987) as an extension to the OA (OA/ER, ER = Equality Relaxation) and by Viswanathan and

Grossmann (1990) (AP/OA/ER, AP = Augmented Penalty). The AP/OA/ER method has been commercialised and available by the trade name DICOPT++.

The extended cutting plane method (ECP) is another method for solving MINLP problems. It is an extension of the cutting plane method of Kelley (Kelley, 1960). In Kelley's cutting plane method LP sub-problems are solved. In the ECP-method an initial solution is produced first by linearization of the original MINLP problem and used then in solving an MILP sub-problem. In the MILP sub-problem the non-linear constraints are approximated with a set of linear constraints. For convex problems the set is a valid under-estimator. The method requires solving only one MILP sub-problem in every iteration step and has been shown to have global convergence in convex MINLP problems (Westerlund and Pettersson, 1995).

A modification of the ECP method, called α-ECP-method (Westerlund et al. 1998), was applied in Paper III, to the heat exchanger network synthesis problem with concave equipment cost data. The nonlinear objective function was transformed to a linear form as presented in Eq. (6.3.4) in section 6.3. The method guarantees global optimum solutions for convex and pseudo-convex problems.

A retrospective on optimisation is presented in Biegler and Grossmann (2004) and added with a future perspective in Grossmann and Biegler (2004).

5.2 Stochastic methods

From the different available stochastic methods genetic algorithms have been chosen to be applied in this work, and they will next be described briefly.

Genetic Algorithms

Evolutionary programming methods, e.g. Genetic Algorithms (GA), are general stochastic techniques that can deal with large problems without being restricted by non-convexities or discontinuities of the models. GA was initially proposed by Holland (1975), as a biologically inspired optimisation method, where the obtained solution cannot be guaranteed to be the global optimum. However, the genetic algorithms are able to deal with a large set of possible solution candidates and are thus assumed to have good properties in screening for the most promising regions of the feasible search space.

GA is based on the concepts of natural selection and genetics. The conventional steps are

1. Initialisation by constructing a solution population with a number of randomly chosen individuals. Their fitness values for the objective are determined.

2. Selection of the individuals from the population to take part in the production of offspring.

3. Offspring production for example by cross-over.

4. Repeating the procedure until a predetermined stopping criterion is reached, for instance the number of iteration loops.

The structure of an individual is often based on a sequence of binary variables, called genes, but also other sequences have been used successfully. Individuals that are better fitted to the environment, i.e. correspond to better solutions of the optimisation problem at hand, have a higher probability of surviving in the process. Every individual represents a possible solution to the optimisation problem. A fitness value corresponds to the goodness of the solution. The chosen selection mechanism picks individuals from the population in such a way that an individual's chance of being selected increases with its fitness value. Some offspring might suffer a mutation during the process, i.e. their genes, which code the values of the unknown variables of the optimisation problem, are randomly changed by a low probability. Elitism may also be used, i.e. a given number of the most fitted individuals in the previous generation are transferred directly to the new population.

6 Discussion of the included papers

6.1 Paper I

Structural and operational optimisation of distributed energy systems

6.1.1 Problem definition

In a distributed energy system optimisation problem, discussed in Paper I, a geographical region is considered comprising a number of energy plants that supply heat and/or electric power and a number of energy consumers that have given heat and power demands in different time periods.

The objective of the DES optimisation task was defined as the following: in a specific region find the optimal design and locations for both heat and electric power generation plants, the optimal routing for the district heating network pipelines and the optimal locations and design of heat storages, all in accordance with the locations of the heat and power consumers and their variable heat and power demands. An MILP model for the DES problems was developed and the problems were solved by Branch and Bound method. A solution is a global optimum for the defined problem.

The approach comprises

1. Energy supply

For the energy supply different options were included. They were combined heat and power (CHP), thermal boiler plant, supplying only heat, and wind power, supplying only electricity. For each option cost functions for the investment and running costs were established.

The model is not limited to these examples. Other types of conversion technologies can be added in the same manner, like fuel cells, solar heat, photovoltaic power, hydro power, diesel engines, gas turbines, Stirling engines, etc.

A supplier can be situated in the region in a number of predetermined locations. Sites can have any number of the given types of energy units.

The region is considered as self-contained with respect to satisfying the total heating demand. Consumers can purchase electricity from the national main grid or from the local suppliers. The power from the grid is considered to be abundant and purchased with given tariffs that can be different between day and night and between different seasons.

2. Energy consumption

A consumer has defined heat and power demands at different time periods. A consumer can buy the district heat from any of the suppliers or produce its own heat with a heat pump. If a heat pump is installed at a consumer site, additional electric power is required at the site.

3. Energy distribution and storage

The district heating network is modelled with main pipelines and consumer pipelines. Additionally hot water storages are included in the DES model. The distances between supplier and consumer sites are calculated separately prior to the optimisation and used as input data. For district heating, the main pipeline routing is given.

The included energy technologies and the costs are presented in Söderman et al., (2005). Investment costs were formed for the included equipment as linear price functions with a fixed part and a size-dependent part multiplied by an annuity factor. The principle of linear costs is shown in Fig 6.1.1. For the included equipment suitable application ranges were chosen.

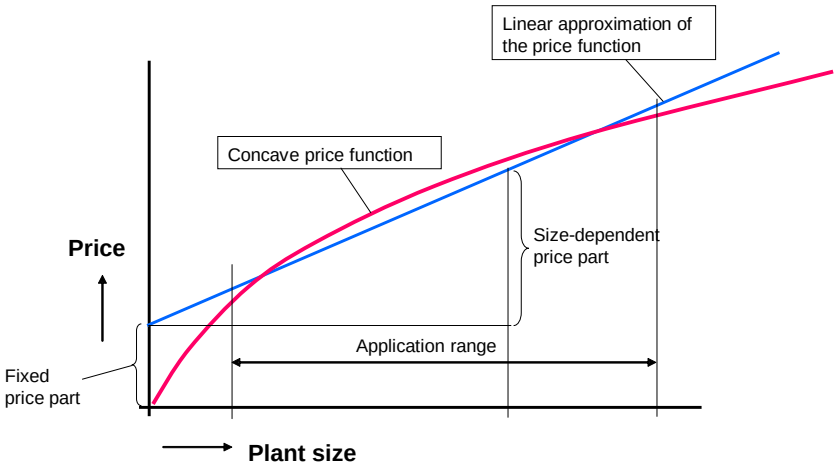

Figure 6.1.1. Formation of linear investment prices from concave price functions.

The costs in a DES optimisation problem include the heat and power supplier equipment and running costs, district heating network investment and running costs and the costs for heat storage tanks. The distances between supplier and consumer sites and a district heating main line routing are defined prior to the optimisation and used as input data.

6.1.2 MILP model

The model formulations are presented in paper I. The main features of DES were presented in section 2.

Objective Function

The objective in a DES problem is to minimise the total cost, denoted by C_{DES}. It is the sum of running and investment costs, denoted by $C_{Oper,DES}$ and $C_{Inv,DES}$:

$$\min \quad \left\{ \quad C_{DES} = C_{Oper,DES} + C_{Inv,DES} \quad \right\} \tag{6.1.1}$$

Investment costs are calculated with different annuity factors, depending of the type of equipment or pipeline. The equipment prices are modelled linear with a fixed part of the investment costs multiplied by a binary variable, getting value 1 at the existence and 0 at the non-existence of the equipment. The size-dependent part is modelled directly proportional to the capacity of the equipment.

Running costs are calculated with cumulative thermal or electrical energy for each period and for each production unit and pipeline part multiplied by a unit operational cost factor.

Consumer heat demand

The heat flow to a consumer is the sum of direct heat flow from supplier to consumer, added by the heat flow from storage to the consumer, the heat flow from main lines and the consumer's own heat production at the site.

The heat flow to a consumer *Cm* at period *p*, denoted by $\dot{Q}_{Cm,p}$, is

$$\dot{Q}_{Cm,p} = \sum_{i=1}^{n_S} \dot{Q}_{Si,Cm,p} + \sum_{k=1}^{n_R} \dot{Q}_{Rk,Cm,p} + \sum_{j=1}^{n_L} \dot{Q}_{Lj,Cm,p} + \dot{Q}_{Om,p} \quad \forall \ m \in M, \ p \in P \tag{6.1.2}$$

$\dot{Q}_{Si,Cm,p}$ is the direct heat flow from supplier *Si* to consumer *Cm*, $\dot{Q}_{Rk,Cm,p}$ is the heat flow from storage *Rk* to the consumer, $\dot{Q}_{Lj,Cm,p}$ is the heat flow from district heating line part *Lj* to the consumer and $\dot{Q}_{Om,p}$ is the consumer's own heat production at the site.

Supplier heat delivery

The heat flow from a supplier at period *p* is the direct heat flow from the supplier to the consumers, added by the heat flow to the storages and to the district heating main line

The heat flow from a supplier *Si* at period *p*, denoted by $\dot{Q}_{Si,p}$, is

$$\dot{Q}_{Si,p} = \sum_{m=1}^{n_C} \dot{Q}_{Si,Cm,p} + \sum_{k=1}^{n_R} \dot{Q}_{Si,Rk,p} + \sum_{j=1}^{n_L} \dot{Q}_{Si,Lj,p} \quad \forall \quad i \in I, \quad p \in P \tag{6.1.3}$$

$\dot{Q}_{Si,Cm,p}$ is the direct heat flow from supplier *Si* to consumer *Cm*, $\dot{Q}_{Si,Rk,p}$ is the heat flow to storage *Rk* and $\dot{Q}_{Si,Lj,p}$ is the heat flow to the district heating line part *Lj*.

District heating network

DH pipeline lengths were calculated prior to the optimisation run for a number of options: lines from the main pipelines to supplier sites, to storage sites and to consumer sites. The shortest distance between the sites and the main pipeline parts were used. Additionally, individual pipelines from any supplier or storage site to any consumer as well as from any supplier site to any storage site were calculated.

Line costs can be modelled as a fixed part and a size-dependent part, which can be included as proportional to the flows in the pipelines. In the same way the pumping costs were included as proportional to the flow rates in the pipelines.

Heat storages

Heat flow into and out from a storage are defined from the supplier and consumer heat flows. Input and output flows must not be equal, as the heat content in the storage can vary. Heat input and output flows must, however, be connected in such a way that a continuous system is obtained. In the illustrative example (cf. Subsection 6.1.3) the storage heat content is defined to be the same after a day- and night-period in each season.

Consumer power demand

The power demand of a consumer is the sum of the basic power demand and the possible additional power consumption due to a heat pump at the consumer site. Power consumption of a heat pump and the heat production are linked together by a COP number, which depends on the construction, working fluids and the prevailing temperatures at the heat pump.

Main grid

A consumer has a basic electricity demand. Electricity can be produced locally within the district or bought from the national grid. Different prices for the power at day- and night-time and in different seasons can be used. The main grid is considered as an abundant source of electricity at given tariffs that may vary at different periods.

Existence constraints

Existence constraints of production units, storage units and DHN pipeline parts were defined by binary variables, with sufficiently large numbers.

For instance, existence of different types of heat and power production units at a supplier site was defined by the constraints as below for CHP plants

$$\dot{Q}_{Si,CHP} + P_{Si,CHP} - U_{CHP} \cdot y_{Si,CHP} \leq 0 \quad \forall \quad i \in I \tag{6.1.4}$$

where $\dot{Q}_{Si,CHP}$ is the heat generation at the CHP plant, $P_{Si,CHP}$ the power generation, U_{CHP} a sufficiently large number calculated from the regional heat and power demands

and $y_{Si,CHP}$ a binary variable, with value 1, if a CHP plant is built at the supplier site *Si* or 0, if a CHP plant is not built at the site.

6.1.3 Illustrative example

Problem size

The illustrative example in Paper I included three types of energy units, five site options, three heat storage site options and 12 consumer sites. Consumer heat and power demands were defined for 8 periods. A period represents the day time or the night time of a season. The model included 225 binary variables and 3000 constraints.

Solutions

The solutions of a DES optimisation problem show the sites where the energy plants and storages are built as well as the routing of the district heating pipelines. It also gives the design parameters of the included equipment. Finally, when a multi-period approach is used the solution gives also the operational parameters, the heat or power capacities of the plants, the water flows in the pipelines and the electricity transmissions in the district network in different periods.

The solution of the example shows, for instance, that the district power demand can be satisfied optimally by combining the locally produced power from the small scale CHP plants and the power from the national grid. The local power supply and purchased power are shown in different periods in Fig. 6.1.2.

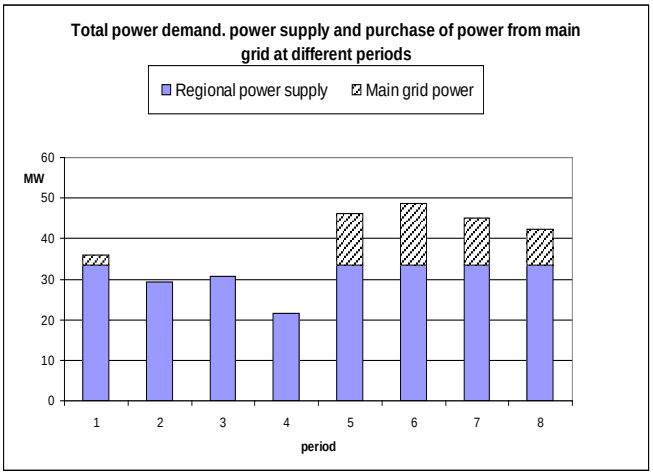

Figure 6.1.2. Total power demand with regional power supplies and purchased power from the national grid.

6.2 Paper II

Optimisation of district cooling networks in urban regions

An MILP model that was developed for optimisation of district cooling (DC) network is discussed in Paper II. The approach is similar to the one in Paper I, but the number of consumers is increased. This became possible without an increase of the calculation time because only one option for the energy generation was included instead of three in Paper I.

The objective was to study optimisation of the district cooling systems in regions with the focus on energy efficiency and the overall economy of the system. Additionally, cold water storage was included for the district cooling networks in order to have the option to balance the operation of the cooling plants at different cooling demand situations.

The obtained solutions are good starting points for the design of a DC network for a new region or in expanding or retrofitting existing district cooling networks. In the tested case the model gave realistic solutions.

The illustrative case was an urban region with a consumption data for the year 2006 and a prediction to year 2020.

Problem definition

A district cooling system (DCS) comprises generation and demand of cooling effect, transport of cold water in the DC pipelines and storage of cold water. The obtained solutions show the DCS structure as well as the operational parameters. The structure data in the solution comprises the equipment design parameters and equipment locations, i.e., the production units, distribution pipelines and cold media storages that shall be built and the dimensions of this equipment. The operational data of the solution specifies, e.g., what the flows of cold water in the pipelines are and how the cooling plants and storages shall be run in different periods of the year.

The cooling plants cool the circulating water in the district cooling network from return water temperature to feed water temperature, for instance from 16 °C to 6 °C. The storages store the circulation water during low consumption hours and supply the water into the network during high consumption hours.

Consumers have two options to get the cooling effect: either from an own cooling unit/plant or from the generation plants. Own cooling plant means an investment cost and operational costs. Electric power for the cooling machines is taken from the grid.

The district cooling main pipeline routing options are given prior to the optimisation. The lines are underground double pipelines comprising a feed line and a return line, Fig. 6.2.1.

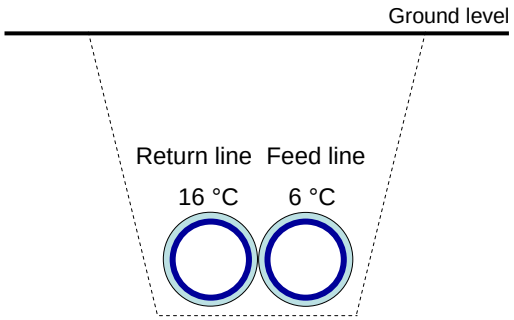

Figure 6.2.1. District cooling pipelines.

The cooling demand is strongly dependent on the season and on the time at a day. At summer day time peak demand is reached during the afternoon hours.

A set of periods is therefore included in the model, similarly as described earlier in section 6.1. for district heating.

The cooling effect can be transferred from a cooling plant to a consumer either directly or via DC main pipelines. The cooling effect can similarly be transferred from a cooling plant to a storage directly or via the main pipelines.

Objective function

The objective of a DCS optimisation problem is to minimise the overall cost of DCS. The cost is defined as the sum of the running costs of the included operations and the annualised investment costs of the included equipment.

Equipment investment prices are modelled with fixed price parts and size-dependent price parts, as described earlier in section 6.1. The investment costs are calculated from the equipment prices by utilising the annuity method. Different annuity factors can be used for different equipment. The overall investment cost is the sum of all the included equipment, the cooling plants and storages, the pipelines and the consumer cooling equipment.

Similarly, the sum of the running costs of the cooling plants and storages, the pipelines and the consumer cooling equipment is calculated in each period and the annual running

costs are the sum of the costs of the periods. Running costs are defined linearly proportional to the generated, stored, consumed or distributed cooling effect.

Illustrative Case

An urban region with cooling demands for the 2006 situation and predicted future situation for the year 2020 was studied.

District Cooling System with 2006 data

The locations of the consumers, possible sites for cooling plants and cold water storages and DC network mainline routes are shown in Fig. 6.2.2. for the 2006 situation. Coordinates are given in kilometres.

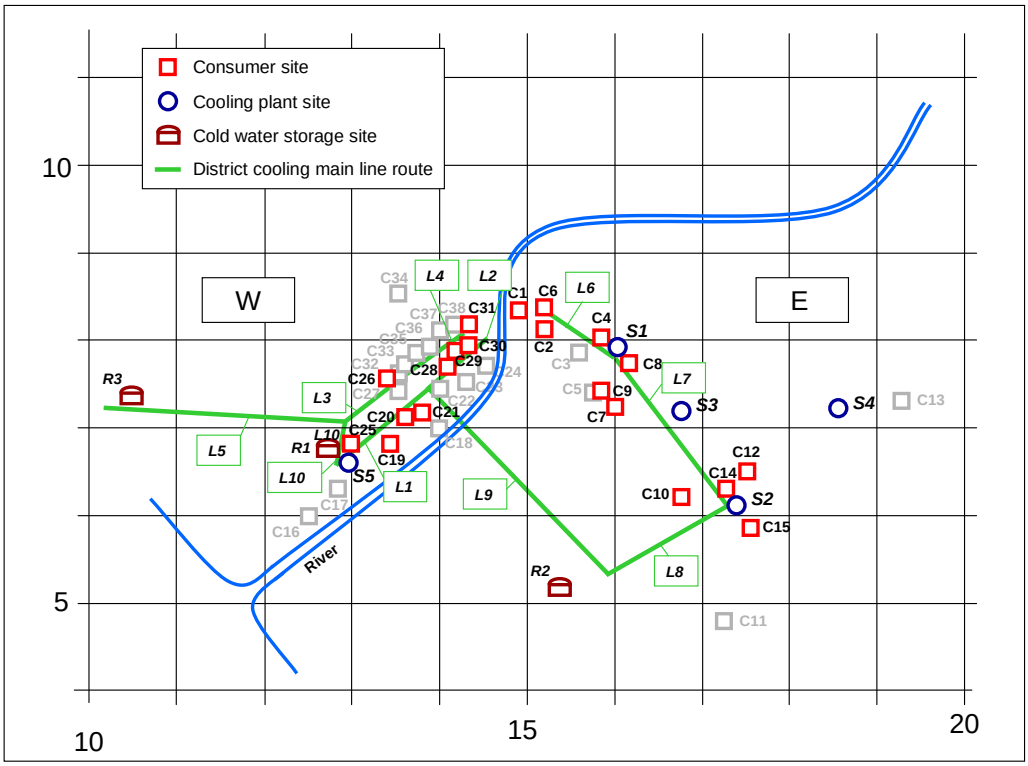

Figure 6.2.2. Locations of the consumers, options for cooling plant and storage sites and DC network mainline routes at 2006. The squares denote consumer sites, the circles optional cooling plant sites, the tanks cold water storage tanks and the lines district cooling main line route options.

In 2006 there are 20 consumers with a peak cooling demand of 11785 kW(th) at a summer day (period 3). The obtained optimal system structure is shown in the map, in Fig. 6.2.3. Black lines show the pipelines that are included in the system and weak grey lines the mainline routes that are not used. Similarly, cooling plants and storages that are included in the system are shown with black and the sites that are not used with grey.

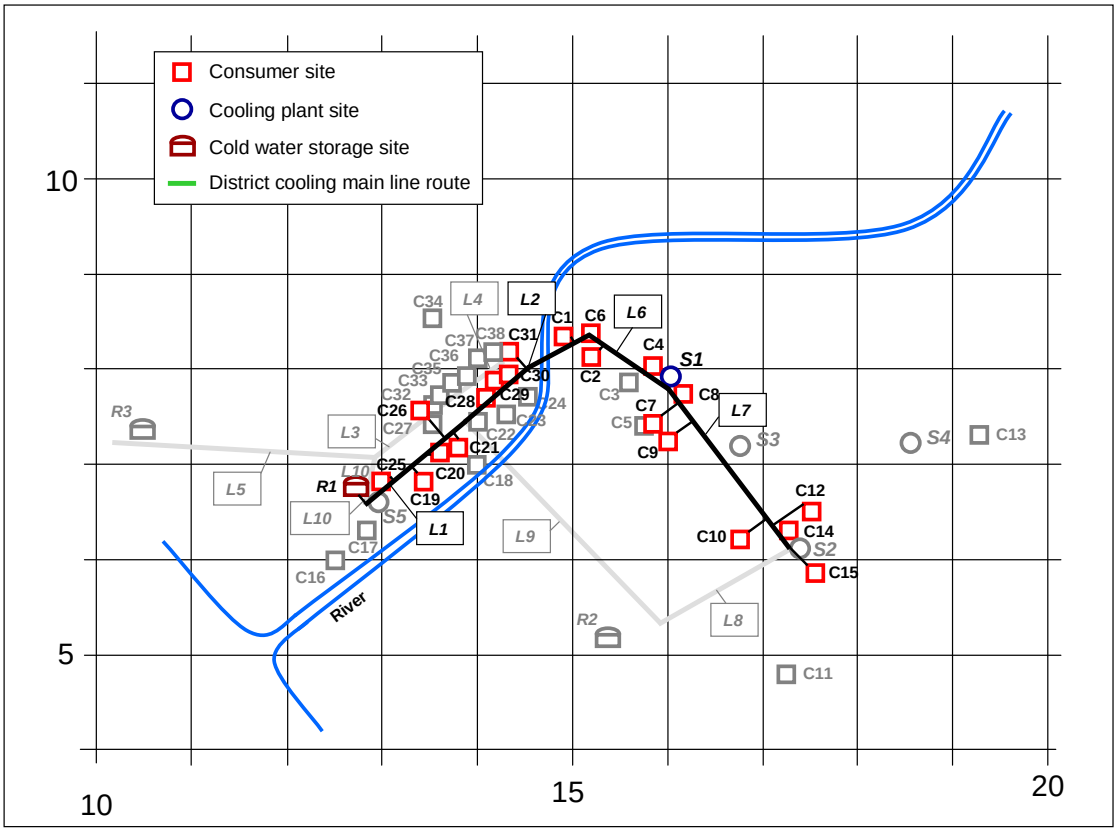

Figure 6.2.3. Solution for the year 2006. System parts that are grey coloured are excluded from the solution.

The optimal system structure comprises one generation plant (at site S1). Its optimal cooling capacity is 8260 kW(th). This covers, however, only 70 % of the peak demand during a summer day.

The lacking effect, 3525 kW(th) is taken from a cold water storage (at site R1). The storage is discharged during the peak demand hours on summer days and recharged during the following night.

The cooling plant at site S1 is run at its full capacity during both summer days and nights (p3 and p4). In the night time the storage is charged and in the day time it is discharged, Fig.6.2.4.

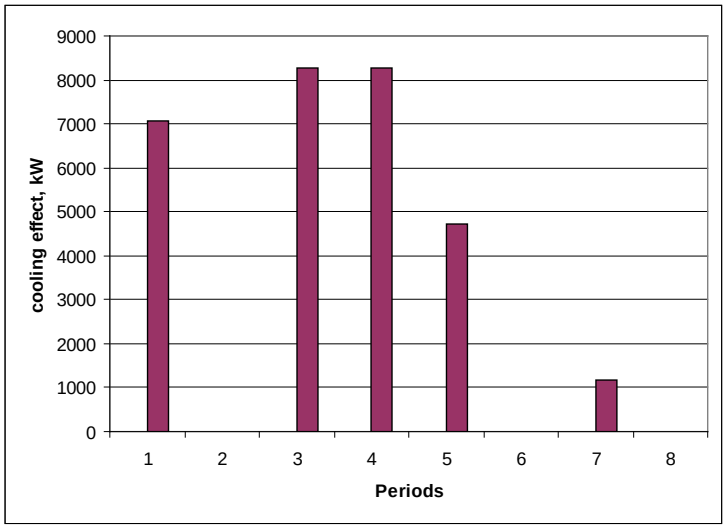

Figure 6.2.4. Operation of the cooling plant in site S1 in different periods.

The solution further shows the needed pipelines and the flow rates of cold water in the pipelines during the different periods.

Water flows are given as their cooling effect in kW(th), Fig. 6.2.5. A cooling effect of 1000 kW(th) equals a water flow of about 24 kg/s, when the temperature difference between the supply water and the return water is 10 °C.

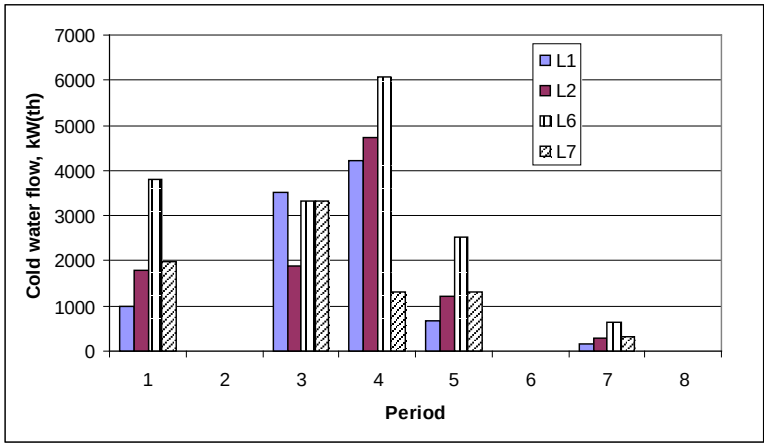

Figure 6.2.5. Cold water flow rates in different periods.

The flow rates are highest during period 4 (summer night). In the night time the water flow direction is from the cooling plant S1 to the storage R1. The cooling plant distributes the cold water into L6 and water is pumped to storage R1 from mainline L1 (cf. Figs 6.2.6 and 6.2.7).

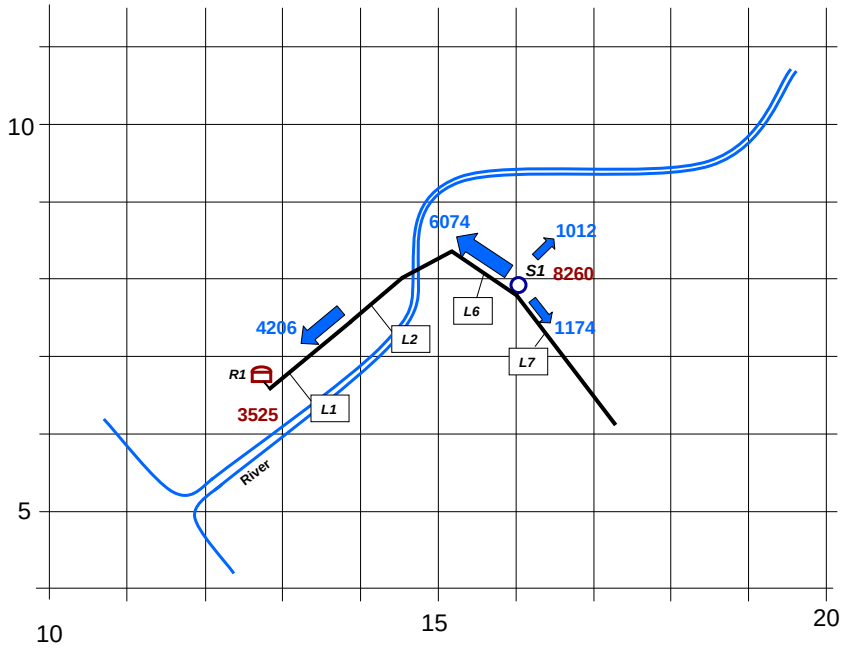

Figure 6.2.6. Cold water flows in different parts of the DC-networks during summer night (period 4). DC-water is pumped to storage tank R1 that is recharged by 3525 kW cooling effect during twelve hours period.

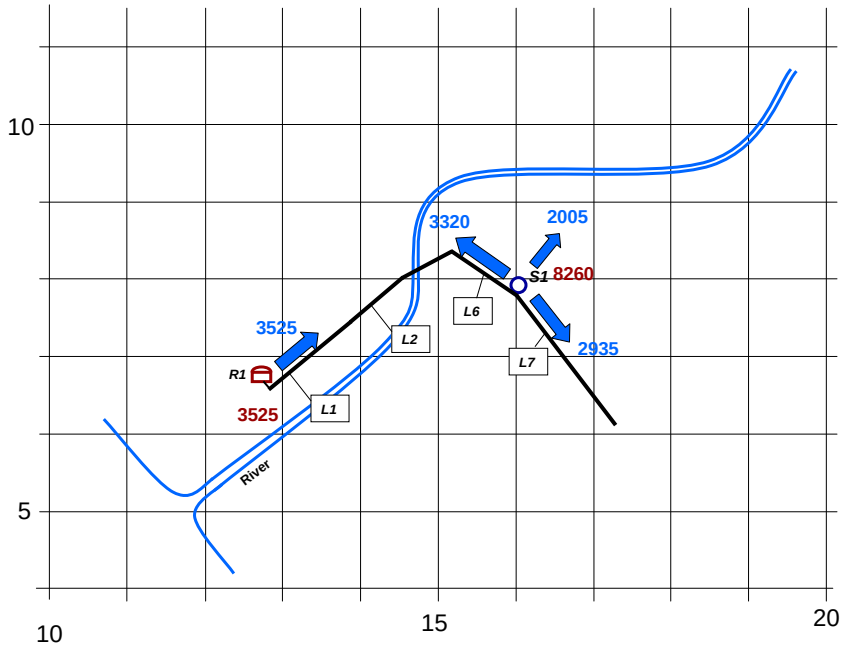

Figure 6.2.7.Cold water flows during summer day (period 3). The storage tank R1 is discharged with 3525 kW cooling effect.

District Cooling System with 2020 data

In addition to the consumers in 2006 new cooling consumers are predicted for 2020 with an important demand increase. The distances from many of these consumer sites to the city centre are relatively long compared to the distances of the consumers in 2006.

53 consumers are included and the predicted total cooling demand is 136 MW(th) in 2020. The consumers are shown on the region map in Fig. 6.2.8.

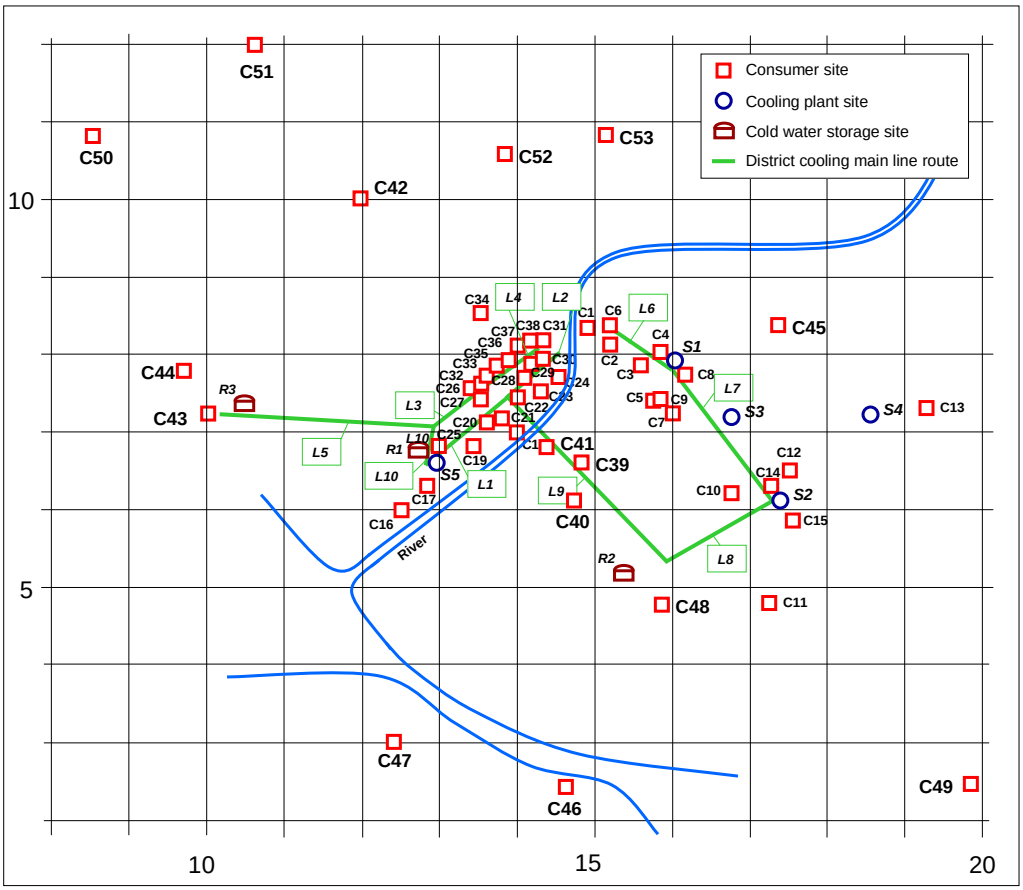

Figure 6.2.8. Locations of the consumers, options for cooling plant and storage sites and DCN mainline routes in 2020.

The obtained solution is shown in Fig. 6.2.9. Now there are two sites, S1 and S5 that shall have a cooling plant. The cooling capacities of the plants are 42.4 MW and 43.1 MW, respectively.

A cold water storage shall be built as earlier on the same site R1. Now the cooling output is 37 MW and the storage volume is 37750 m^3.

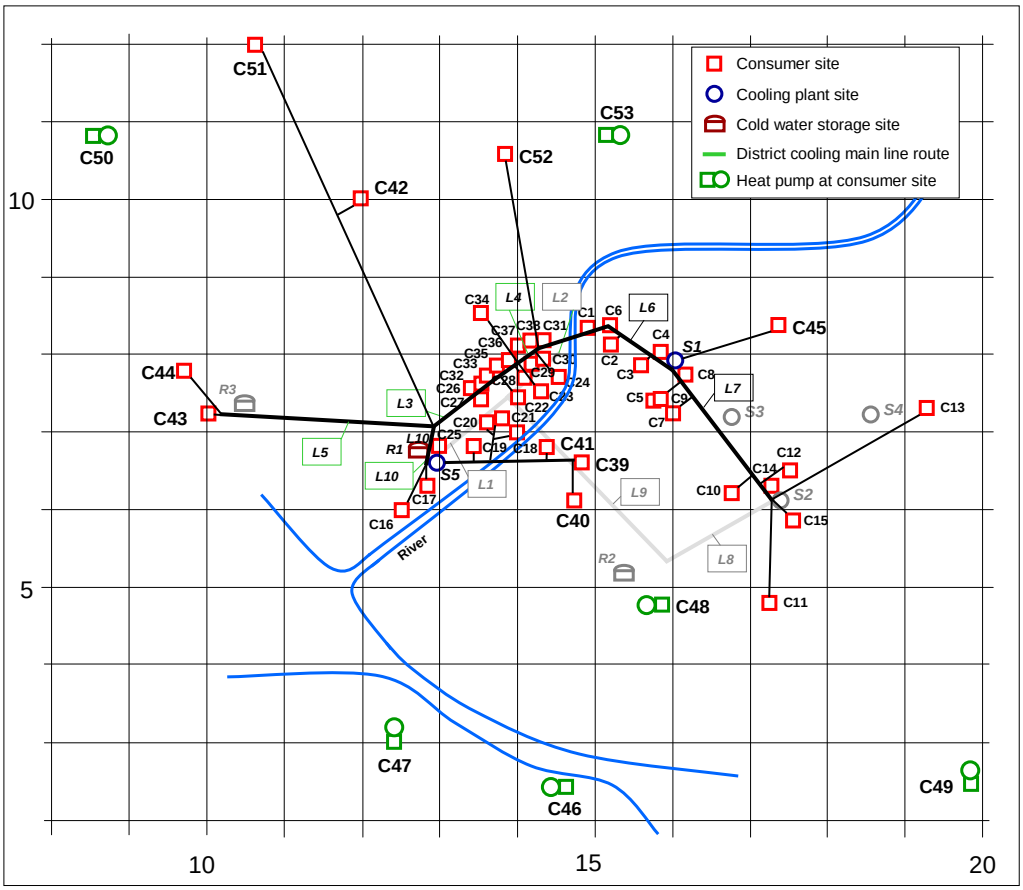

Figure 6.2.9. Solution for the year 2020. A part of regional cooling demand is satisfied with heat pumps at some consumer sites.

The solution for 2020 comprises also consumers that are left out of the network. In their case own cooling machines are more economic than their coupling in the district cooling network. By this way the maximum network capacity is obtained, which in this case is 89.7 % of the total peak demand.

Consumers with own cooling machines are situated relatively far from the city centre. Their machine capacities are together 14 MW or 10.3 % of the total cooling demand in the region. From the remaining demand of about 122 MW the cooling plants in S1 and S5 cover about 70 % and the cooling effect from storage R1 about 30 %.

It can be noted that the consumer C51 is connected to the district cooling network in spite of the long distance to the city centre. This is due to the relatively high cooling demand of the consumer.

The operation of the plants S1 and S5 at different periods is shown in Fig. 6.2.10.

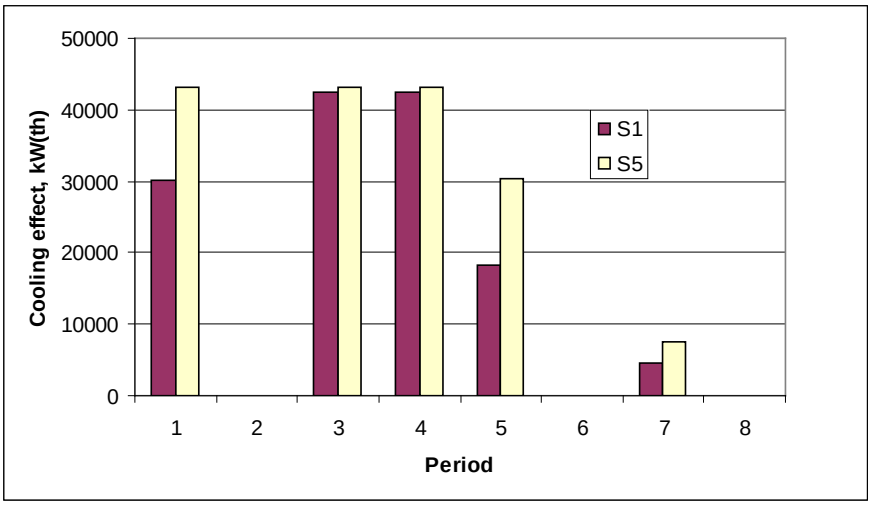

Figure 6.2.10. Cooling effect generation in different periods in 2020 with the cooling generation plants at sites S1 and S5 that are included in the optimal solution.

Solution time

The developed model was tested with several different DCS problem sizes. The number of consumers, generation plant sites, storages and mainline routes were varied. The problems were solved with the CPLEX 9.0 Solver and a 1.4 GHz Pentium M processor. The solution times varied strongly with increased problem size. Table 6.1 shows a number of problem sizes, defined by the number of binary variables in the problem, and the respective solution times.

Table 6.1. Solution time as a function of the number of binary variables in a DCS problem.

Number of binary variables	Solution time sec.
100	0.32
130	0.37
244	0.75
302	1.90
404	3.89
520	8.81
616	37.23
643	439.9
738	547.2
869	1720.3
989	22616.7

The described DCS problem was solved in a very short time as long as the number of binary variables was below 500. Above that the solution time increased considerably. Now also the variations in the solution time with the same number of binaries became considerable. The solution time varied strongly in different solutions, depending on the used price and cost parameters. A certain set of parameters could cause an unpredictedly long solution time. The model was tested with different cost parameters at the size of 643 binary variables, and the solution time was found to vary between 112 and 1518 seconds at this problem size. The mean value of twelve runs was 440 seconds. When the problem size was increased to 1000 binaries the solution time increased to over 6 hours.

To be able to solve large energy network problems in a reasonable time, a procedure for merging different consumers in a region to form combined consumers and by this way reducing the size of the problem was developed. The problem with the year 2020 cooling demand data was solved in approximately 180 seconds by modifying the problem so that the final number of consumers was 25. The procedure seeks to combine the consumers in such a way that the impact of the combination on the overall system is minimised. The developed procedure makes it possible to optimise large district cooling systems.

In the optimisation based on predictions of the future cooling demand, valuable guidance was obtained on how the DC network should be expanded, i.e. where and with what capacity the new cooling generation capacity should be built, where and what size the cold media storages should be built, where and what size the district cooling pipelines should be built.

Additionally, the solutions contain information about how the district cooling network should be operated in different time periods, e.g. the cold media flows in different parts of the network during day and night times and in different seasons and the charging and discharging of the storages.

6.3 Paper III

Optimisation of paper machine HRS

In this section an optimisation model for paper machine heat recovery systems (HRS) with single-period and multi-period formulations, described in Paper III, is tested with different cost functions. The tests are based on measured process data from a large paper machine with conventional cylinder drying.

6.3.1 HRS model

In a paper machine HRS the heat flow rates and the heat transfer coefficients vary strongly, because of condensation inside the heat recovery exchangers.

A HRS comprises a set of hot streams, *H* and a set of cold streams, *C*. The number of included hot streams is denoted by n_H and the number of cold streams by n_C. Individual hot streams are denoted by subscript *h* and cold streams by *c*. The index sets for the hot and cold streams are

$$\begin{array}{lll} h \in H & H = \{1,2,\ldots,n_H\} & \text{hot streams} \\ c \in C & C = \{1,2,\ldots,n_C\} & \text{cold streams} \end{array} \qquad (6.3.1)$$

The overall temperature range of the HRS, $\Delta\theta_{tot}$, is the difference of the highest temperature $\theta_{\max}$ and the lowest temperature $\theta_{\min}$ of the inlet and outlet temperatures of the involved streams. The temperature range $\Delta\theta_{tot}$ is partitioned into a suitable number of temperature intervals, denoted by n_{TI}. The hot stream temperature intervals are denoted by subscripts *i* and the cold stream temperature intervals by *j*. The index sets are *I* and *J*, respectively

$$\begin{array}{lll} i \in I & I = \{1,2,\ldots,n_{TI}\} & \text{hot stream temperature intervals} \\ j \in J & J = \{1,2,\ldots,n_{TI}\} & \text{cold stream temperature intervals} \end{array} \qquad (6.3.2)$$

A hot stream interval *h,i* is cooled from the interval upper border temperature, $\theta_{h,i,u}$, to the interval lower border temperature, $\theta_{h,i,l}$. The heat flow that must be transferred from the interval, denoted by $\dot{Q}_{h,i}$, is equal to the enthalpy drop of the stream *h* at the temperature drop $\theta_{h,i,u} - \theta_{h,i,l}$. Correspondingly, a cold stream interval *c,j* is heated from the interval lower border temperature, $\theta_{c,j,l}$, to the interval upper border temperature, $\theta_{c,j,u}$ and the heat flow, $\dot{Q}_{c,j}$, that must be transferred to the interval is equal to the enthalpy rise of the cold stream at the temperature rise $\theta_{c,j,u} - \theta_{c,j,l}$.

Heat Table

The heat flow rates of the formed intervals can be presented in a heat table. An example of a heat table is shown in Fig. 6.3.1.

A heat flow from a humid air stream is dependent on its moisture content and temperature. In the interval, where condensation starts, the hot stream heat flow rate per degree Celsius becomes much larger than in the preceding intervals, i.e. around 50 - 60 °C in the given example. The condensation takes place in all successive intervals towards the outlet temperature. The saturation moisture content is maintained in the descending air temperature.

The heat table can be compared with the corresponding composite curves in Fig. 6.3.1. The hot and cold composite curves are formed from the heat table as the cumulative sums of the hot and cold stream interval heat flow rates.

Upper and Lower Temp.,°C	Interval Number	Hot streams			Cold streams		
		1	2	3	1	2	3
100 - 90	1	0	0	0	271	0	0
90 - 80	2	0	0	151	695	0	0
80 - 70	3	99	376	295	694	0	0
70 - 66	4	166	171	118	278	0	0
66 - 62	5	166	171	118	277	0	0
62 - 58	6	166	935	118	277	0	0
58 - 54	7	2146	2353	118	277	277	0
54 - 50	8	1877	1900	1115	277	1106	0
50 - 46	9	1531	1549	1143	277	1105	4736
46 - 42	10	1258	1273	940	277	1105	4735
42 - 38	11	1041	1054	778	277	1105	4733
38 - 34	12	866	877	647	277	1105	4733
34 - 30	13	725	734	541	277	1105	3513
30 - 20	14	1360	1377	1016	0	2763	0
20 - 10	15	917	929	685	0	2764	0
10 - 0	16	0	0	0	0	829	0

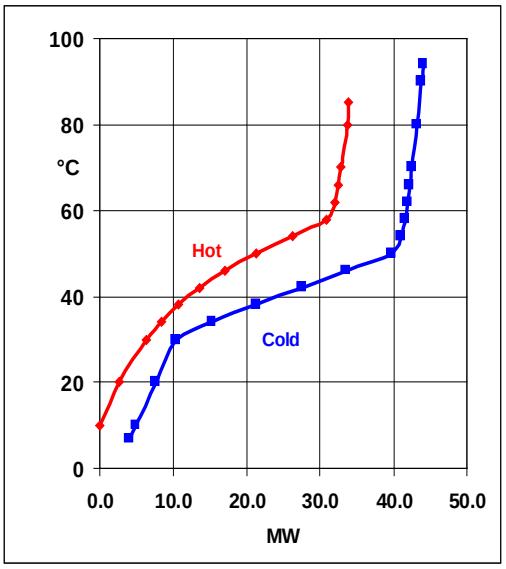

Figure 6.3.1. A heat table and the corresponding composite curves.

Objective function

The objective for the HRS optimisation is to maximise the savings in the mill's energy costs that are obtainable by installing and operating the HRS. Maximum savings are obtained by minimising the sum of the running and investment costs of the HRS, denoted by C_{HRS}. The objective function is

$$\min \quad \left\{ C_{HRS} = C_{Oper,HRS} + C_{Inv,HRS} \right\} \qquad (6.3.3)$$

$C_{Oper,HRS}$ is the sum of the hot and cold utility costs. $C_{Inv,HRS}$ is the sum of the heat recovery exchanger costs. An exchanger area cost function can for instance be linear, piecewise linear or concave. The optimisation problem is a MILP-problem with linear or

piecewise linear area costs and a MINLP-problem with concave area costs. Labour and maintenance costs are considered unchanged, regardless the size of HRS equipment and are not included in the objective function.

The nonlinear objective function with concave exchanger area cost functions is denoted by $f(\mathbf{x},\mathbf{y})$. The objective function was made linear by introducing a new variable, μ that was minimised instead of the nonlinear objective function. A nonlinear inequality constraint was added, the difference between the nonlinear objective function and the variable μ. The HRS problem was defined as

$$
\begin{aligned}
&\min_{x,y} \mu \\
&\text{s.t.} \\
&f(\mathbf{x},\mathbf{y}) - \mu \le 0 \\
&\mathbf{Ex} + \mathbf{Fy} = \mathbf{k} \\
&\mathbf{Ax} + \mathbf{By} \le \mathbf{d} \\
&\mathbf{h}(\mathbf{x},\mathbf{y}) = \mathbf{0} \\
&\mathbf{g}(\mathbf{x},\mathbf{y}) \le \mathbf{0} \\
&\mathbf{x} \ge \mathbf{0} \qquad \mathbf{x} \in \mathbf{X} \subseteq R^n \\
&\mathbf{y} = \mathbf{0,1} \quad \mathbf{y} \in \mathbf{Y} \subseteq R^n
\end{aligned}
\tag{6.3.4}
$$

The linear process constraints are given by a set of inequalities and by a set of equations, where **A, B, E** and **F** denote the constraint matrices and **d** and **k** parameter vectors. The sets of nonlinear equality and inequality constraints are denoted by **h**(**x,y**) and **g**(**x,y**).

The nonlinear problems studied in Paper III have several concave exchanger area cost functions. With the applied optimisation method the global optimality cannot be guaranteed. Therefore, in the work it was analysed, how the MINLP-solutions differ from the respective global optimal MILP-solutions that were obtained with linear and piecewise linear area cost functions.

The constraints in the model are the heat balances, the heat transfer area constraints and the existence constraints. The heat balance in an interval is fulfilled either by heat transfer between the intervals or by hot and cold utilities or by discharging heat from a hot stream interval into the atmosphere. The objective function and the constraints are described in detail in Paper III.

Modelling the condensate streams in intervals

The condensate is considered to participate in the heat transfer inside the interval, where it is formed. The condensate is cooled in the interval to the same outlet temperature as the air stream. The condensate is modelled to run out from the heat transfer surfaces before the next interval and not to take part in the heat transfer in the later intervals. The condensate streams are shown schematically in Fig. 6.3.2. The chosen approach is close to the actual situation in many heat exchanger types, e.g. horizontal shell and tube exchangers or plate heat exchangers.

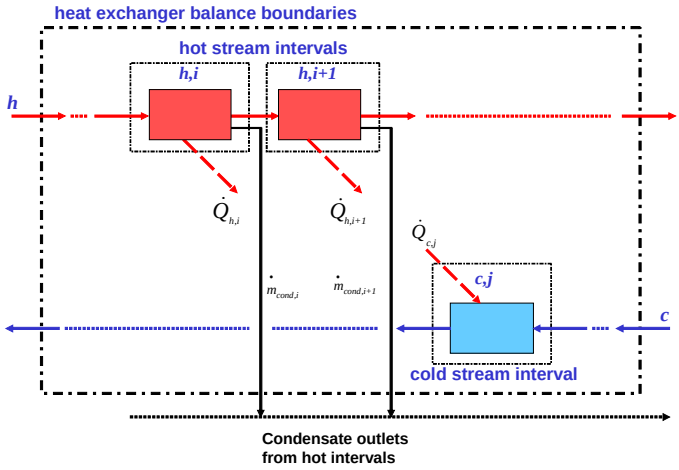

Figure 6.3.2. Model of the condensate streams.

6.3.2 Input data of the tests of the HRS model

In paper III four different paper mill sites were considered. The annual duration curves of the outdoor air temperatures and the raw water temperatures at the sites and a multi-period model with nonlinear price functions were applied. The structures of the optimal HRS for the mills were presented in the paper.

Here a comparison between different cost functions is made by testing both single-period and multi-period models with linear, nonlinear and piecewise linear price functions.

Process streams

The test cases comprise a set of three hot, humid exhaust air streams from the paper machine dryer section, denoted by H1, H2 and H3, and a set of three cold process streams, denoted by C1, C2 and C3. The types of the hot and cold streams are defined in Table 6.3.1. The temperature range, the intervals and the border temperatures that are given in the heat table in Fig. 6.3.1 are applied in the cases.

Table 6.3.1. Hot and cold stream types in the test cases.

Hot stream types		Cold stream types	
H1	exhaust air	C1	supply air
H2	exhaust air	C2	process water
H3	exhaust air	C3	glycol-water

Matching these stream types leads to two heat recovery exchanger types, the air-to-air and the air-to-water heat exchangers.

Test data

A series of measurements were made at a large paper machine with cylinder drying. The input data for the cases is based on these measurements. Stream data is shown in Table 6.3.2.

Table 6.3.2. Stream data for the test cases.

Hot streams	**H1**	**H2**	**H3**
Mass flow rate, kg da/s	33.6	34.2	26.7
Temperature in, °C	73.0	80.0	86.0
Temperature out, °C	10.0	10.0	10.0
Moisture content, kg H_2O/ kg da	0.1410	0.1560	0.1140
Cold streams	**C1**	**C2**	**C3**
Mass flow rate, kg/s	66.0	66.5	204.0
Temperature in, °C	37.0	25.0	38.5 *)
Temperature out, °C	92.7	55.0	51.0
Moisture content, kg H_2O/ kg da	0.0100	-	-

*) glycol-water temperature is calculated, see below.

The source temperature of the cold stream C3 depends on the circulation flow rate of the glycol-water and the heat transfer to the machine hall ventilation air. The glycol-water circulation is defined according to the flow diagram in Fig. 6.3.3.

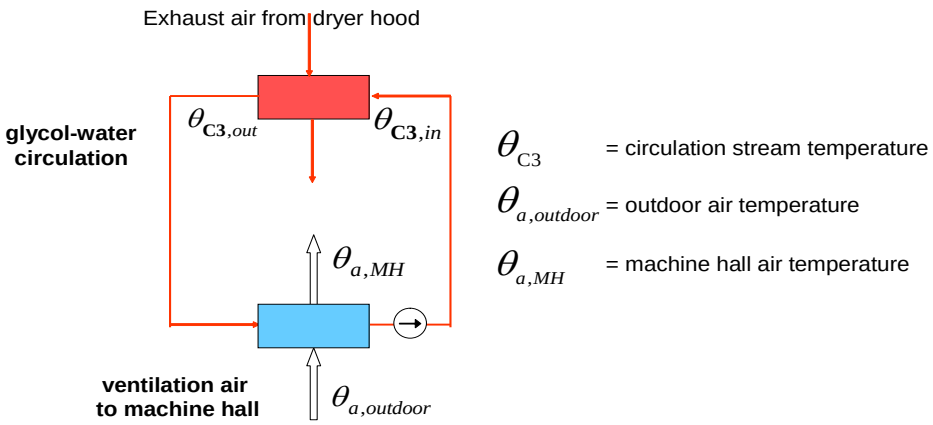

Figure 6.3.3. Heating of machine hall ventilation air by the circulating glycol-water stream.

The ventilation air flow rate is 450 kg/s and its moisture content 0.005 kg H_2O/ kg da. The air is heated from the outdoor air temperature of 2.6 °C to the machine hall air temperature of 25 °C by the circulating glycol-water stream, which is then reheated in the HRS.

In all test cases a constant atmospheric pressure of 101.325 kPa is applied for the calculation of saturation temperatures. Pressure drops in the equipment are not taken into account.

Specific heat capacities c_p and heat transfer coefficients α

Specific heat capacities and heat transfer coefficients for the process streams are given in Table 6.3.3.

Table 6.3.3. Specific heat capacities for the process streams.

	c_p kJ/kgK	α kW/m²K
dry air	1.008	0.05
vapour	1.900	0.06
water	4.186	3.00
10 % glycol-water	4.007	2.60

The glycol content of the glycol-water is taken as 10 %. The specific heat capacity for the mixture is calculated from the c_p values of water and 100 % glycol (= 2.40 kJ/kg).

For the overall heat transfer coefficients, calculated coefficients for each interval pair were applied. The approach is described in Paper IV. In the approach the moist air heat transfer coefficient is obtained by multiplying the dry air heat transfer coefficient with a condensation factor. The condensation factor is calculated for each pair of hot and cold stream intervals. It depends on the temperature of the heat transfer wall between the hot and cold streams. The wall temperature is calculated in this work by iteration. The iteration approach is based on the interval halving (Bolzano search).

The measured overall heat transfer coefficients for the air-to-air heat exchangers were 20 - 30 W/m^{2}K and for the air-to-water exchangers 200 - 600 W/m^{2}K, i.e. 10 to 20 times higher due to the condensation at the hot side surfaces. The calculated heat transfer coefficients are in good conformity with the measured values.

Utility costs

Three different hot utilities are included in the model, low-pressure steam, denoted by UL, medium-pressure steam, denoted by UM and gas, denoted by UG, with temperatures 120, 160 and 300 °C, respectively. The minimum approach temperature for the hot utility heaters is defined as 10 °C. The utility prices for UL, UM and UG are 16, 20 and 24 €/MWh. In the test cases only cylinder drying was considered, so only the hot utility UL was applied. In the impingement drying case, discussed in paper VI, other utilities were also used.

The given prices include all the costs that are involved when a utility is used, i.e. the costs for fuel, production facilities, heat exchangers, pipelines, control systems, etc. The heat transfer areas for the utility matches are therefore not included separately in the formulation. A utility is considered abundant, i.e. any demand that is set up by the optimisation can be satisfied.

The exhaust air streams are discharged into the atmosphere after the HRS without any temperature limitations. No cost of discharge is applied.

6.3.3 Heat exchanger area price functions

The annual area costs are calculated from the equipment prices with the annuity method. An annuity factor of 0.16 is used, covering 10 years depreciation time and 10 % interest rate.

Linear price functions

An area cost in the objective function comprises two parts, a fixed cost part and an area-dependent cost part. A linear price is defined as

$$P_l = P_{f,l} + P_{A,l} \cdot A \tag{6.3.5}$$

where P_l is the exchanger price with an exchanger area A, $P_{f,l}$ is the fixed price and $P_{A,l}$ is the unit price, e.g. in €/m^2. Both the investment and the running costs are transformed to hourly costs by dividing the annual costs with the annual running hours of the HRS, denoted by t_{Oper}. In this work it is defined as 8000 h/a. The cost factors are obtained by

$$c_{f,l} = \frac{a}{t_{Oper}} \cdot P_{f,l} \quad ; \quad c_{A,l} = \frac{a}{t_{Oper}} \cdot P_{A,l} \tag{6.3.6}$$

where the annuity factor is denoted by a, $c_{f,l}$ is the fixed cost and $c_{A,l}$ is the unit cost of an exchanger.

With linear price functions the HRS problem has a global optimum and can be solved in a relatively short computation time. Linear costs are also practical, as the exchanger prices are often given as unit prices or as a total price for a certain exchanger size, from which a unit price can be obtained. Linear functions do not, however, take into account the economy of scale.

Nonlinear price functions

A nonlinear price function is defined as

$$P_{nl} = P_{f,nl} + P_{A,nl} \cdot A^{\beta} \tag{6.3.7}$$

The price curve is concave with the area price exponent $\beta < 1.0$. The fixed price is denoted by $P_{f,nl}$ and the area dependent unit price by $P_{A,nl}$.

The nonlinear price function takes into account the economy of scale. Its disadvantage is that the problem becomes an MINLP problem with longer computation times than with the linear prices. A global optimality is not guaranteed for an MINLP solution with the method applied in this work.

Heat transfer area costs

Running-hour-based heat transfer area costs are calculated with an annuity factor, an annual runtime of the paper machine and the exchanger prices, given in Table 6.3.4.

The nonlinear price functions are firstly defined for two different types of heat recovery exchangers, air-to-air and air-to-water heat exchangers. The corresponding linear prices are then defined so that relatively good conformities between the two price functions for both exchanger types are obtained in a chosen exchanger area range, i.e., between 500 m^2 and 3000 m^2, which is a conventional range for practical HRS design.

The following data has been defined

Table 6.3.4. Linear and nonlinear exchanger price data.

		fixed price M€	unit price €/m^2	price at 1000 m^2 M€	exponent β
Type 1	linear	0.14	120	0.26	
	nonlinear	0.02		0.26	0.6
Type 2	linear	0.10	160	0.26	
	nonlinear	0.04		0.26	0.8

Type 1 simulates the air-to-air heat exchangers. The nonlinear function is defined with a fixed price of 0.02 M€, a price of 0.26 M€ at 1000 m^2 and an exponent $\beta = 0.6$. The fixed price for the corresponding linear price is 0.14 M€ and a slope of 0.12 M€/1000 m^2

is applied to conform to the nonlinear curve. A high conformity between the two functions is obtained in the range between 800 m^2 and 2500 m^2. The prices are shown in Fig. 6.3.5.

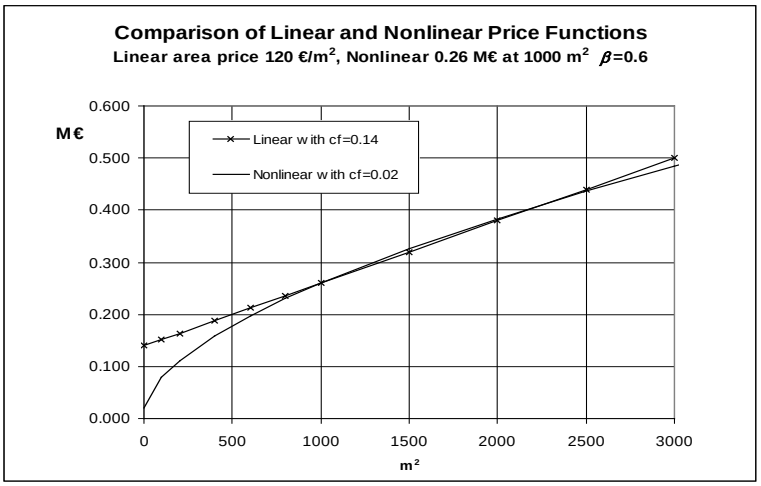

Figure 6.3.5. Linear and nonlinear price functions, Type 1. $\beta = 0.6$.

Type 2 simulates the air-to-water heat exchangers. The nonlinear price has a fixed price part of 0.04 M€ and the price at 1000 m^2 is 0.26 M€. The exponent β for the price curve is 0.8. A corresponding linear price is applied with a fixed price of 0.10 M€ and the slope of 0.16 M€/1000 m^2.

The price differences, ΔP, between the nonlinear and linear area prices, are shown in Fig. 6.3.6, for the two types. The differences are smaller than ± 2 % in the area range from 800 m^2 to 2700 m^2.

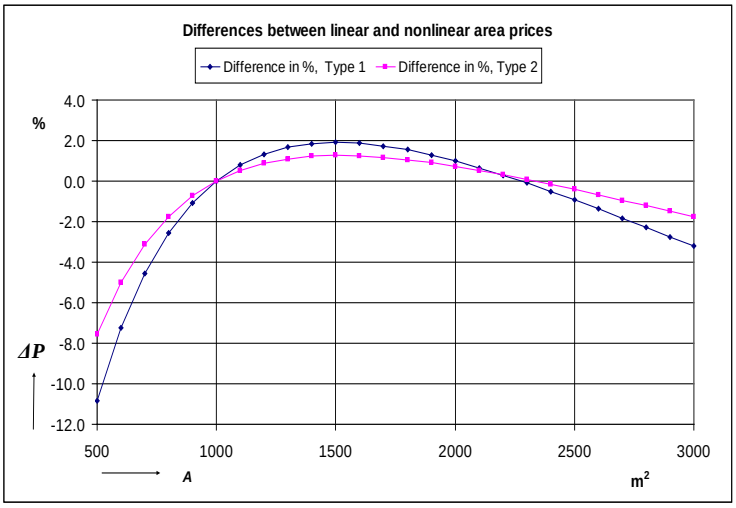

Figure 6.3.6. Differences between nonlinear and corresponding linear prices, with $\beta = 0.6$ (Type 1) and $\beta = 0.8$ (Type 2).

Piecewise linear price functions

A piecewise linear price function is built by dividing the chosen heat transfer area range into a number of steps. The price is defined as

$$P_{A,pl} = P_{f,pl} + \sum_{s=1}^{N_s} P_{A,s} \cdot (A_s - A_{s-1}) \qquad (6.3.8)$$

The exchanger price is denoted by $P_{A,pl}$. The subscript s denotes a step and N_s the total number of steps. $P_{f,pl}$ denotes the fixed price, $P_{A,s}$ the specific area price in a step, A_s the area at the upper step border and A_{s-1} the area at the lower step border.

A schematic figure of the piecewise linear price is shown in Fig. 6.3.7.

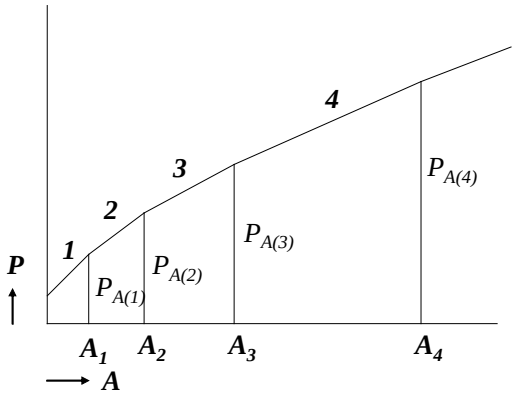

Figure 6.3.7. Schematic picture of a piecewise linear cost function.

The area points are denoted by A_s for the steps s = 1,2,...,N_s , and the area prices at the area points are denoted by $P_{A(s)}$. The area dependent linear prices between two area points are denoted by $P_{A,s}$ and are given by

$$P_{A,s} = \frac{P_{A(s)} - P_{A(s-1)}}{A_s - A_{s-1}} \qquad (6.3.9)$$

For a heat transfer match between hot stream h and cold stream c the heat transfer area is defined with the following constraints

1) For each step

$$A_{h\_c(s)} \le (A_s - A_{s-1}) \cdot y_{h\_c(s)} \qquad \text{for} \quad s = 1,2,...,N_s \qquad (6.3.10)$$

The area in a step s is denoted by $A_{h\_c(s)}$ and the binary variable for defining the existence or nonexistence of area in the step by $y_{h\_c(s)}$. If there is an area between the area points A_s and A_{s-1} then $y_{h\_c(s)}$ is 1 and the partial area can have a positive value up to the maximum of the given step area (A_s - A_{s-1}).

If there is no area in the step *s*, then $y_{h\_c(s)}$ can be 0 or 1. A second constraint is inserted to define which one is valid.

2) An unbroken chain of successive step areas are needed until the total area for the match has been reached, defined with the constraints

$$y_{h\_c(s)} - y_{h\_c(s+1)} \geq 0 \qquad \text{for} \quad s = 1,2,...,(N_s\text{-}1) \tag{6.3.11}$$

3) For the unbroken chain the former step area must be completely used, before an area in the next step can be included in the total area

$$A_{h\_c(s)} \geq (A_s - A_{s-1}) \cdot y_{h\_c(s+1)} \qquad \text{for} \quad s = 1,2,...,(N_s\text{-}1) \tag{6.3.12}$$

4) The total area of the match *h,c*, is equal to the sum of the defined areas in the steps

$$A_{h\_c} = \sum_{s=1}^{N_s} A_{h\_c(s)} \tag{6.3.13}$$

The piecewise linear price functions are built from the nonlinear price data from Table 6.3.1 so that the prices coincide with the nonlinear prices at the area points of 500, 1000, 2000 and 4000 m^2. The price functions are defined in Table 6.3.5.

Table 6.3.5. Piecewise linear exchanger prices.

Fixed price, M€				
Type 1 (air-to-air)				0.02
Type 2 (air-to-water)				0.04
Step	**1**	**2**	**3**	**4**
Area, m2	0 - 500	500 - 1000	1000 - 2000	2000 - 4000
Price at the end of step, M€				
Type 1	0.1784	0.2600	0.3838	0.5714
Type 2	0.1664	0.2600	0.4230	0.7070

A piecewise price built in this way is an under-estimator of the corresponding nonlinear price function in the given range. The differences between the piecewise linear and nonlinear prices for the exchangers with β = 0.6 (Type 1) and with β = 0.8 (Type 2) are shown in Fig. 6.3.8, and are seen to be less than 1.4 % in the range of A= 500 - 4000 m^2.

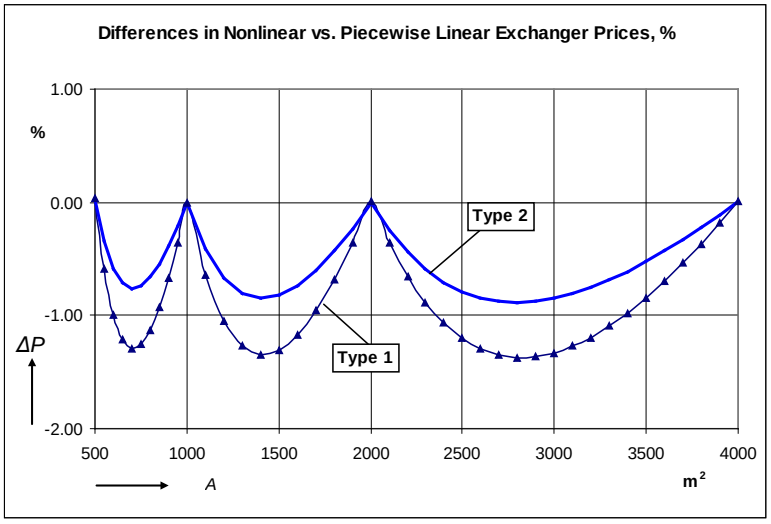

Figure 6.3.8. Differences between the piecewise linear and nonlinear prices for two heat exchanger types (Type 1 and 2), in the area range from 500 to 4000 m^2.

Outside the given range with match areas larger than 4000 m^2 the piecewise linear costs are obtained by extrapolating the price line of step 4 with the same slope.

With the piecewise linear prices the optimisation problem is an MILP-problem and has a global optimal solution. On the other hand, because of additional binary variables the computation time is longer than with linear or nonlinear prices.

Stepwise exchanger costs

The heat exchanger manufacturers strive to standardise and modularise the exchangers. This means that the exchanger prices are actually defined with stepwise changes. A stepwise exchanger price, denoted by $P_{step,s}$, can be obtained from the piecewise formulation by replacing the area dependent step price with a fixed step price, i.e. the piecewise linear unit price in the step multiplied by the area at the upper step border

$$P_{step,s} = P_{A(s)} \cdot A_s \tag{6.3.14}$$

The step price function is written as

$$P_{A,step} = P_{f,step} + \sum_{s=1}^{N_s} P_{step,s} \cdot y_{h\_c(s)} \qquad s = 1,2,...,N_s \tag{6.3.15}$$

The total step price is denoted by $P_{A,step}$ and the fixed price by $P_{f,step}$.

A solution with the step cost model gives the heat transfer areas equal to the upper border values of the area steps, i.e. the standard sizes. In this work, however, the continuous price models are used in order to make a comparison between the different cost functions.

Layout costs

Costs of the pipelines and ducts at a paper machine HRS, denoted here generally as lay-out costs, depend on the distances between the heat exchangers and the source and target points of the process streams. The layout costs are included in the test cases according to the schematic drawing, shown in Fig. 6.3.9. The three hot exhaust air ducts are placed along the dryer section. The supply air, C1, enters the HRS directly from the machine hall so no duct costs are included for C1. The process water, C2, is defined to have its source and target point near the press section. The circulating glycol-water stream, C3, is defined to have its source and target points near the dry end of the dryer section.

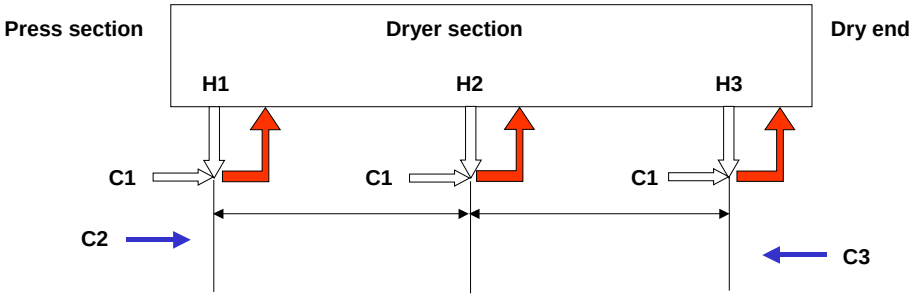

Figure 6.3.9. A schematic drawing of a paper machine for the layout costs.

The layout prices for the nine exchanger matches are given in Table 6.3.6.

Table 6.3.6. Layout prices.

cold stream	**C1**	**C2**	**C3**
matched with	M€	M€	M€
H1	0	0.02	0.06
H2	0	0.04	0.04
H3	0	0.06	0.02

6.3.4. Test cases

Three single-period and three multi-period cases are tested. Cases are named with letters TC and a running number. The cases are described in Table 6.3.7.

Table 6.3.7. Test cases.

Test case name	cost data type	number of periods
TC-1	linear	1
TC-2	non-linear	1
TC-3	piecewise linear	1
TC-4	linear	4
TC-5	non-linear	4
TC-6	piecewise linear	4

Single-period test cases

Test case TC-1

The obtained solution of the test case TC-1 with linear cost function and single-period formulation is shown in Fig. 6.3.10. Five matches are included in the solution. The sum of the heat exchanger areas is 9046 m^2. The hot utility demand is 1614 kW or about 7 % of the total heating demand of the cold streams. The annual HRS cost is 0.5166 M€.

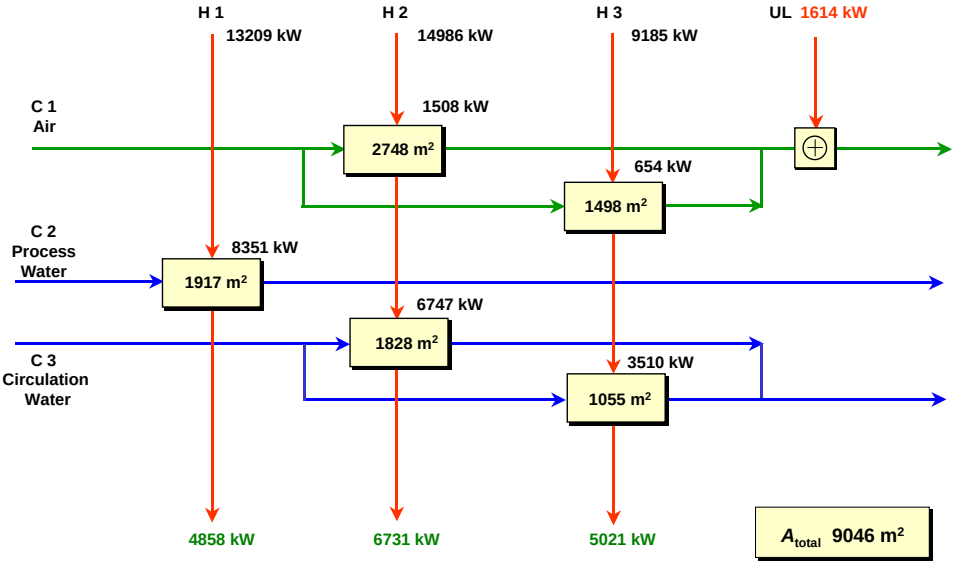

Figure 6.3.10. HRS structure for the linear, single-period test case, TC-1.

Test case TC-2

In the test case TC-2 the linear exchanger prices are replaced with non-linear cost functions and the non-convex MINLP problem is solved with the α-ECP-method. The obtained solution for the test case TC-2 has the same HRS structure as was obtained in TC-1. Total heat exchanger area is 9629 m^2 and the hot utility demand 1539 kW. The annual cost is 0.5146 M€.

Test case TC-3

In the test case TC-3 the linear exchanger prices are replaced with piecewise linear price functions. The solution gives a lower bound to the nonlinear case TC-2. The obtained solution structure of the test case TC-3 is again the same as in TC-1 and TC-2. Total area is 9615 m^2 and the hot utility demand 1539 kW. The annual cost is 0.5132 M€.

Comparison of single period test cases TC-1, TC-2 and TC-3

The three single period cases are compared in Table 6.3.8.

Table 6.3.8. Comparison of the single-period test cases.

		TC-1		TC-2		TC-3	
		A	*Q*	*A*	*Q*	*A*	*Q*
match		m²	kW	m²	kW	m²	kW
	Inlet heat H1		13209		13209		13209
H1-C2		1917	8351	1917	8351	1917	8351
	Outlet heat H1		4858		4858		4858
	Inlet heat H2		14986		14986		14986
H2-C1		2748	1508	3598	1714	3568	1714
H2-C3		1828	6747	1889	6841	1897	6841
	Outlet heat H2		6731		6431		6431
	Inlet heat H3		9185		9185		9185
H3-C1		1498	654	1208	523	1208	523
H3-C3		1055	3510	1018	3415	1026	3415
	Outlet heat H3		5021		5246		5246
	Hot utility to C1		1614		1539		1539
Annual cost, M€		0.5166		0.5146		0.5132	

From the table it can be noted that the differences of the solutions are small and can be regarded as insignificant for a practical design work. The comparison indicates that any of the formulations could be applied satisfactorily.

Multi-period test cases

The heat table in Fig. 6.3.1 represents a situation at the paper machine at one moment of a year. The question arises whether this data set can give a satisfactory solution with respect to the prevailing seasonal variations. A paper machine can be considered to run fairly unchanged throughout the year so the hot streams can be considered to remain relatively constant but, on the other hand, some of the cold streams are influenced significantly by seasonal variations, especially in the Nordic climates.

The influence of the annual variations of the outdoor air temperature and the temperature of the inlet raw water is tested here with three additional cases having multi-period data. A year is divided into a number of time periods and the air and water temperature variations are obtained from the temperature duration curves.

The formation of time periods is shown schematically in Fig. 6.3.11. Time periods are denoted by index p and the number of time periods by n_P. An index set P is defined as

$$p \in P \quad p = \{1,2,\ldots,n_P\} \tag{6.3.16}$$

The mean temperatures for the periods $\theta_{m,p}$ are applied in the model.

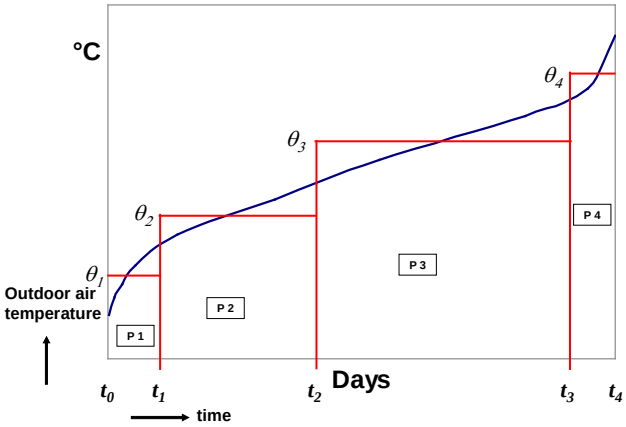

Figure 6.3.11. Time periods and mean temperatures derived from the outdoor air temperature duration curve.

Data for multi-period tests

Data for the multi-period test cases is shown in Table 6.3.9. The periods are denoted by p1, p2, p3 and p4. The temperature values are defined at five day points, 0, 20, 140, 330 and 365 days, from the annual duration curves.

Table 6.3.9. Data for the multi-period test cases.

Day points, days	**0**	**20**	**140**	**330**	**365**
Outdoor air temperature ($\theta_{a,outdoor}$), °C	-34	-15	0	16.5	28
River water temperature ($\theta_{w,river}$), °C	2	2	6	16	20
Period		**p1**	**p2**	**p3**	**p4**
Period length, days		20	120	190	35
Running time, hours		438	2630	4164	768
Mean outdoor air temperature ($\theta_{a,outdoor}$), °C		-24.5	-7.5	8.25	22.25
Mean river water temperature ($\theta_{w,river}$), °C		2	4	11	18
Air humidity, outdoor, kg H_2O/kg da		0.002	0.003	0.007	0.01
Air humidity, indoor, kg H_2O/kg da		0.007	0.008	0.01	0.014
Proportionality factor, $f_{pg,}$ for glycol-water flow rate		1.25	1.1	0.9	0.75
Flow rate of glycol-water , kg/s		255	224.4	183.6	153

The moisture content of the indoor air varies due to the outdoor air humidity and the many sources of humidity increase inside the mill, like the open wet end at the paper machine, the floor channels of condensates, tank ventilations etc.

For the glycol-water circulation flow rates a proportionality factor f_{pg} is defined for the different periods in relation to a basic value of 204 kg/s. The ventilation airflow rate of 450 kg/s d.a. and the machine hall temperature of 25 °C are considered to remain unchanged throughout the year.

The hood supply air intake to HRS is commonly placed at an upper level in the machine hall beside the paper machine with a significantly higher temperature than prevailing in general in the machine hall. The temperature increase above the machine hall temperature is defined in this work as 12 °C.

Similarly, the inlet process water temperature increases in the mill before entering HRS in the process water pipe lines, intermediate storage tanks, etc. This temperature increase is here taken to be 15 °C.

Test case TC-4

The solution of the linear multi-period test case TC-4 is shown in Fig. 6.3.12.

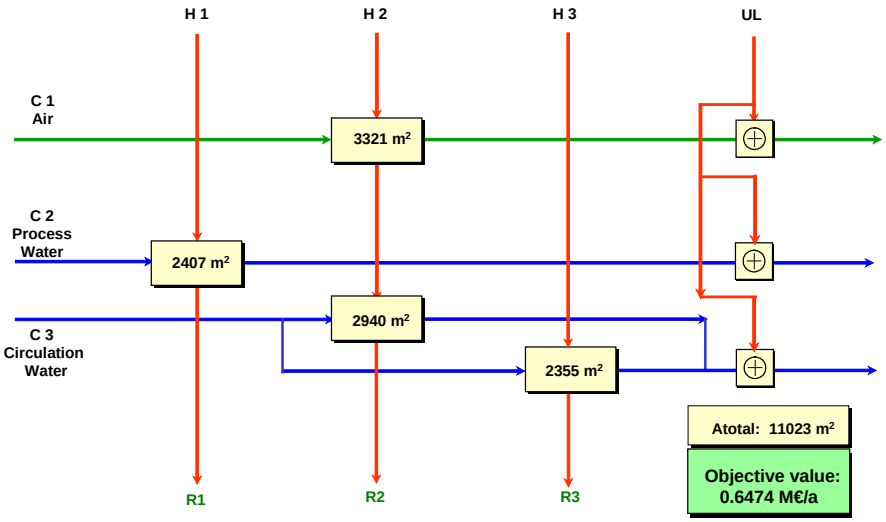

Figure 6.3.12. Solution of the test case TC-4.

Table 6.3.10 shows the hot utility demand in different periods in the test case TC-4 for the cold streams C1, C2 and C3, denoted by $\dot{Q}_{(HU\_1),p}$, $\dot{Q}_{(HU\_2),p}$ and $\dot{Q}_{(HU\_3),p}$ respectively. The periodic hot utility consumptions, in MWh, are calculated with the running hours of the periods. The annual average hot utility demand is 2369 kW.

Table 6.3.10. Hot utility consumption in different periods and the average HU-consumption in the test case TC-4.

Period	Hot utility heat flows $\dot{Q}_{(HU\_1),p}$ kW	$\dot{Q}_{(HU\_2),p}$ kW	$\dot{Q}_{(HU\_3),p}$ kW	$\dot{Q}_{HU,p}$ kW	Hot utility consumption MWh
p1	2432	173	5104	7709	3377
p2	2167			2167	5700
p3	1999			1999	8322
p4	2020			2020	1551
total				MWh/a	18950
Average hot utility consumption				2369 kW	

Test case TC-5

The nonlinear area price functions with the multi-period data are used in the test case TC-5. The solution is shown in Fig. 6.3.13. Compared with the linear case TC-4 the match H2-C1 is replaced with two matches, H1-C1 and H3-C1. The total heat transfer area is larger and the hot utility costs are smaller in the test case TC-5 than in the test case TC-4.

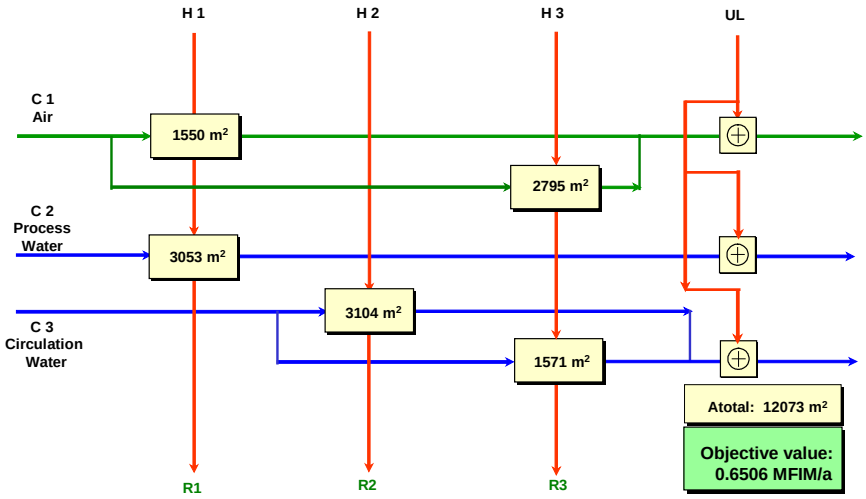

Figure 6.3.13. Solution of the test case TC-5.

Table 6.3.11 shows the hot utility demand in different periods.

Table 6.3.11. Hot utility demand of the test case TC-5 in different periods.

Period	Hot utility heat flows $\dot{Q}_{(HU\_1),p}$ kW	$\dot{Q}_{(HU\_2),p}$ kW	$\dot{Q}_{(HU\_3),p}$ kW	$\dot{Q}_{HU,p}$ kW	Hot utility consumption MWh
p1	2007	157	5181	7345	3217
p2	1831			1831	4817
p3	1758			1758	7321
p4	1779			1779	1366
total					16722
Average hot utility demand				2090 kW	

The hot utility demands are denoted in the same way as in Table 6.3.10. The annual average hot utility demand in the nonlinear multi-period test case TC-5 is 2090 kW.

Test case TC-6

The test case TC-6 is formulated with the piecewise linear price functions so that a lower bound for the nonlinear multi-period test case TC-5 is obtained. The solution for TC-6 is shown in Fig. 6.3.14. The HRS structure is the same in TC-6 as in the linear multi-period test case TC-4. The heat transfer areas are slightly larger in TC-6 than in TC-4.

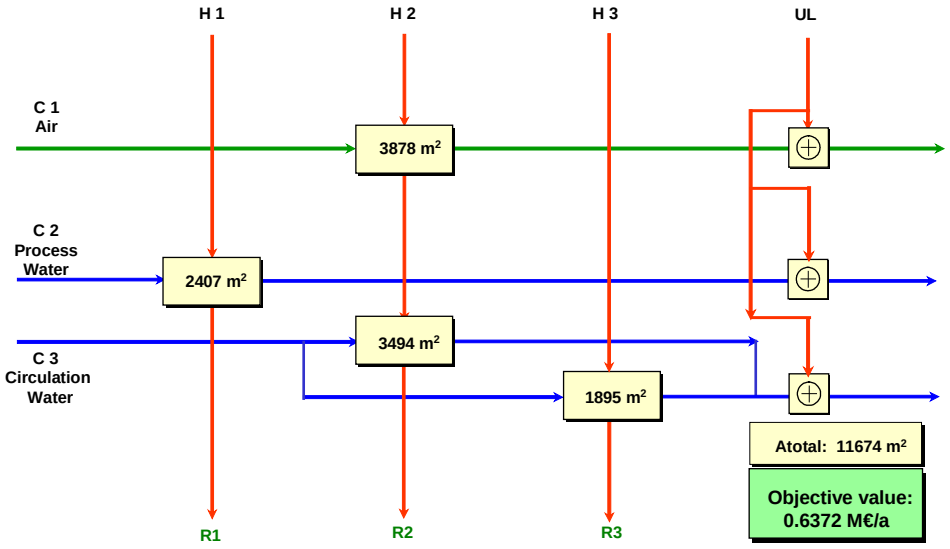

Figure 6.3.14. Solution of the test case TC-6.

Table 6.3.12 shows the hot utility demand in different periods in TC-6 for the cold streams C1, C2 and C3.

Table 6.3.12 Hot utility demand of the test case TC-6 in different periods.

Period	Hot utility heat flows				Hot utility consumption
	$\dot{Q}_{(HU\_1),p}$ kW	$\dot{Q}_{(HU\_2),p}$ kW	$\dot{Q}_{(HU\_3),p}$ kW	$\dot{Q}_{HU,p}$ kW	MWh
p1	2339	173	5152	7664	3357
p2	2069			2069	5442
p3	1903			1903	7924
p4	1923			1923	1477
total					18200
Average hot utility demand				2275 kW	

The hot utility demands in different periods are denoted as in Table 6.3.10. The annual average hot utility demand in the piecewise linear multi-period test case TC-6 is 2275 kW.

Comparison of test cases TC-4, TC-5 and TC-6

A comparison of the costs of the linear test case TC-4, the nonlinear test case TC-5 and the piecewise linear test case TC-6 is shown in Table 6.3.13.

Table 6.3.13. Comparison of the costs of the test cases TC-4, TC-5 and TC-6.

Relative costs	TC-4	TC-5	TC-6
Area costs	0.512	0.572	0.515
Hot utility costs	0.468	0.413	0.450
Lay-out costs	0.020	0.020	0.020
Total HRS-cost	1.000	1.005	0.985

The total HRS-cost of TC-5 is approx. 0.5 % higher than TC-4, while for TC-6 the cost is approximately 1.5 % smaller than in TC-4. The area costs of TC-6 are approximately 10 % smaller than of TC-5, but are compensated by higher hot utility costs. The lay-out costs are equal in all three cases, approximately 2 % of the total HRS-costs.

Comparison of single-period test cases vs. multi-period test cases

A significant difference can be noticed between the single-period vs. multi-period solutions in respect of the hot utility consumptions and the total heat exchanger areas. The ratio between the objective functions of TC-4 and TC-1 is 1.253, between TC-5 and TC-2 1.264 and between TC-6 and TC-3 1.242. The input data for the multi-period cases lead to higher hot utility demands and also higher total HRS exchanger areas than in corresponding single-period cases.

Concluding remarks

From the obtained solutions of the test cases it can be stated that all three heat exchanger price models can be used satisfactorily in the optimisation and give a good starting point for the practical HRS design work. The differences between the single-period and multi-period cases are, however, significant. Therefore, the multi-period approach is preferred.

6.4. Paper IV

Influence of cost factor variations in energy systems structures

The optimal structure of an energy system is dependent on a large amount of process data and cost factors. A solution is a point in an n^{th} dimensional space. A question is how the optimal solution changes when one or some of the data is changed. Paper IV studies the influence of the data variations on the optimal heat recovery exchanger systems that have moist air streams as heat sources.

6.4.1. Influence of annuity factor and hot utility price

Two cost factors were chosen to represent the different data involved in the studied energy system, namely the annuity factor and the hot utility price. The annuity factor influences the investment costs and the hot utility price the running costs. The annuity factor includes both depreciation and interest rate and is a measure of the price of the invested money.

Influence of annuity factor at a constant hot utility price

In the first test series the annuity factor was increased from a low level of 0.01 to a level where the investment on HRS was no more economical. In the studied case the zero investment level was reached at the annuity factor of 4.0. The decrease of the total heat exchanger area in HRS from the maximum value to zero is shown in Fig. 6.4.1.

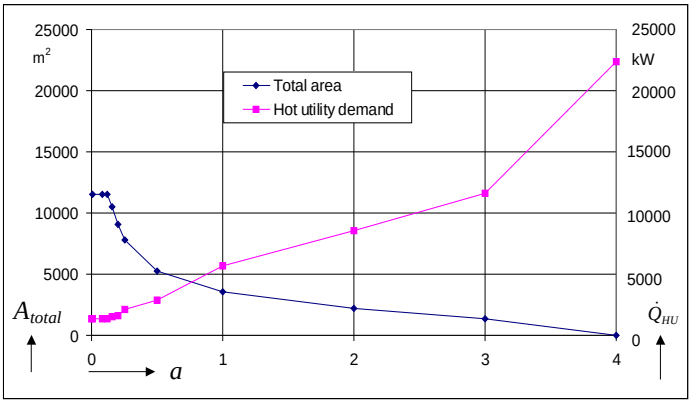

Figure 6.4.1. Total heat transfer area, A_{total} and the hot utility demand, $\dot{Q}_{HU}$ as a function of the annuity factor, a.

With a low annuity factor a minimum hot utility demand is required in the optimal system. This means also at the same time that the maximum heat exchanger area is

required. In the studied case the minimum hot utility demand is $\dot{Q}_{HU}$ =1342 kW and the maximum optimal heat exchanger area is 11562 m^2. When increasing the annuity factor the hot utility demand remains at the minimum level and the optimal area at the maximum level until the annuity factor of a = 0.12. A threshold is obtained after which the hot utility demand starts increasing and the total heat transfer area starts decreasing.

At the annuity factor of a = 4.0 the whole heating demand of the cold streams, ≈ 23 MW, is satisfied by the hot utility.

At a paper machine the three hot exhaust air streams have quite similar stream data and are relatively easily interchangeable in the optimisation solution. Therefore, when the heat exchanger area decrease as a function of the annuity factor was considered, the sum of the exchanger areas with respect to the cold streams was followed together with the individual match areas. The cold stream C1, C2 and C3 heating areas are shown in Fig. 6.4.2.

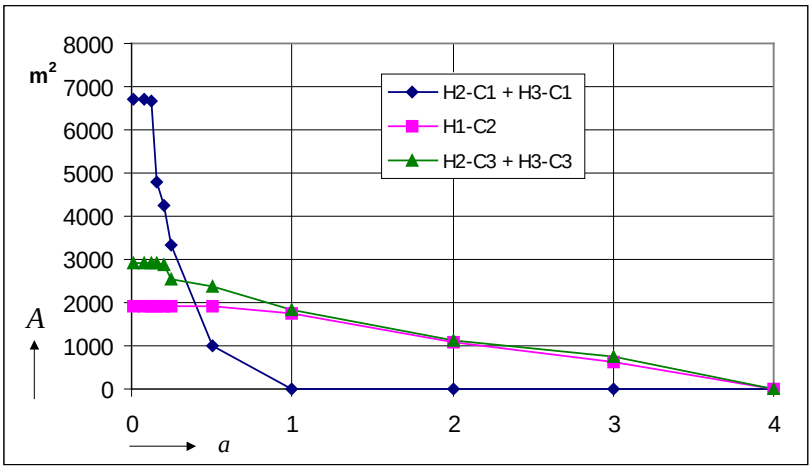

Figure 6.4.2. Exchanger areas in respect of cold streams C1, C2 and C3 as a function of the annuity factor. HU price is 16 €/MWh. Two matches H2-C1 and H3-C1 are in the solutions for C1, H1-C2 is the only match for C2 and two matches H2-C3 and H3-C3 are for C3.

It can be seen from Fig. 6.4.2 that the exchangers for C1, supply air heaters, have the largest areas of the cold streams as long as the annuity factor is low. After the threshold value of a ≈ 0.12 the optimal exchanger areas for C1 decrease fast as the annuity factor increases. On the other hand, the optimal heat exchanger areas for C2 and C3, process water and circulation water, decrease fairly smoothly with the increasing annuity factors.

Influence of hot utility price at a constant annuity factor

The influence of the hot utility price was studied by fixing the annuity factor to a = 0.16 and varying the hot utility cost. The exchanger area increases are shown in Fig. 6.4.3. With sufficiently high HU price the areas become constants, evidently the same areas as with low annuity factors in Fig. 6.4.2. The limit of the hot utility price below which no heat recovery match is economical was in this case 0.68 €/MWh. For supply air heating the HU price limit was 4 €/MWh.

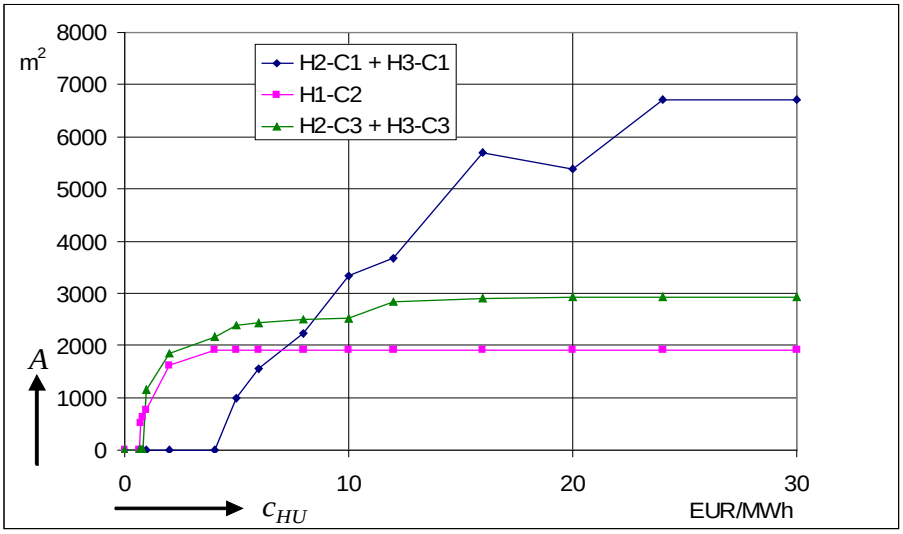

Figure 6.4.3. Sum of exchanger areas as a function of the hot utility price. Annuity factor is 0.16.

The total heat transfer area and the hot utility demand as a function of the HU price are shown in Fig. 6.4.4. The minimum hot utility demand is reached at 24 €/MWh. A further increase of the price can not decrease the hot utility demand.

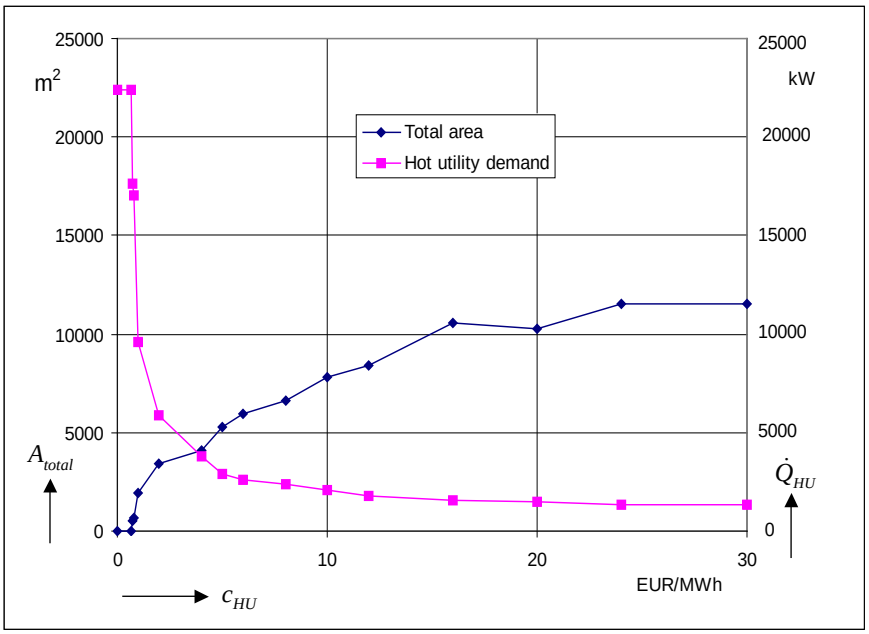

Figure 6.4.4. Total heat transfer area and hot utility demand as a function of the hot utility price.

The influence of both the annuity factor and the HU-price on the number of matches in the optimal solution is shown in Fig. 6.4.5. Boundary lines between the regions with a given number of matches are denoted by B(0/1), B(1/2) etc. The numbers in the parentheses indicate the change of the number of matches. For example at the boundary

line B(4/5) the hot utility price is about 11 €/MWh with the annuity factor of 0.16 and about 20 €/MWh with the annuity factor of a = 0.3.

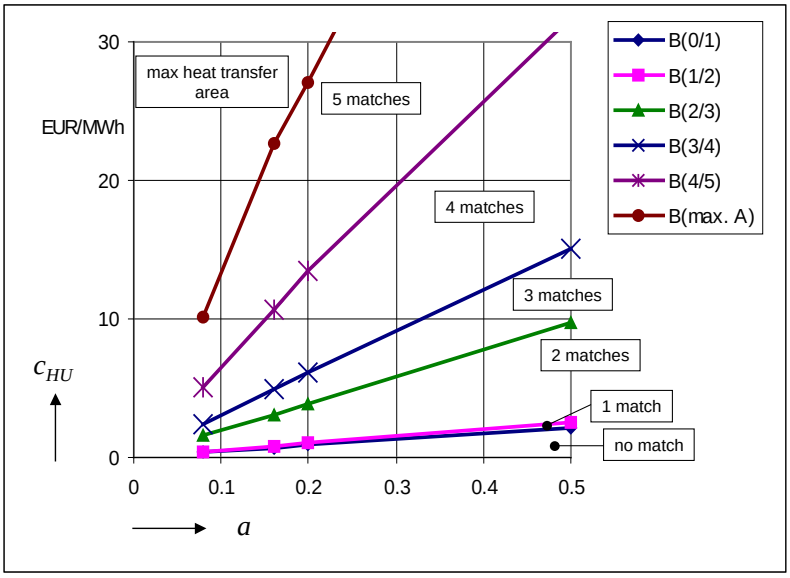

Figure 6.4.5. Optimal number of matches in HU-price vs. annuity factor diagram.

The region with five matches at the upper left part of the diagram is divided into two regions with a boundary line denoted by B(max. A). Starting from the boundary line B(4/5) the area increases until it reaches the maximum area at the boundary B(max. A). The minimum hot utility consumption prevails on the maximum area region.

6.4.2. Area Cost Sensitivity

The sensitivity of the optimal structure of the energy systems with respect to the heat exchanger area costs was analysed by solving the nonlinear test case TC-2, defined in section 6.3, with different fixed total area cost values. Both smaller and larger costs than the optimal area cost were used. Two optimum points from different regions of the HU price vs. annuity factor map, Fig. 6.4.5, were chosen for the analysis.

Test runs with a five-match optimum

An optimum point with the HU price of 16 €/MWh and the annuity factor a = 0.16 was chosen from Fig. 6.4.5 as the reference point for the first analysis.

In Fig. 6.4.6 the hot utility cost and the total HRS cost of the solutions are shown as a function of the relative area cost.

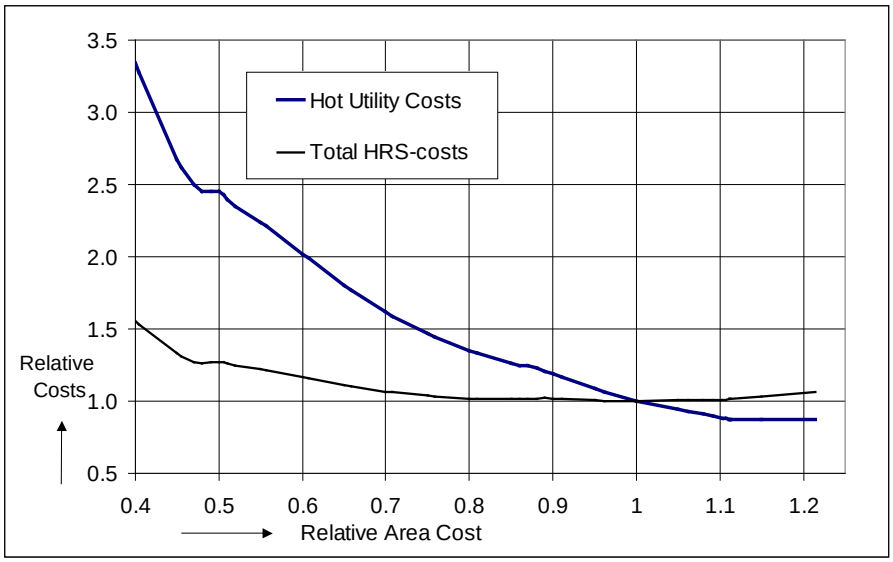

Figure 6.4.6. Relative hot utility costs and total HRS costs as a function of the relative area costs. Annuity factor is 0.16 and HU-price 16 €/MWh.

The hot utility cost in Fig. 6.4.6 decreases until a minimum level, at the relative hot utility cost of approx. 0.85, is reached. Two zones above the optimum point can, however, be noticed, where the hot utility consumption remains constant regardless a change in the relative area cost. At the same zones the total HRS cost has local minima.

The two zones are caused by the change of the number of matches in the solution, from three to four matches at the relative area cost of 0.50 and from four to five matches at 0.88. Above the optimum area cost the total HRS cost increases slowly before the minimum hot utility consumption is reached at the relative area cost of 1.1. After that a further increase in the area increases only the total HRS cost.

The individual match areas are shown in Fig. 6.4.7 as a function of the relative area cost. Both zones with a change in the number of matches show significant changes in the exchanger areas.

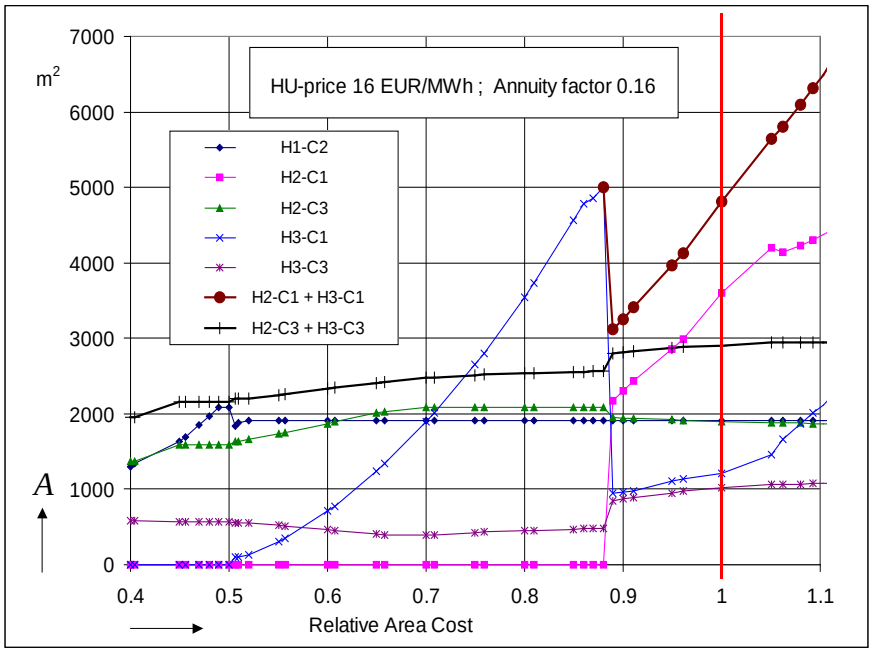

Figure 6.4.7. Match areas as a function of the relative area costs. Annuity factor is 0.16 and HU price 16 €/MWh.

At the relative area cost level of 0.4 three exchanger matches, H1-C2, H2-C3 and H3-C3 are included in the solution. They are all air-to-water exchangers. Moving towards the optimum cost level, an air-to-air heat transfer match, H3-C1, becomes economical at the relative area cost of 0.5.

Each match has a fixed cost, as described in section 6.3, causing a threshold that have to be passed before a match is added in the solution. In this case a threshold is formed between the relative cost of 0.48 and 0.50. At the relative area cost of 0.48 the heating demands of C2 and C3 are covered fully by the recovered heat, while the heat demand of C1 is covered fully by the hot utility. The HU consumption remains constant in the zone, equal to the total heat demand of the cold stream C1, until a fourth match becomes economical.

The area of the fourth match H3-C1 increases to 5000 m^2 as the relative area cost is increased from 0.5 to 0.88. The fifth match, H2-C1, being easily interchangeable with H3-C1, then becomes economical. A new balance between the areas of the matches is obtained, where the sum of areas of H2-C1 and H3-C1 is smaller than the area of H3-C1 was alone.

The area of H1-C2 shows no change at the match number change. That is evident, as it is the only match for both H1 and C2 in the solutions. The areas of H2-C3 and H3-C3 show mirror-like area patterns, compensating each other. The sum of the areas of the two exchanger matches is only slightly increasing over the range from 0.4 to 0.89. At that upper boundary, the sum jumps to a new level and then remains nearly constant despite further increase of the relative area cost.

Test runs with a four-match optimum

A similar analysis as above was made with a four-match optimum, chosen from Fig. 6.4.5. The optimal solution was obtained with a = 0.2 and the c_{HU} = 8 €/MWh.

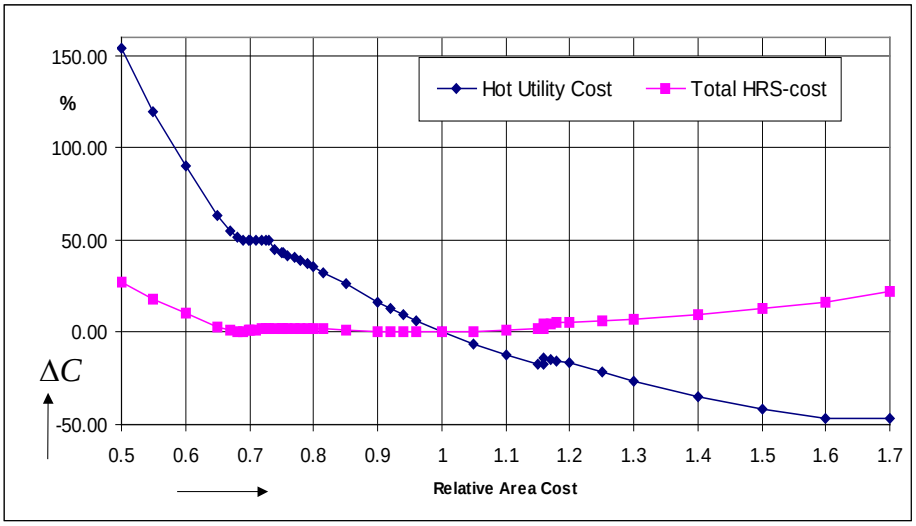

Figure 6.4.8. Hot utility consumption and total HRS-cost as a function of the relative area costs. a = 0.20 and c_{HU} = 8 €/MWh.

.

In Fig. 6.4.8, as in Fig. 6.4.6, two zones of constant hot utility costs are seen. Firstly, the hot utility consumption has a constant level, about 50 % above the optimum HU consumption, in a zone at the relative area cost 0.68 - 0.73. Near the zone the total HRS cost shows a local optimum, which nearly reaches to the global optimum value level.

The second zone of constant hot utility cost is in this case at a relative area cost level higher than the optimum, i.e., at the relative area cost of 1.16. The minimum hot utility consumption is reached at the relative area cost of about 1.6.

The changes in the individual match areas are shown in Fig. 6.4.9. At the relative area cost of 0.5 the number of matches is three, H1-C2, H2-C3 and H3-C3, actually the same matches as above in the five-match-optimum case. At an area cost level of around 0.7 the number of matches changes from three to four. The supply air heat exchanger H3-C1 is included. The total HRS cost in Fig. 6.4.8 decreases very slowly with increased area of H3-C1. This is due to the relatively small benefit that the heat recovery to cold stream C1 brings to the total HRS cost.

The change from four to five matches takes place in this case after the optimum area cost. Another supply air heater H2-C1 is included at that level in the solution.

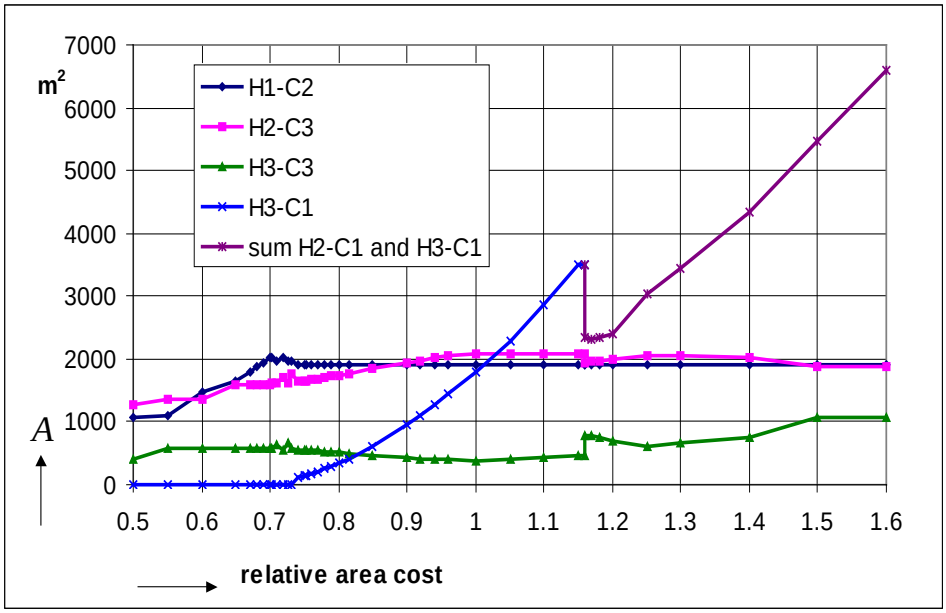

Figure 6.4.9. Match areas as a function of the relative area costs. a = 0.20 and c_{HU} = 8 €/MWh.

Concluding remarks

The optimal energy system structure can be defined as a point-optimal solution with the deterministic optimisation methods and the developed models. The sensitivity analysis is a valuable tool in showing how the optimal structure changes when different data is changed. Sensitivity analysis diagrams show the influence of, for example, different cost factors defining the regions on the diagrams where different optimal system structures prevail. In energy systems a large number of sensitive cost factors can be identified. Multi-dimensional sensitivity analysis can be made and visualised as tables or diagrams as shown in this study. The analysis time can be kept reasonable with a suitable problem formulation that gives sufficiently short computation time for each optimal solution, each as one point in the variable space.

The benefit of the sensitivity analysis is that the influence of the cost parameter variations on the objective value can be determined so that the designer has a quantitative evaluation of the costs of the different solutions before the detailed engineering. Consequently, a practical design structure can be found that is both cost-effective and nearly the global optimum. In Paper V the discussion is continued with a robust design approach taking into account variations of some process parameters.

6.5 Paper V

Design of robust paper machine HRS

The optimisation of paper machine heat recovery systems (HRS), as discussed in sections 3 and 6.3, has the synthesis task to minimize the overall costs, considering simultaneously both energy and investment costs. The optimal solution is obtained with a set of fixed parameters, i.e. a point-optimal solution. If, however, the parameter values are known to vary within certain ranges it is not evident that the point-optimal solution is the most economic one.

In Paper V the discussion was therefore broadened to take also into account variations of the operational parameters. The aim was to compare the point-optimal solutions to solutions with accepted parameter variations, i.e., robust solutions. A process system design is considered to be robust, if it is capable of handling all evolving operation situations. The state-of-art in robust design optimisation is reviewed in a comprehensive survey of Beyer and Sendhoff (2007).

A possible approach to model design uncertainties is to use a multi-data set model. Different expected operational conditions are points in the data set. The target is the best possible solution, where all the points in the set are considered. The problem size will, however, often become extensive with this approach in industrial cases. Therefore, a hybrid method based on evolutionary programming and non-linear programming was chosen in this study. Additionally, a robust design of HRS was obtained by taking into account predetermined variation ranges of two selected parameters.

A HRS with three hot streams and three cold streams was considered, similarly as in Paper III. Condensation can take place in the heat exchangers causing both the specific heat capacity and the overall heat transfer coefficient vary strongly. Calculation of the overall heat transfer coefficient and the specific heat content for condensing streams is presented in Paper IV.

A superstructure was defined for the given HRS synthesis problem, shown in Fig. 6.5.1.

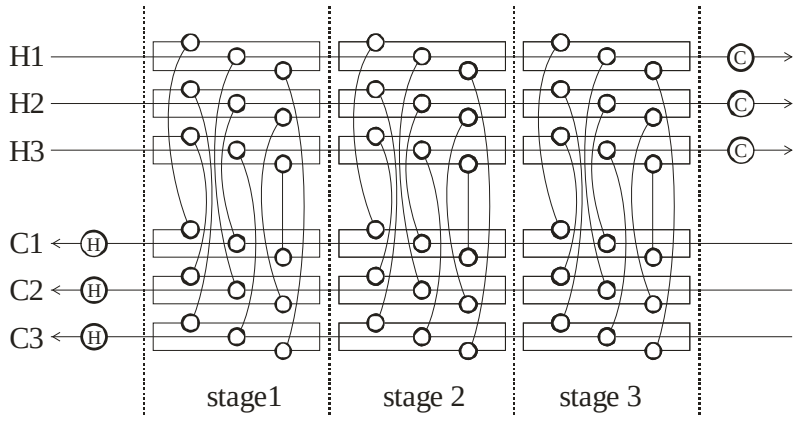

Figure 6.5.1. Superstructure for the HRS design problem with three stages.

The matches between the hot and cold streams are separated into a number of stages. More than one match per stream in one stage indicates a split stream. A solution design may encounter non-isothermal mixing. The approach does not need a fixed minimum approach temperature difference. With three stages and the given number of streams there are 2^{27} or about 135 million different ways to connect the streams within the given superstructure. The supersturture is the same as introduced by Yee and Grossmann (1990).

The objective function was defined as in Paper III to minimise the total annual costs of HRS, i.e. the sum of the investment and running costs of HRS. A heat exchanger investment price was defined by a fixed price part and an area-dependent price part. Concave price functions were applied, as in Paper III.

Hybrid method with GA

A hybrid approach based on GA and NLP is proposed in paper V for solving the robust HRS synthesis problem. The problem is decomposed into a GA part and an NLP part. GA generates decisions about the matches as well as the size of the heat exchanger areas in the network. Each individual in the population represents a possible heat recovery network.

One possible way to represent a design structure is to define for each exchanger one binary variable indicating its existence or non-existence and one real valued variable describing its heat transfer area. In this study the binary variable and the area variable were combined into one real variable bounded between 0 and 1. Thus, in the problem with 3 hot and 3 cold streams in 3 stages each individual consisted of 27 genes with real values between 0 and 1.

An NLP problem was posed to obtain the annual overall cost for every solution candidate in the evolving populations. The minimum utility consumption was determined for the structure and the heat transfer areas for the individuals. In the NLP problem the objective was to minimise the hot utility consumption by deciding an appropriate set of temperatures and split factors. The developed NLP-approach was based on the bisection method (interval halving, Bolzano search).

The values of the genes were transformed to corresponding heat exchanger areas by using a threshold value v_{th}. Two cases were defined. If the value of a gene v is smaller than or equal to the threshold value then the heat transfer area is defined as 0, according to first inequality in Eq. (6.5.1). If v is larger than v_{th} then an area value between the predefined maximum feasible area A_{max} and minimum feasible area A_{min} is defined by second inequality in Eq. (6.5.1)

$$A = \begin{cases} 0 & \text{if } v \le v_{th}, \\ (v - v_{th}) \cdot \dfrac{A_{\max} - A_{\min}}{1 - v_{th}} + A_{\min} & \text{if } v > v_{th} \end{cases} \qquad (6.5.1)$$

The proposed approach was stated as following

1. Randomly generate an initial population.
2. Evaluate fitness for each individual in the population.
2.1 Determine the network structure and available heat transfer areas from the individual using Eq. 6.5.1.
2.2 Solve for the temperatures and split factors, included in the NLP master problem (e.g. using a gradient based search algorithm).
2.2.1 For each function evaluation of the NLP master problem, a number of sub-problems are solved where the remaining temperatures are obtained using the approach based on the Bisection method.
2.3 The sum of the costs for utility consumption arrived at in 2.2 and the investment costs obtained from the utilized heat transfer areas in 2.2.1 is the fitness value for the current individual.
3. Selection and pairing of fit individuals is based on the roulette wheel selection scheme.
4. For mating, the two-point-cross-over, is used to give offspring forming a new population.
5. The new population is finally submitted to mutation, where each gene may change its value randomly with a low probability. If the defined maximum number of generations has been reached, stop the search, otherwise go to step 2.

Case study

The variations in the moisture content of the exhaust air streams, denoted by x, and the flow rate of process water, denoted by F, were chosen to obtain a robust design. The robust design was compared with two point-optimal solutions.

Point-optimal design A

For a point-optimal solution, denoted by design A, the moisture content of the exhaust air was fixed to x=135 gH_2O/kg dry air and the flow rates of process water and circulation water were fixed at 70 and 200 kg/s, respectively. The supply air flow rate was fixed to 70 kg/s and the exhaust air flow rates were fixed to 30 kg/s from each of the three discharge points. Fixed prices and area-dependent prices as well as the hot utility cost, the annuity factor and the exponents for air-to-air and air-to-water matches were taken the same as in Paper IV. With the given set of parameters a point optimal design A, was obtained, shown in Fig. 6.5.2. A population of 20 individuals in 100 generations with the mutation probability of 1% was used in the GA search.

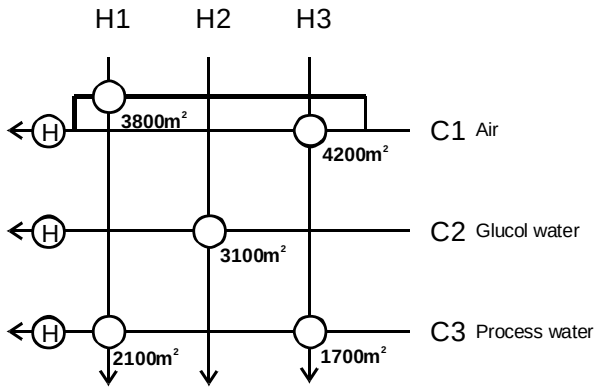

Figure 6.5.2. Point optimal design A.

Robust design R

A robust design, denoted by R, was obtained for the given variations of two operational parameters, the mean moisture content, *x*, and the mean process water flow rate, *F*. The probability for different operational situations was modelled with a normal distribution function. The assumed variations were described by a mean moisture content x = 135 gH_2O/kg dry air with a variance of 20 gH_2O/kg dry air and by a mean process water flow rate F = 70 kg/s and a variance of 5 kg/s. The probabilities for different operational points are shown in Fig. 6.5.3. The obtained robust design R is shown in Fig. 6.5.4.

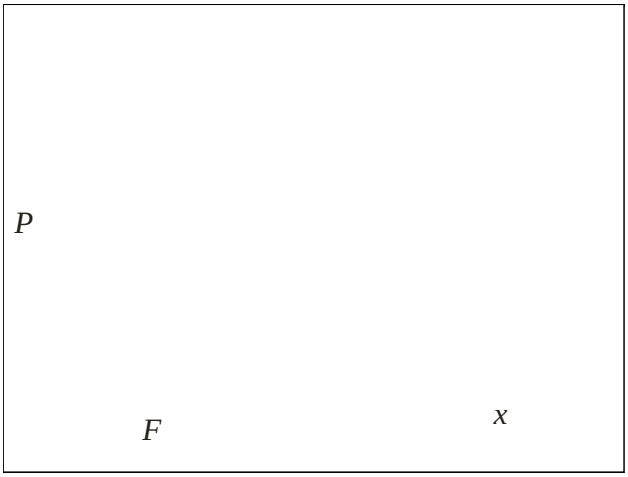

Figure 6.5.3. Overall distribution surface indicating probabilities for different operational points. *F* is the flow rate of process water (kg/s) and *x* is the moisture content of the dryer hood exhaust air (gH_2O/kg dry air).

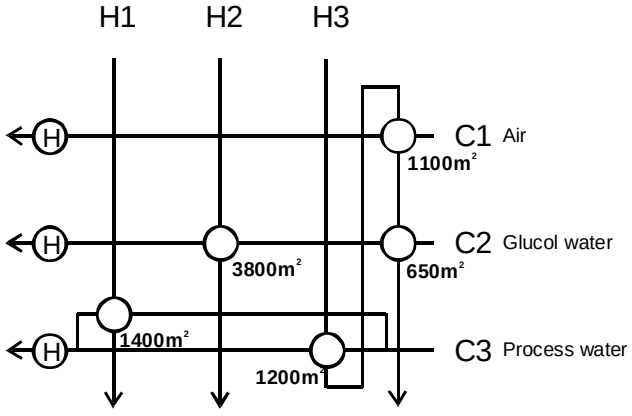

Figure 6.5.4. Robust design R.

When comparing the designs A and R, it can be noted that the robust design R has a considerably smaller total heat transfer area than the point-optimal design A. The biggest difference is in the air-to-air matches.

With the parameter values of x=135 gH_2O/kg dry air and F=70 kg/s, the total annual costs are 0.634 M€ for the point-optimal design A and 0.697 M€ for the robust design R respectively. However, when the given ranges are taken into account the robust design

becomes more economic in large parts of the variation range field. The differences between the costs for the point-optimal design A and the robust design R are shown in Fig. 6.5.5. The negative values indicate the region where the point-optimal solution is more economic, i.e. in the upper left corner.

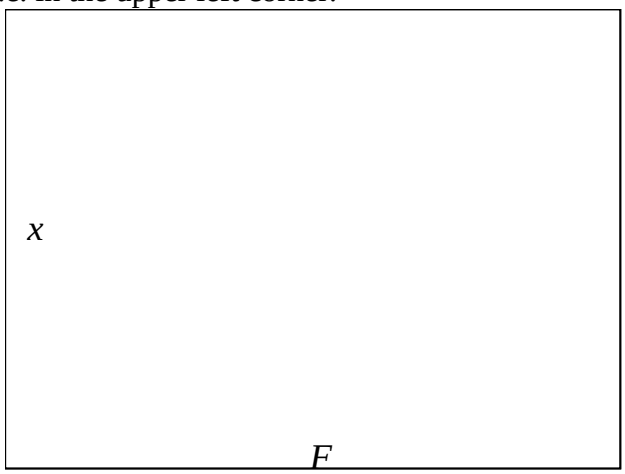

Figure 6.5.5. Differences between the total annual costs (M€/a) of the point-optimal design A and the robust design R.

Point-optimal design B

For the sake of comparison, parameter values were fixed as x=120 and F=75 for a new point optimal solution, denoted by design B. The optimal solution is shown in Fig. 6.5.6. The total annual cost differences between the point-optimal design B and the robust design R are shown in Fig. 6.5.7.

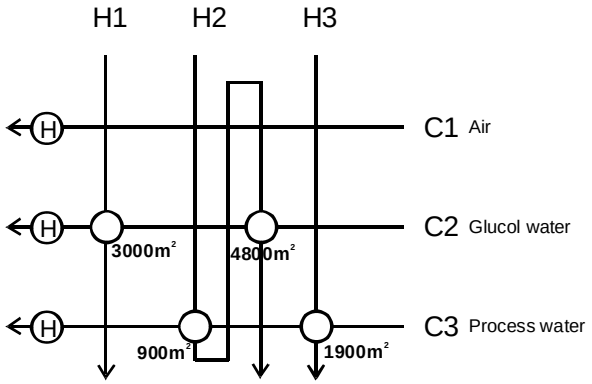

Figure 6.5.6. The point-optimal design B.

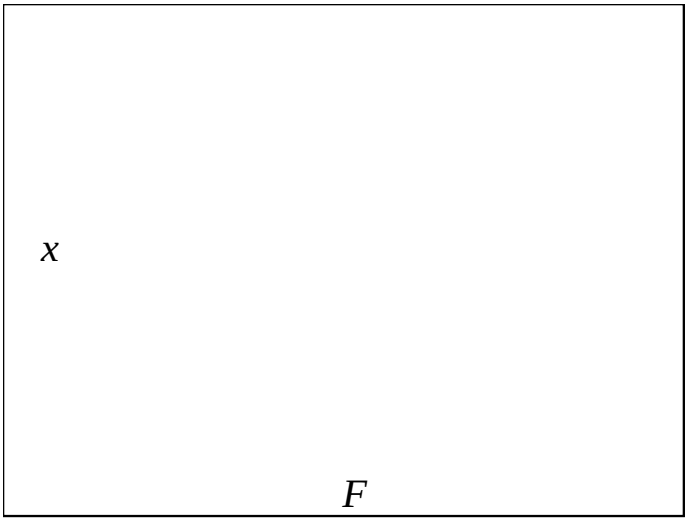

Figure 6.5.7 Differences in the total annual costs (M€/a) of the point-optimal design B and the robust design R.

At a region in Fig 6.5.7, near the fixed parameter values, the difference is negative, i.e. the point-optimal solution B is more economical than the robust solution R. In the other parts of the field the robust design is more economical.

6.6 Paper VI

Enhanced utilisation of excess heat

6.6.1 Heat recovery at Impingement Drying

New drying technologies have been developed that operate with higher temperatures and higher air humidity than those used in the conventional cylinder drying. This opens new possibilities for heat recovery. Impingement drying is one such technology, described comprehensively, e.g., in Sundqvist and Kiiskinen, 2000.

The temperature level in the impingement drying is much higher than in the conventional cylinder drying. An air jet stream at a temperature of 350 °C and a velocity of 90 m/s is blown against the paper web, yielding a drying rate of about 100 kg H_2O/m^2h. This is to be compared with the drying rate of around 30 kg H_2O/m^2h at the conventional cylinder dryer. The higher drying rate means that with the impingement drying the dryer section can be built shorter. Combined dryer systems are built, for instance systems with one third of the total drying realised with impingement drying and two thirds by cylinder drying.

For the heat recovery the impingement drying means that a moist air stream is obtained both at higher temperature and at higher humidity. The exhaust air temperature from the impingement dryer part can be at the level of 200 - 250 °C. This means that heat recovery systems with higher exergy level than before can be built or makes it even possible to convert the available heat into electricity.

The impingement drying has been used on tissue machines with Yankee cylinders. Its application for newspaper or fine paper machines has, however, been lagging behind. A schematic flow sheet of an impingement dryer unit is shown in Fig. 6.6.1.

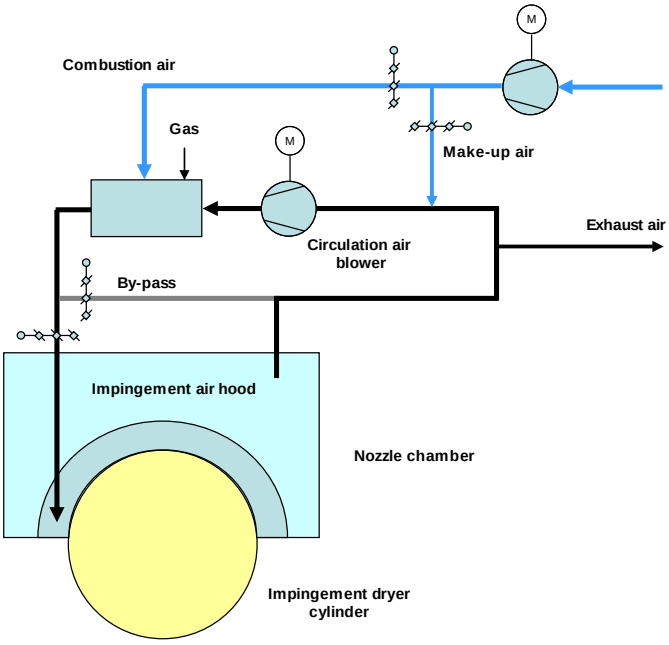

Figure 6.6.1. Impingement dryer unit (modified from Sundqvist and Kiiskinen, 2000).

The dryer cylinder is covered partly by a nozzle chamber where the air nozzles are placed in a short distance from the web surface at the rotating cylinder. The hot air is blown with high speed against the web, causing the high-rate evaporation of the water from the web. After the contact with the web the air is passed to the air hood and further to the suction side of the circulation air blower. The inlet of combustion air and a possible make-up air are balanced by the exhaust air stream. An air by-pass is needed for the sheet break situations.

Test cases with impingement drying

For a paper machine with partial impingement drying an example of input data for heat recovery optimisation is given in Table 6.6.1.

Table 6.6.1. Set of hot and cold stream data for a paper machine with impingement drying.

HOT STREAMS	H1	H2	H3
stream type	exhaust air	exhaust air	exhaust air
air flow, kg d.a./s	30.5	17.2	30.5
temperature, °C	85	236	82
moist.cont., kg H_2O/kg d.a.	0.17	0.26	0.15

COLD STREAMS	C1	C2	C3	C4	C5
stream type	imp.supply air	hood supply air	wire pit water	process water	circ.water
air, kg d.a./s; water, kg/s	17.2	48.9	190	100	150
temperature in, °C	28	28	51	32	28
temperature out, °C	350	95	60	60	45
moist.cont., kg H_2O/kg d.a.	0.02	0.02	-	-	-

C1 is the supply air to the impingement part with a temperature of 350 °C at the impingement nozzles. C2 is the supply air to the cylinder dryer parts with a temperature of 95 °C. Both are taken from the machine hall at an inlet temperature of 28 °C.

C3, C4 and C5 are different process waters that shall be heated. Their flow rates, inlet and outlet temperatures are given in the table.

H1 and H3 are the exhaust air streams from the cylinder drying parts and H2 is the exhaust air from the impingement part. The moist air temperature after the impingement dryer part is 236 °C and the moisture content 0.26 kg H_2O/kg da.

The total available heat from the hot streams is about 45 MW, i.e. from H1 about 15 MW, H2 about 16 MW and H3 about 14 MW.

The layout costs are defined according to the principle drawing, shown in Fig. 6.6.2. The three exhaust air ducts are placed in three positions along the dryer section with the impingement part exhaust air in the middle. The supply air to the impingement drying part, C1 and the two supply air streams to cylinder parts, C2, are entering the HRS directly from the machine hall. C1 and C2 can be heated with any of the hot streams. Wire-pit water, C3, and process water, C4, have their source and target points near the press section and the glycol-water stream, C5, near the dry end.

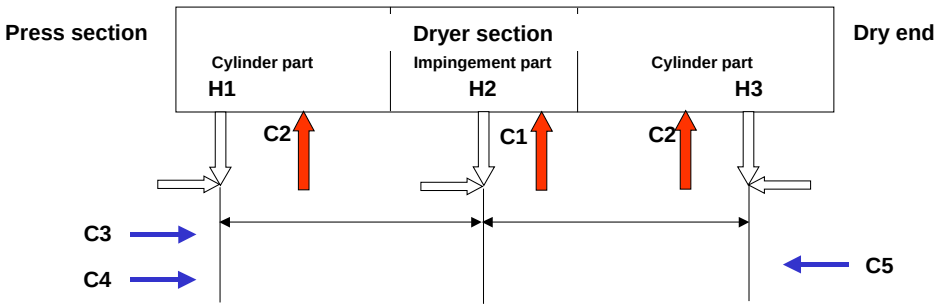

Figure 6.6.2. Principle drawing for the layout costs of HRS with impingement drying.

The chosen prices of the pipelines for the matches are given in Table 6.6.2.

Table 6.6.2. Layout prices for HRS with impingement drying.

cold stream	**C1**	**C2**	**C3**	**C4**	**C5**
matched with	M€	M€	M€	M€	M€
H1	0	0	0.02	0.02	0.06
H2	0	0	0.04	0.04	0.04
H3	0	0	0.06	0.06	0.02

A broad temperature range has to be covered when modelling a heat recovery system with impingement drying. In order to avoid an unnecessary large number of intervals the overall temperature range was partitioned so that in the lower part of the range, from 0 to 30 °C, three intervals, each of 10 °C, from 30 to 150 °C 24 intervals, each of 5 °C, and in the upper part from 150 to 350 °C four intervals, each of 50 °C, were defined. Thus, totally 31 intervals were considered in the overall temperature range from 0 to 350 °C.

Three test cases were considered in order to study the influence of a large number of intervals and a broad temperature range. The cost data and the HRS model from section 6.3 were applied.

Linear, single-period impingement test case, TI-1

The first test case with the impingement drying was a single-period case, denoted by TI-1. The total heating demand of the cold streams was approx. 38 MW. The heat demand of the supply air for the impingement drying part was approx. 6 MW and for the cylinder parts approx. 3 MW. The heat demand of the three process water streams was together approx. 29 MW.

The solution for a single-period impingement test case is shown in Fig. 6.6.3.

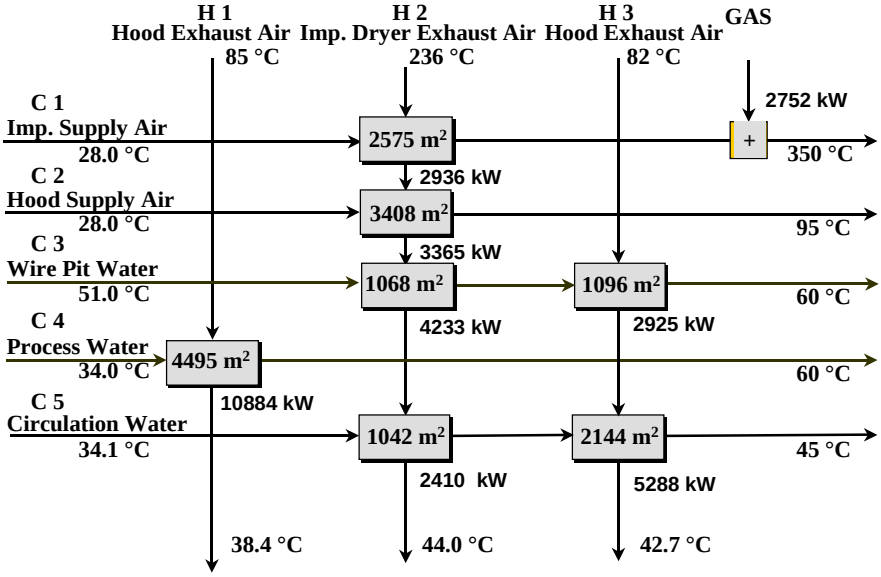

Figure 6.6.3. Solution of the test case TI-1.

Seven matches are obtained in the optimal solution. The total heat transfer area of the matches is 15828 m^2 and the objective value is 0.991 M€/a. A gas burner is used to raise the impingement supply air to 350 °C. The costs of the burner and other equipment for the hot utility are included in the applied utility price of 24 €/MWh. The gas demand is 2.75 MW.

Nonlinear, single-period impingement test case TI-2

Nonlinear area price functions, the same as in section 6.3, were applied with the impingement dryer in the second test case, denoted by TI-2. The objective value was 1.021 M€/a or 3 % higher than with the linear exchanger prices. In the solution the gas demand was 2.70 MW together with a small preheating with low-pressure steam of 130 kW.

Linear, multi-period impingement test case TI-3

In the third test case, denoted by TI-3, the same seasonal temperature data were applied as in section 6.3 to formulate a multi-period model. The total area in TI-3 was about 15830 m^2 and the objective value 1.210 M€/a. The hot utility demands in different periods are shown in Table 6.6.3.

Table 6.6.3. Cold stream heat balances in different periods in the test case TI-3.

	p1	**p2**	**p3**	**p4**
period	MW	MW	MW	MW
heating demand	53.35	44.81	34.79	25.50
recovered heat	39.20	38.03	32.04	22.69
gas	2.64	2.64	2.75	2.77
low-pressure steam	11.51	4.14	0	0.04

When comparing the solution of the linear multi-period test case TI-3 with the solution of the linear single-period test case TI-1 the same 7 matches were included. The total heat transfer area is actually the same, while the objective value is significantly higher in the test case TI-3 than in the test case TI-1, because of higher hot utility demands.

Concluding remarks

In the test cases with impingement drying the number of cold streams was larger than in the test cases in section 6.3. This gave the opportunity to utilise the available excess heat from the impingement drying effectively inside the heat recovery system. Excess heat can also be used in several other ways, for instance in process water evaporators operating at low temperatures and low pressures. Other alternatives could be utilisation of the heat outside the mill for other drying processes or generation of electric power.

6.6.2. Upgrade of secondary heat streams

Absorption heat transformers (AHT) can be used to elevate a stream temperature above the temperature of excess heat stream. In Paper VI AHT is proposed to be used for upgrading of the heat of the exhaust air streams from a paper machine. A large amount of low grade heat is usually available at paper mills without a meaningful utilisation.

In Paper VI, as an example, the supply air to a paper machine dryer with cylinder drying is proposed to be heated to the usual inlet temperature of 95 °C by an absorption heat transformer. The working principle of AHT is shown in Fig. 6.6.4.

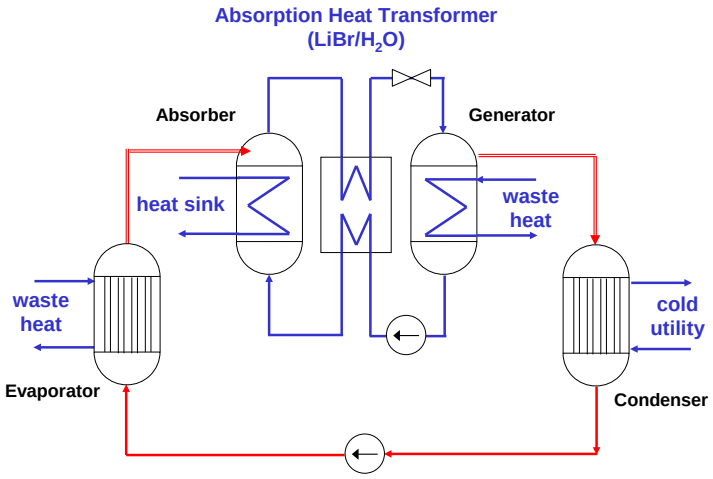

Figure 6.6.4. Working principle of absorption heat transformer.

The respective pressure vs. temperature diagram is shown in Fig. 6.6.5, where LiBr/H_2O mixture is considered as the working fluid.

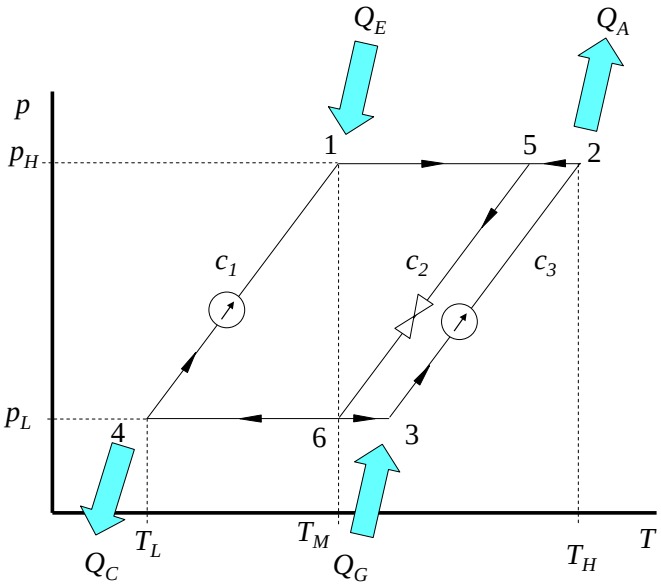

Figure 6.6.5. p,T-diagram of an AHT.

The COP of AHT is defined as

$$\mathrm{COP}_{\mathrm{AHT}} = \frac{\dot{Q}_A}{\dot{Q}_E + \dot{Q}_G} \tag{6.6.1}$$

$\dot{Q}_A$ is the heat flow from the absorber at an elevated temperature T_H. $\dot{Q}_E$ and $\dot{Q}_D$ are the waste heat flows at the medium temperature T_M into the evaporator and the generator respectively. Both flows can have approximately same temperature, so they can be the same waste heat stream, split into two parts. $\dot{Q}_C$ is the heat flow from the condenser at a lower temperature T_C.

In AHT two excess heat streams are used as heat sources. The temperature of a heat sink stream is raised above the temperature of the heat sources. With Li/Br-water as the working fluid AHT can have up to 50 °C temperature difference between the heat sources and the heat sink. The coefficient of performance is about 0.5.

One possible use of AHT at a paper mill is shown in Fig. 6.6.6. The supply air is heated in the absorber. Additionally, glycol water for the machine room ventilation air heaters is heated with the exhaust air (1) and the mill process waters are heated with the exhaust air (2) after the generator.

Two exhaust air streams of around 60 kg d.a./s, both at around 85 °C and with 0.160 kg H_2O/kg da are used as heat sources. Water vapour is produced in the evaporator at around 0.15 bar and 55 °C with the heat of the exhaust air (1) and absorbed in the absorber into a circulating lithium bromide solution. The LiBr-concentration of the solution is about 60 %. It is diluted in the absorber by the water vapour to about 55 %. The heat sink in the absorber is the supply air that is taken from the machine hall at around 30 °C and heated up to around 95 °C.

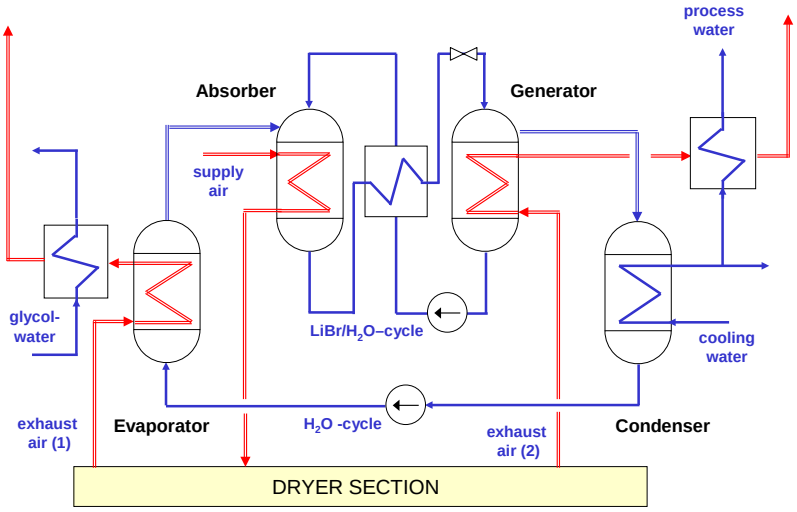

Figure 6.6.6. Schematic flow diagram of AHT for paper machine dryer section.

The LiBr-solution is led to the generator via an intermediate heat exchanger, causing an improvement of the performance of the AHT. In the generator the water, which was absorbed in the absorber, is evaporated by the heat of the exhaust air (2). The concentrated LiBr-solution is pumped via an intermediate heat exchanger back to the absorber. The obtained water vapour from the generator is condensed at the condenser by the cooling water. The condensate from the condenser is pumped back to the evaporator.

The exhaust air streams are cooled in the evaporator and generator to around 60 °C. With an additional heat exchanger the process water, which has been preheated as part of the condenser cooling water, can be heated further to 55 °C.

Around 3 MW of low pressure steam is saved in the given example by the use of AHT in comparison with a conventional dryer. Around two thirds of the moisture content of the exhaust air is condensed for water reuse, i.e. about 13 kg/s in the present case.

In the proposed AHT all the heat exchangers have a liquid phase at least on one side. Additionally, all the exhaust air-to-liquid heat exchangers have condensation of the air humidity. This means that the heat transfer coefficients of the heat exchangers are relatively high.

6.6.3. Power from low grade heat

The Organic Rankine Cycle (ORC) is an interesting option for the electric power generation from low grade heat. The ORC-technology has been applied for instance in many geothermal power plants. The basic ORC is a power cycle with a one-component organic working fluid. The possibilities to use ORC for power generation at paper mills are discussed in Paper VI.

ORC with high-speed technology has been studied intensively (e.g. Larjola, 1995). In a high-speed construction the turbine, the generator and the circulation pump are built on the same shaft. The unit can be built hermetic. The rotational speed of the turbine is much higher than in a conventional ORC and consequently the equipment sizes are strongly reduced.

An ORC process at an integrated paper mill with thermo-mechanical pulp (TMP) production is proposed in Paper VI. The TMP heat recovery steam (HR steam) is usually used at the paper machine for the cylinder drying. If, however, impingement drying is applied at the paper machine, the low-pressure steam consumption is reduced strongly, as a part of it is replaced by the hot impingement air, heated by gas burners.

A schematic flow diagram of an ORC is shown in Fig. 6.6.7, with the TMP-heat recovery steam as the heat source and the paper mill process water as the heat sink. The cycle efficiency can be improved with a recuperator between the turbine and the condenser.

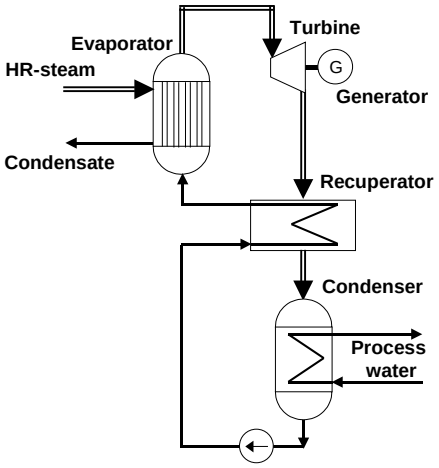

Figure 6.6.7. Flow diagram of an ORC with TMP heat recovery steam as the heat source.

A newsprint machine with a paper basis weight of 40 g/m^2 absolute dry web, a machine speed of 1700 m/min and a web width of 10 m is taken here as an example. The paper production at the machine is 12.3 kg/s air-dry paper with 92 % dry solids. With a specific energy consumption at the TMP-refiners of 2000 kWh/t pulp of 90 % dry solids the installed refiner effect is about 100 MW and the steam production about 1 ton steam/MWh.

The paper machine dryer section in this example is assumed to have 30 % impingement drying and 70 % cylinder drying. The paper is further assumed to be dried in the dryer section from 48 % to 92 % dry solids. With these figures it can be estimated that 6 kg/s of TMP-steam becomes excessive and available for ORC.

Different working fluids can be considered for ORC. One option is ammonia. The pressure of the NH_3-gas before the turbine would be about 90 bar(a) and the temperature 120 °C. The condensation pressure of the NH_3 would be about 12 bar(a). The relatively high pressures lead to elevated plant costs. Other suitable working fluids could be isobutane or isopentane, with the known risks of inflammability. The critical point of isobutane is at 36 bar(a) and 135 °C and of isopentane at 34 bar(a) and 187 °C.

With isopentane as working fluid an overall efficiency of 14 % for the power generation could be obtained. With 6 kg/s TMP-steam 1.8 MW power could be generated. A specific plant price assumed in Paper VI is 2000 €/kW. The price assumption is comparable with prices for other power generation technologies. The specific price would mean an investment of 3.6 million €. With the given data and with depreciation of 10 years and interest rate of 10 % (annuity factor = 0.16) the investment cost would be 0.04 €/kWh. If the TMP heat recovery steam can be supplied without an internal charge, the price of the generated electricity would be competitive.

An idea of reducing the assumed investment price above is presented in Paper VI. The steam directly from the TMP-refiners could possibly be used in ORC, instead of the steam from the TMP heat recovery system. This would mean that a part of the reboilers in the heat recovery system could be omitted. The idea is based on the consideration that the construction of an ORC-evaporator is close to the reboiler construction. Possible technical obstacles are not evaluated in the paper.

In Paper VI an improvement of the basic ORC, the Kalina cycle, is discussed briefly. A binary working fluid NH_3/H_2O, for instance 80 % NH_3 and 20 % H_2O, is used in the Kalina cycle. A schematic flow diagram of one type of Kalina cycles (from Leibowitz and Mlcak, 1999) is shown in Fig. 6.6.8 with TMP heat recovery steam as the heat source.

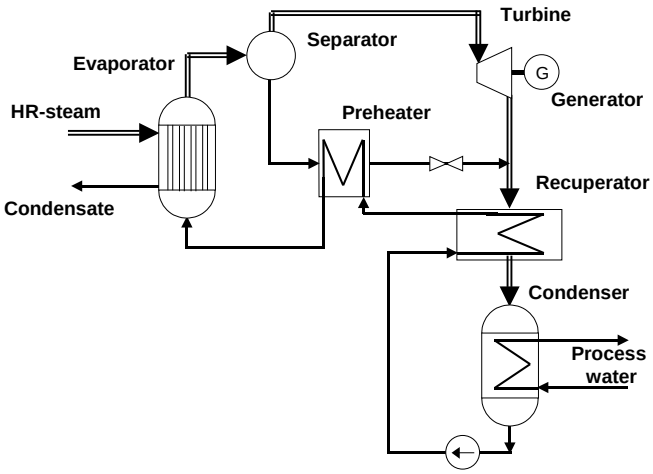

Figure 6.6.8. A Kalina Cycle for power generation from TMP heat recovery steam.

In the Kalina cycle in Fig. 6.6.8 the vapour from the evaporator is partitioned into an NH_3-rich gas stream that is led to the turbine, and an H_2O-rich stream that is cooled in a preheater and mixed back with the NH_3-rich stream after the turbine.

7 Conclusions

Optimisation of different energy systems were studied in the present work, considering both structural and operational optimisation. The aim of the work was to put forward different model formulations and to study how the developed models perform in different design situations. The cases that were studied were taken from industrial processes and from large regional energy distribution systems. The studied energy systems were the distributed energy systems comprising different energy conversation technologies, district cooling systems with cold water chillers, heat recovery systems in connection with humid air streams and a selection of processes for enhanced utilisation of excess heat.

The developed optimisation models were based on mixed integer linear programming (MILP), mixed integer nonlinear programming (MINLP) and on a hybrid approach with nonlinear programming (NLP) and genetic algorithms (GA).

A model for the optimisation of decentralised or distributed energy systems (DES) was developed in the work, studying how the DES should be built in a given region and the most cost effective way of the system operation, with respect to the annual variations of consumer demands of heating and electrical power. Different technologies for generation of distributed energy were taken into account. The combined heat and power plant was found to be a preferred alternative for DES with the given set of design and cost data in comparison with thermal boilers for heat production and wind turbines for electricity generation.

For optimisation of District cooling systems (DCS) an MILP model was developed and tested in a region with different cooling demand situations. A study was made to predict with a long term design perspective how a regional district cooling system should be optimally expanded based on the consumer cooling demand development.

The optimisation models for the DES and DCS problems give valuable guidance for planning and design of district heating and cooling systems. The developed approaches should be available for all stakeholders in the energy supply field, the energy plants, the equipment suppliers, the design engineers, the energy consumers and the authorities to enable them to make right decisions in the design processes.

Models for optimisation of heat recovery systems (HRS) were also developed in the work. The focus was on systems with moist air streams, such as different dryers, but the formulations are applicable also in other types of heat exchanger network synthesis problems. A simultaneous optimisation approach was chosen with the objective to minimise the total cost of a recovery system with a set of hot and cold streams. A partitioning of the overall temperature range of the system into a number of temperature intervals was chosen in order to take into account the strong nonlinearities due to condensation inside the heat recovery exchangers.

The optimisation models were first tested with data from a large paper machine with a conventional cylinder dryer section. Secondly, the influence of impingement drying on the optimisation was studied with higher exhaust temperatures and moisture contents than in the conventional cylinder drying. The high exergy heat in the exhaust air stream from the impingement part was effectively utilised inside the heat recovery system.

The HRS optimisation models were built with linear, nonlinear and piecewise linear heat transfer area cost functions. Models with linear area costs showed good results and are preferable especially in large systems due to relatively short computational times. Piecewise linear cost functions were used as under-estimators for the concave cost functions in order to obtain a lower bound for the respective nonlinear solution. The influence of the yearly variations of the mill-site outdoor air temperature and the river water temperature on the optimisation was studied in multi-period cases.

The influence of variations in the hot utility prices and the annuity factors for investment costs on the solutions was analysed on a broad scale. Boundary values of the two parameters for the changes in the number of matches, included in the solution, were defined. The flatness of the objective function in the region near the optimum was shown with the area cost tests. The areas of the individual matches showed strong variations at the structure boundaries.

The solution of an energy system optimisation depends on a large amount of process data and cost factors. With fixed parameters the solution is a point in an *n*-dimensional space. The question is how the optimal solution changes when some of the data is changed. The influence of the data variations was studied in the work on heat recovery systems with moist air streams as heat sources. The aim was to compare the point-optimal solutions with robust solutions within given parameter variation ranges. A hybrid approach based on evolutionary programming and non-linear programming was applied to solve the problem. The importance of considering varying parameters in the design of paper machine HRS was demonstrated with a case study.

The possibilities to apply Absorption Heat Transformers (AHT) in elevating a stream temperature above the temperature of a low temperature excess heat stream, for instance, the exhaust air streams from a paper machine, were studied. Large amount of low grade heat is usually available at paper mills without a meaningful utilisation. A system developed for paper machine dryer section was proposed where low pressure steam could be saved by AHT.

The Organic Rankine Cycle (ORC) was studied for electric power generation from low grade heat. The ORC technology has been applied for instance in many geothermal power plants. In connection with an integrated paper mill with thermo-mechanical pulp production and impingement drying power generation with ORC was considered. In the discussed situation and with the given cost structure an ORC power generation plant could generate electricity at a competitive price.

The model development always includes an uncertainty of the practical use of the results. The aim in this work was to create models that give solutions usable as starting points for engineering in the practical energy systems design. Different users of the models with different computer facilities are considered when the model sizes are evaluated. The trade-off between the computation time and the inclusion of details has

been the basic guideline for the modelling. For a formulation that makes it possible to solve a problem in a feasible computation time, many assumptions are normally needed. The models developed in this work have, therefore, been given sufficient detail in order to avoid oversimplifications, but have been formulated general enough to make the computation time in a standard personal computer feasible. This was verified in the test cases by evaluating the obtained results with known practical designs and noting that the computation time was not prohibitive on a conventional PC.

Notations

Variables

A	Heat transfer area, m^2
C	Cost, €/year
c	Unit cost coefficient
c_p	Specific heat capacity, kJ/kg K
E	Electricity, kW
f_{cond}	Condensation factor, -
$\dot{m}$	Material flow, kg/s
n_S	Number of supplier sites
n_C	Number of consumer sites
n_R	Number of storage sites
n_L	Number of pipeline parts
n_P	Number of periods
P	Power transmission rate, kW
P	Price, €
$\dot{Q}$	Cooling effect flow rate, kW
$\dot{Q}$	Heat flow rate, kW
t	Time, h
U	Overall heat transfer coefficient, kW/m^2 K
U	A large number
x	Air moisture content, kg H_2O/kg d.a.
y	Binary variable
α	Heat transfer coefficient, kW/m^2 K
β	Mass transfer coefficient, m/s
θ	Temperature, °C
$\Delta\theta$	Difference in temperature, °C
ΔH_{cond}	Latent heat of condensation, kJ/ kg H_2O
ε	Acceptance criterion, -

Subscripts and abbreviations

a	Air
bar(a)	absolute pressure in bar
c	Cold stream
cap	Capacity
CHP	Combined Heat and Power
Cm	Consumer site
cond	Condensation, condensate
CU	Cold utility
d	Dry part

da	Dry air
DC	District Cooling
DCS	District Cooling System
DES	Distributed Energy System
DH	District heating
E	Heat exchanging
F	Fixed investment cost
Gm	Main grid power at consumer site *Cm*
h	Hot stream
HRS	Heat Recovery System
HU	Hot utility
i	Hot stream interval
i	Supplier
in	Input
Inv	Investment cost
j	Pipeline
j	Cold stream interval
k	Storage
k	Calculated value
kW(th)	kW thermal effect
l	Lower
Lb	Pipeline part
Lj	Pipeline part
lm	logarithmic mean
m	Consumer
m	Mean
ma	Moist air
n	Number of units in a set
Om	Own heat production at consumer site *Cm*
Oper	Running cost
ORC	Organic Rankine Cycle
out	Output
p	Period
Q	Heat containing
R	Residual heat, discharged heat
Rk	Storage site
sat	Saturated
SD	Size-dependent investment cost
Si	Supplier site
tot	Total
u	Upper
w	Wall
x	Trial value
XP	Site without power generation
XH	Site without heat production
Zm	Own heat pump at consumer site *Cm*

Index sets

C	Set of cold streams
H	Set of hot streams
I	Set of hot stream intervals
I	Set of supplier sites
J	Set of cold stream intervals
J	Set of line parts
K	Set of heat storage sites
M	Set of consumers
N_{HU}	Set of hot utilities
P	Set of periods

References

Alanne K., Saari A., Distributed energy generation and sustainable development, Renewable and Sustainable Energy Reviews, 10, 2006, 539–558.

Aye, L., Charters, W.W.S., Electrical and engine driven heat pumps for effective utilisation of renewable energy resources, Appl. Thermal Eng., 23, 2003, 1295–1300.

Barbaro, A., Bagajewicz, M.J., New rigorous one-step MILP formulation for heat exchanger network synthesis, Comp. Chem. Eng., 29, 2005, 1945–1976, with Corrigendum, Comp. Chem. Eng., 30, 2006, 1310–1313.

Benders, J.F., Partitioning procedures for solving mixed-variables programming problems, Numerische Matematik, 4, 1962, 238–252.

Beyer H-G., Sendhoff, B., Robust optimization - A comprehensive survey, Comp. Methods in Appl. Mech. and Eng., 196, 2007, 3190–3218.

Bidini, G. Desideri, U., Di Maria, F., Baldacci, A., Papale, R., Sabatelli, F., Optimization of an integrated gas turbine-geothermal power plant, Energy Conversion and Management, 39, 1998, 1945–1956.

Biegler, L.T., Grossmann, I.E., Retrospective on optimization, Comp. Chem. Eng., 28, 2004, 1169–1192.

Biegler, L.T., Grossmann, I.E., Westerberg, A.W., Systematic Methods of Chemical Process Design, Prentice Hall, 1997.

Burer, M., Tanaka, K., Favrat, D., Yamada, K., Multi-criteria optimization of a district cogeneration plant integrating a solid oxide fuel cell–gas turbine combined cycle, heat pumps and chillers, Energy, 28, 2003, 497–518.

Cena, V., Mustacchi, C. Natali, F., Synthesis of heat exchange networks: a non-iterative approach, Chem. Eng. Sci., 32, 1977, 1227–1231.

Cerda, J., Westerberg, A.W., Mason, D. Linnhoff, B., Minimum utility usage in heat exchanger network synthesis, Chem. Eng. Sci., 38, 1983, 373–387.

Cerda, J., Westerberg, A.W., Synthesizing heat exchanger networks having restricted stream/stream matches using transportation problem formulations, Chem. Eng. Sci., 38, 1983, 1723–1740.

Chan, A.L.S., Chow, T.T., Fong, S.K.F., Lin, J.Z., Performance evaluation of district cooling plant with ice storage, Energy, 31, 2006, 2750–2762.

Chen, J.J.J., Comments on improvements on a replacement for the logarithmic mean, Chem. Eng. Sci., 42, 1987, 2488–2489.

Chinese, D., Meneghetti, A., Optimisation models for decision support in the development of biomass-based industrial district-heating networks in Italy, Applied Energy 82, 2005, 228–254.

Chow, T.T., Fong, K.F., Chan, A.L.S., Yau, R., Au, W.H., Cheng, V., Energy modelling of district cooling system for new urban development, Energy and Buildings, 36, 2004, 1153–1162.

Ciric, A.R., Floudas, C.A., Heat exchanger network synthesis without decomposition, Comp. Chem. Eng., 15, 1991, 385–396.

Cormio C., Dicorato M., Minoia A., Trovato M., A regional energy planning methodology including renewable energy sources and environmental constraints, Renewable and Sustainable Energy Reviews, 7, 2003, 99–130.

Crowder, H.P., Johnson, E.L., Padberg, M.W., Solving large-scale zero-one linear programming problems, Oper. Res., 31, 1983, 803–834.

Curti, V., von Spakovsky, M.R., Favrat, D., An environomic approach for the modeling and optimization of district heating network based on centralized and decentralized heat pumps, cogeneration and/or gas furnace. Part I: Methodology, Int. J. Therm. Sci, 39, 2000, 721–730. (a)

Curti, V., Favrat, D., von Spakovsky, M.R., An environomic approach for the modeling and optimization of district heating network based on centralized and decentralized heat pumps, cogeneration and/or gas furnace. Part II: Application, Int. J. Therm. Sci, 39, 2000, 731–741. (b)

Daichendt, M.M., Grossmann I.E., Preliminary Screening Procedure for the MINLP Synthesis of Process Systems- II. Heat Exchanger Networks, Comp. Chem. Eng., 18, 1994, 679–709.

Danzig, G.B., Linear Programming and extensions, Princeton University Press, 1963.

Duran, M.A., Grossmann, I.E., An outer-approximation algorithm for a class of mixed-integer nonlinear programs, Math. Progr., 36, 1986, 307–339.

Fishbone L.G., Abilock H.M., MARKAL, a linear programming model for energy systems analysis: technical description of the BNL version, Int. J. of Energy Research 1981, 353–375.

Floudas, C.A., Ciric, A.R., Grossmann, I.E., Automatic synthesis of optimum heat exchanger network configurations, AIChE J., 32, 1986, 276–290.

Fuglsang, P., Madsen, H.A., Optimization method for wind turbine rotors, J. of Wind Engineering and Industrial Aerodynamics, 80, 1999, 191–206.

Galli, M.R., Cerdá, J., A Customized MILP approach to the synthesis of heat exchanger networks reaching specified topology targets, Ind. Eng. Chem. Res., 37, 1998, 2479–2495.

Galli, M.R., Cerdá, J., Synthesis of heat exchanger networks featuring minimum number of constrained-size shells of 1-2 type. Appl. Thermal Eng., 20, 2000, 1443–1467.

Geoffrion, A.M., Generalized Benders Decomposition, J. Optim. Theory and Appl., 10, 1972, 237–260.

Gomory, R.E., An algorithm for the mixed integer problem, Technical report RM-2597, The Rand Corp.,1960.

Grohnheit P.E., Economic interpretation of the EFOM model. Energy Economics 1991; 13(2):143–152.

Grossmann, I.E., Biegler, L.T., Future perspective on optimization, Comp. Chem. Eng., 28, 2004, 1193–1218.

Grossmann, I.E., Caballero, J.A., Yeomans, H., Advances in mathematical programming for automated design, integration and operation of chemical processes, Proc. of PI'99, Int. Conf. on Process Integration, Vol. I, 37–65, Copenhagen, 1999.

Grossmann, I.E. and Sargent, R.W.H., Optimum design of heat exchanger networks, Comp. Chem. Eng., 2, 1978, 1–7.

Grossmann, I.E., Mixed-integer optimization techniques for algorithmic process synthesis, Advances in Chem. Eng., 23, 1996, 171–246.

Gundersen, T., A process integration primer, Report on IEA Implementing Agreement on Process Integration, SINTEF Energy Research, 2000.

Gundersen, T., Grossmann, I.E., Improved optimization strategies for automated heat exchanger network synthesis through physical insights. Comp. Chem. Eng., 14, 1990, 925–944.

Gundersen, T., Naess, L., Synthesis of cost optimal heat exchanger networks. An industrial review of the state of the art, Comp. Chem. Eng., 12, 1988, 503–530.

Hillier, F. S., Lieberman, G. J., Introduction to operations research, 5th ed., McGraw-Hill, 1980.

Hiremath R.B., Shikha S., Ravindranath N.H., Decentralized energy planning; modeling and
application – a review, Renewable and Sustainable Energy Reviews, 11, 2007, 729–752.

Hohmann, E.C., Optimal networks for heat exchange, Ph.D. thesis, Univ. of Southern California, Los Angeles, 1971.

Hohmann, E.C., Lockhart, F.J., Optimum heat exchanger network synthesis, AIChE 82nd National Meeting, Atlantic City, N.J.,1976.

Holland, J., Adaptation in natural and artificial systems, Ann Arbor, Univ. of Michigan Press, 1975.

Huang, F., Elshout, R., Optimizing the heat recovery of crude units, Chem. Eng. Prog., 72, 1976, 68–74.

Hwa, C.S., Mathematical formulation and optimisation of heat exchanger networks using separable programming. AIChE - Ind. Chem. Eng. Symp. Series, nr 4, 1965, 101–106.

International Energy Agency, World Energy Outlook 2004, OECD/IEA, 2004.

Karlsson, M.(ed.), Papermaking, Part 2, Drying, Papermaking Science and Technology, Book 9, Fapet, 2000.

Karmarkar, N., A new polynomial time algorithm for linear programming, Combinatorica, 4, 1984, 373–395.

Kelley, J.E., The Cutting-Plane method for solving convex programs, Journal of SIAM, 8, 1960, 703–712.

Kesler, M. G. and Parker, R. O., Optimal networks of heat exchange, Chem. Eng. Progr. Symp. Series, 65, 1969, 111–120.

Khan, F.I., Hawboldt, K., Iqbal, M.T., Life Cycle Analysis of wind–fuel cell integrated system, Renewable Energy, 30, 2005, 157–177.

Kobayashi, S., Umeda, T. and Ichikawa, A., Synthesis of optimal heat exchange systems - an approach by the optimal assignment problem in Linear Programming, Chem. Eng. Sci., 26, 1971, 1367–1380.

Kocis, G.R., Grossmann, I.E., Relaxation strategy for the structural optimization of process flow sheets, Ind. Eng. Chem. Res., 26, 1987, 869–1880.

Kongtragool, B., Wongwises, S., A review of solar-powered Stirling engines and low temperature differential Stirling engines, Renewable and Sustainable Energy Reviews, 7, 2003, 131–154.

Kuhasalo, A., Niskanen, J., Paltakari, J., Karlsson, M., Introduction to paper drying and principles and structure of a dryer section, Papermaking Science and Technology, Book 9(M. Karlsson, ed.), Ch. 1, 16–53, Fapet, 2000.

Larjola, J., Electricity from industrial waste heat using high-speed organic Rankine cycle (ORC), Int. J. Production Economics, 41, 1995, 227–235.

Lee, K.F., Masso, A.H., Rudd, D.F., Branch and bound synthesis of integrated process designs, Ind. Eng. Chem. Fundamentals, 9, 1970, 48–58.

Leibowitz, H.M., Mlcak, H.A., Design of a 2-MW Kalina Cycle. Binary Module for Installation in Husavik, Iceland, Geothermal Resources Council Trans., 1999, 75–80.

Linnhoff, B., Pinch Analysis - a state-of-the-art overview, Trans. Inst. Chem. Eng., 71, 1993, 503–521.

Linnhoff, B., Flower, J.R., Synthesis of heat exchanger networks, AIChE Journal, 24, 1978, 633–642.

Linnhoff, B., Hindmarsh, E., The Pinch Design Method for heat exchanger networks, Chem. Eng. Sci., 38, 1983, 745–763.

Marbe, Å., Harvey, S., Berntsson, T., Biofuel gasification combined heat and power—new implementation opportunities resulting from combined supply of process steam and district heating, Energy 29, 2004, 1117–1137.

Masso, A.H., Rudd, D.F., The synthesis of system designs: II Heuristic structuring, AIChE Journal, 15, 1969, 10–17.

Nieminen J., Kivelä M., Biomass CFB gasifier connected to a 350 MWth steam boiler fired with coal and natural gas—THERMIE demonstration project in Lahti in Finland, Biomass and Bioenergy, 15, 1998, 251–257.

Nishida, N., Kobayashi, S., Ichikawa, A., Optimal synthesis of heat exchange systems: Necessary conditions for minimum heat transfer area and their application to systems synthesis, Chem. Eng. Sci., 26, 1971, 1841–1856.

Nishida, N., Stephanopoulos, G., Westerberg, A.W., A review of process synthesis, AIChE Journal, 27, 1981, 321–351.

Obernberger I., Decentralized biomass combustion: state of the art and future development, Biomass and Bioenergy, 14, 1998, 33–56.

Paish, O., Small hydro power: technology and current status, Renewable and Sustainable Energy Reviews, 6, 2002, 537–556.

Papoulias, S.A., Grossmann, I.E., A structural optimization approach to process synthesis - II: Heat recovery networks, Comp. Chem. Eng., 7, 1983, 707–721.

Pardalos, P.M., Rosen, J.B., Constrained global optimization: algorithms and applications, vol 268, Lecture notes in Computer Science, Springer, 1987.

Pettersson, F., Synthesis of large-scale heat exchanger networks using a sequential match reduction approach, Comp. Chem. Eng., 29, 2005, 993–1007.

Pettersson, H., External noise control in the pulp and paper industry - efficiency and economy, Proc. of Intern, Congress and Exhibition on Noise Control Eng., The Hague, 2001.

Pho, T.K., Lapidus, L., Topics in computer-aided design: Part II. Synthesis of optimal heat exchanger networks by tree searching algorithm, AIChE J., 19, 1973, 1182–1189.

Pilavachi, P.A., Mini- and micro-gas turbines for combined heat and power, Appl. Thermal Eng., 22, 2002, 2003–2014.

Pohekar S.D., Ramchandran M., Application of multi-criteria decision making to sustainable energy planning – a review, Renew Sustainable Energy Rev., 2004, 365–381.

Ponton, J.W., Donaldson, R.A.B., A fast method for synthesis of optimal heat exchanger networks, Comp. Chem. Eng., 29, 1974, 2375–2377.

Ranta T., Logging residues from regeneration fellings for biofuelproduction - a GIS-based availability analysis in Finland, Biomass and Bioenergy, 28, 2005, 171–182.

Rudd, D.F., The synthesis of system designs: I. Elementary decomposition theory, AIChE Journal, 14, 1968, 343–349.

Sakawa, M., Kato, K., Ushiro, S., Operational planning of district heating and cooling plants through genetic algorithms for mixed 0–1 linear programming, European J. Oper. Res., 137, 2002, 677–687.

Savola, T., Keppo, I., Off-design simulation and mathematical modeling of small-scale CHP plants at part loads, Appl. Thermal Eng., 25, 2005, 1219–1232.

Sen, Z., Solar energy in progress and future research trends, Progress in Energy and Combustion Science, 30, 2004, 367–416.

Shethna, H.K., Jezowski, J.M., Castillo, F.J.L., A new methodology for simultaneous optimization of capital and operating cost targets in heat exchanger network design, Appl. Thermal Eng., 20, 2000, 1577–1587.

Spets, J-P., Ahtila, P., Improving the power-to-heat ratio in CHP plants by means of a biofuel multistage drying system, Appl. Thermal Eng., 22, 2002, 1175–1180.

Sundqvist, H., Dryer section ventilation and heat recovery, Papermaking Science and Technology, Book 9, ed. Karlsson, M., Ch. 9, 295–331, Fapet, 2000.

Sundqvist, H., Kiiskinen, H., Air impingement drying, Papermaking Science and Technology, Book 9, ed. Karlsson, M., Ch. 4, 127–144, Fapet, 2000.

Söderman, J., Heikkilä, P., Calculation of the heat transfer coefficients with condensation in heat recovery systems, Report 2001-1, Åbo Akademi Univ., Heat Eng. Lab., 2001.

Söderman, J., Pettersson, F., Structural and operational optimisation of distributed energy systems, Appl. Thermal Eng., 26, 2006, 1400–1408.

Söderman, J., Pettersson, F., Comparison of solutions with varying cost factors in structural optimisation of paper machine heat recovery systems, Report 2001-3, Åbo Akademi Univ., Heat Eng. Lab., 2001.

Söderman J., Pettersson F., Ahtila, P., Keppo, I., Nuorkivi, A., Sipilä, K., Ikäheimo, J., Design of optimal distributed energy systems, Report 2005-1, Åbo Akademi Univ., Heat Eng. Lab., 2005.

Söderman, J., Westerlund, T., Pettersson, F., Economical optimisation of heat recovery systems for paper machine dryer sections, Proceedings of 2nd Conf. on Process Integration, Modelling and Optimisation for Energy Saving and Pollution Reduction, 607–612, Budapest, 1999.

Söderman, J., Öhman, G., Saxén, H., A periodic process for enhanced district cooling generation, 10th Symposium District Heating and Cooling, Hannover, 2006.

Tessmer R.G., Hoffman K.C., Marcuse W., Behling D.J., Coupled energy system-economic models and strategic planning, Computer and Operations Research, 2, 1975, 213–224.

Trivedi, K.K., O'Neill, B.K., Roach, J.R., Wood, R.M., A new dual-temperature design method for the synthesis of heat exchanger networks, Comp. Chem. Eng., 6, 1989, 667–685.

Umeda, T., Harada, T., Shiroko, K., A thermodynamic approach to the synthesis of heat integration systems in chemical processes, Comp. Chem. Eng., 3, 1979, 273–282.

Umeda, T., Itoh, J., Shiroko, K., Heat exchange system synthesis, Chem. Eng. Prog., 74, Nr. 7, 1978, 70–76.

Umeda, T., Niida, K., Shiroko, K., A thermodynamic approach to heat integration in distillation systems, AIChE Journal, 25, 1979, 423–429.

Van der Voort E., Donni E., Thonet C., Bois d'Enghien E., Dechamps C., Guilmot J.F., Energy supply modelling package EFOM-12C Mark I, Mathematical Description, EUR-8896, Louvian-la-Neuve, Cabay, Commission of the European Communities, 1984.

Vartiainen E., Luoma P., Hiltunen J., Vanhanen J., Decentralized energy production: technology, fuels, market and CO2-emissions, technology review (in Finnish), Edita, 2002.

Viswanathan, J., Grossmann, I.E., A combined penalty function and Outer-Approximation method for MINLP optimization, Comp. Chem. Eng., 14, 1990, 769–782.

Weber C., Maréchal F., Favrat D., Design and optimization of district energy systems, Proceedings of 17th Int. Congr. of Chem. and Proc. Eng.(CHISA 2006), Prague, 2006.

Wene C.O., Rydén B., A comprehensive energy model in the municipal energy planning process, European Journal of Operational Research, 33, 1988, 212–222.

Westerlund, T., Pettersson, F., A Cutting Plane method for solving convex MINLP problems, Comp. Chem. Eng., 19, 1995, S 131–136.

Westerlund T., Skrifvars H., Harjunkoski I. and Pörn R., 1998, An Extended Cutting Plane Method for solving a Class of Non-Convex MINLP Problems. Comp. Chem. Eng., 22, 357–365.

Wu, Y.J., Rosen, M.A., Assessing and optimizing the economic and environmental impacts of cogeneration/district energy systems using an energy equilibrium model, Appl. Energy, 62, 1999, 141–154.

Yee T.F., Grossmann I.E., Simultaneous optimization models for Heat Integration, II: Heat Exchanger Network Synthesis, Comp. Chem. Eng., 14, 1990, 1165–1184.

ISBN 978-952-12-1983-2

UNIPRINT

Åbo 2007